U.S. DEPARTMENT OF THE INTERIOR
U.S. GEOLOGICAL SURVEY

Aquifer Compaction and Ground-Water Levels in South-Central Arizona

Water-Resources Investigations Report 99—4249

Prepared in cooperation with the
CITY OF TUCSON and
ARIZONA DEPARTMENT OF WATER RESOURCES

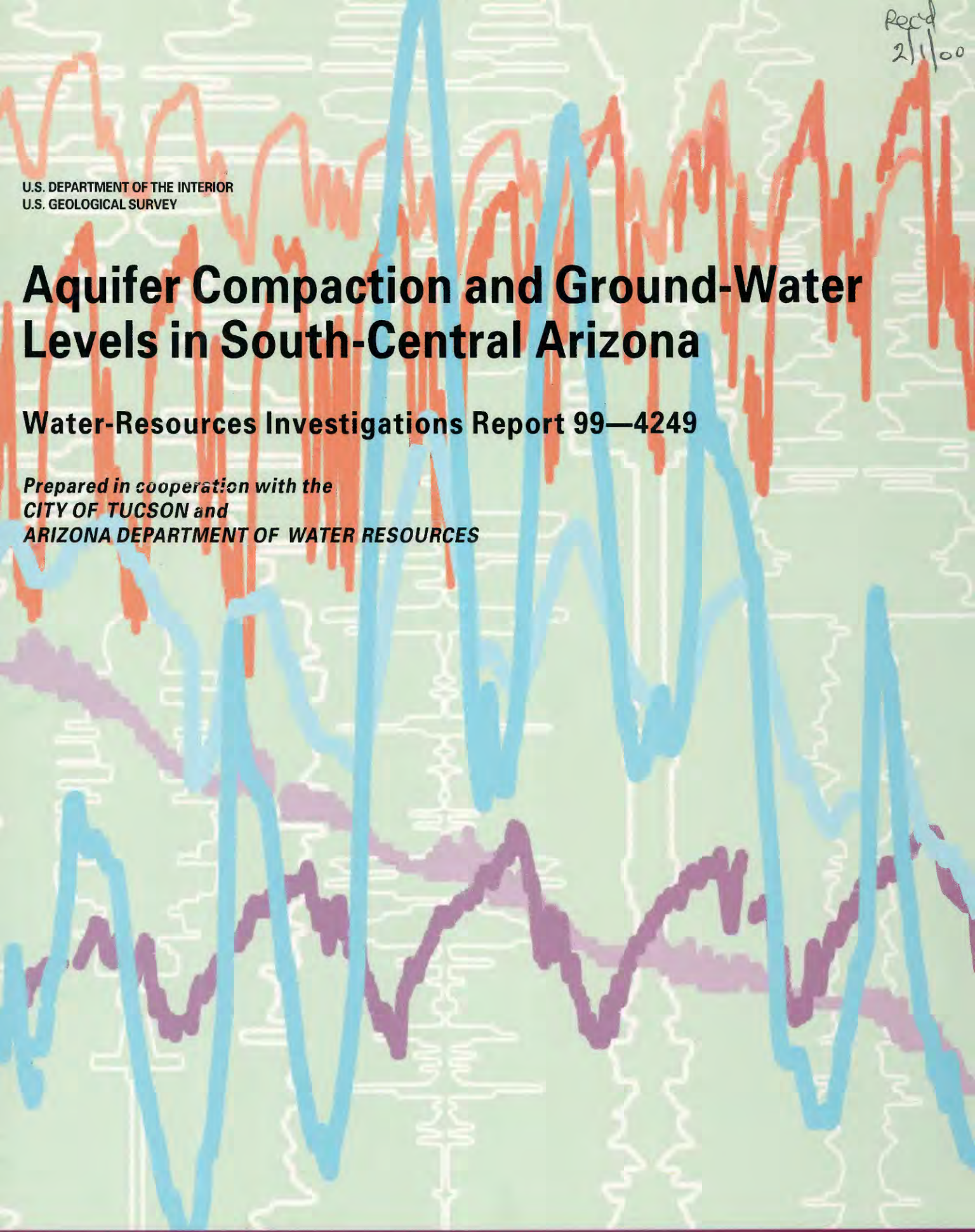

USGS

U.S. DEPARTMENT OF THE INTERIOR
U.S. GEOLOGICAL SURVEY

Aquifer Compaction and Ground-Water Levels in South-Central Arizona

By D.W. EVANS *and* D.R. POOL

Water-Resources Investigations Report 99—4249

Prepared in cooperation with the
CITY OF TUCSON and
ARIZONA DEPARTMENT OF WATER RESOURCES

Tucson, Arizona
2000

U.S. DEPARTMENT OF THE INTERIOR
BRUCE BABBITT, Secretary

U.S. GEOLOGICAL SURVEY
Charles G. Groat, Director

For additional information write to:

District Chief
U.S. Geological Survey
Water Resources Division
520 N. Park Avenue, Suite 221
Tucson, AZ 85719-5035

Copies of this report can be purchased from:

U.S. Geological Survey
Information Services
Box 25286
Federal Center
Denver, CO 80225-0046

CONTENTS

FIGURES

FIGURES—Continued Page

FIGURES—Continued Page

TABLES

CONVERSION FACTORS

Multiply	By	To obtain
inch (in.)	2.54	centimeter
inch (in.)	25.4	millimeter
foot (ft)	0.3048	meter
square mile (mi^2)	2.590	square kilometer
acre-foot (acre-ft)	0.001233	cubic hectometer

Temperature in degrees Celsius (°C) may be converted to degrees Fahrenheit (°F) as follows:

$$°F=1.8(°C)+32$$

VERTICAL DATUM

Sea level: In this report, "sea level" refers to the National Geodetic Vertical Datum of 1929 (NGVD of 1929)—A geodetic datum derived from a general adjustment of the first-order level nets of the United States and Canada, formerly called Sea Level Datum of 1929.

WELL-NUMBERING AND NAMING SYSTEM

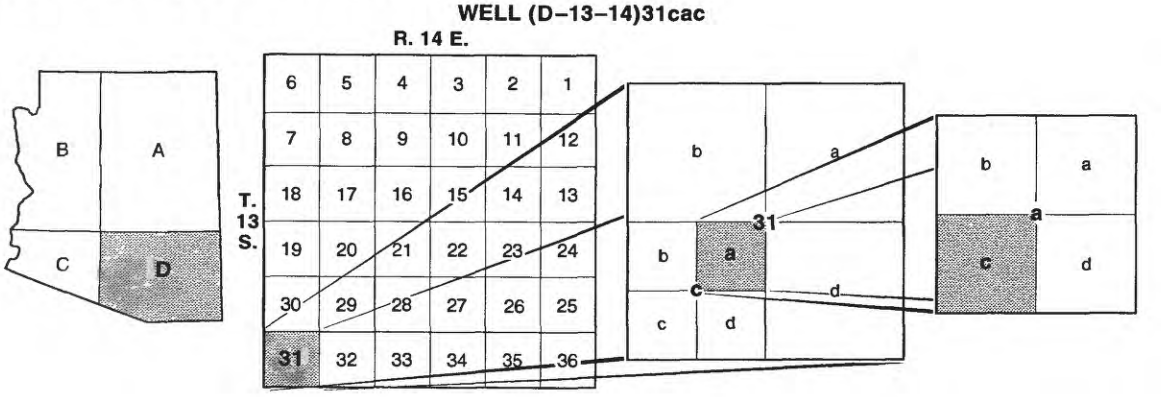

Quadrant D, Township 13 South, Range 14 East, section 31, quarter section c, quarter section a, quarter section c

The well numbers used by the U.S. Geological Survey in Arizona are in accordance with the Bureau of Land Management's system of land subdivision. The land survey in Arizona is based on the Gila and Salt River meridian and base line, which divide the State into four quadrants and are designated by capital letters A, B, C, and D in a counterclockwise direction beginning in the northeast quarter. The first digit of a well number indicates the township, the second the range, and the third the section in which the well is situated. The lowercase letters a, b, c, and d after the section number indicate the well location within the section. The first letter denotes a particular 160-acre tract, the second the 40-acre tract and the third the 10-acre tract. These letters also are assigned in a counterclockwise direction beginning in the northeast quarter. If the location is known within the 10-acre tract, three lowercase letters are shown in the well number. Where more than one well is within a 10-acre tract, consecutive numbers beginning with 1 are added as suffixes. In the example shown, well number (D–13–14)31cac designates the well as being in the SW1/4, NE1/4, SW1/4, section 31, Township 13 South, and Range 14 East.

Aquifer Compaction and Ground-Water Levels in South-Central Arizona

By D.W. Evans *and* D.R. Pool

Abstract

As of 1998, the U.S. Geological Survey is monitoring water-level fluctuations and aquifer compaction at 19 wells that are fitted with borehole extensometers in the Eloy Basin, Stanfield Basin, Avra Valley, and Upper Santa Cruz Basin. Decreased ground-water pumping has resulted in water-level recoveries of more than 100 feet at a well near Eloy and almost 20 feet at a well in Avra Valley. Aquifer compaction has continued in both areas despite the large water-level recoveries in Eloy and the stable water levels in Avra Valley. Extensometer sites in the Upper Santa Cruz Basin have recorded as much as 50 feet of water-level decline and 0.2 feet of aquifer compaction during 1980 to 1996. Rates of compaction vary throughout the extensometer network, with the greater rates of compaction being associated with the more compressible sediments of the Eloy and Stanfield Basins.

INTRODUCTION

Since the 1940's, declines of several feet per year in ground-water levels have resulted in aquifer compaction and measurable land subsidence in the Eloy Basin, Stanfield Basin, Avra Valley, and Upper Santa Cruz Basin in Arizona. Historic overdrafts in the Eloy Basin are responsible for continued dewatering of aquitards and subsequent aquifer compaction and land subsidence even with recent water-level recoveries of more than 100 ft in some areas. Water-level declines in Avra Valley and the Upper Santa Cruz Basin are less than in the Eloy and Stanfield Basins; however, measurable amounts of compaction have been recorded at most of the monitoring stations. The future of the Tucson metropolitan area may be severely affected by ground-water overdrafts and subsidence-related problems because of rapid population growth and the almost exclusive reliance on ground water by the City of Tucson for its water supply.

In 1979, the U.S. Geological Survey (USGS), in cooperation with the City of Tucson, began to monitor aquifer compaction at several sites in the Upper Santa Cruz Basin. In 1983, the study was expanded to include six sites in Avra Valley. In 1989, with the cooperation of the Arizona Department of Water Resources, five sites in the Eloy Basin and one site in the Stanfield Basin were added to the network. Data have been collected continuously since the activation of recording instrumentation in each well. As of 1998, the USGS is monitoring 19 borehole extensometers in wells in south-central Arizona (fig. 1). Continuous water levels and compaction are recorded at each site.

Near Eloy, water-level declines continued at rates of several feet per year from the 1940's until the early 1980's (Hanson, 1989). With the advent of available surface water from the Central Arizona Project and subsequent decreased pumping, water levels began to recover. Since the early 1980's, recoveries of as much as 100 ft have been recorded. The effects of historic pumping on the aquifer are still evident as aquifer compaction and land subsidence have continued in spite of a significant water-level recovery.

Although monitoring of compaction and water levels is ongoing, the scope of this report is limited to data collected between 1980 and 1996 for wells

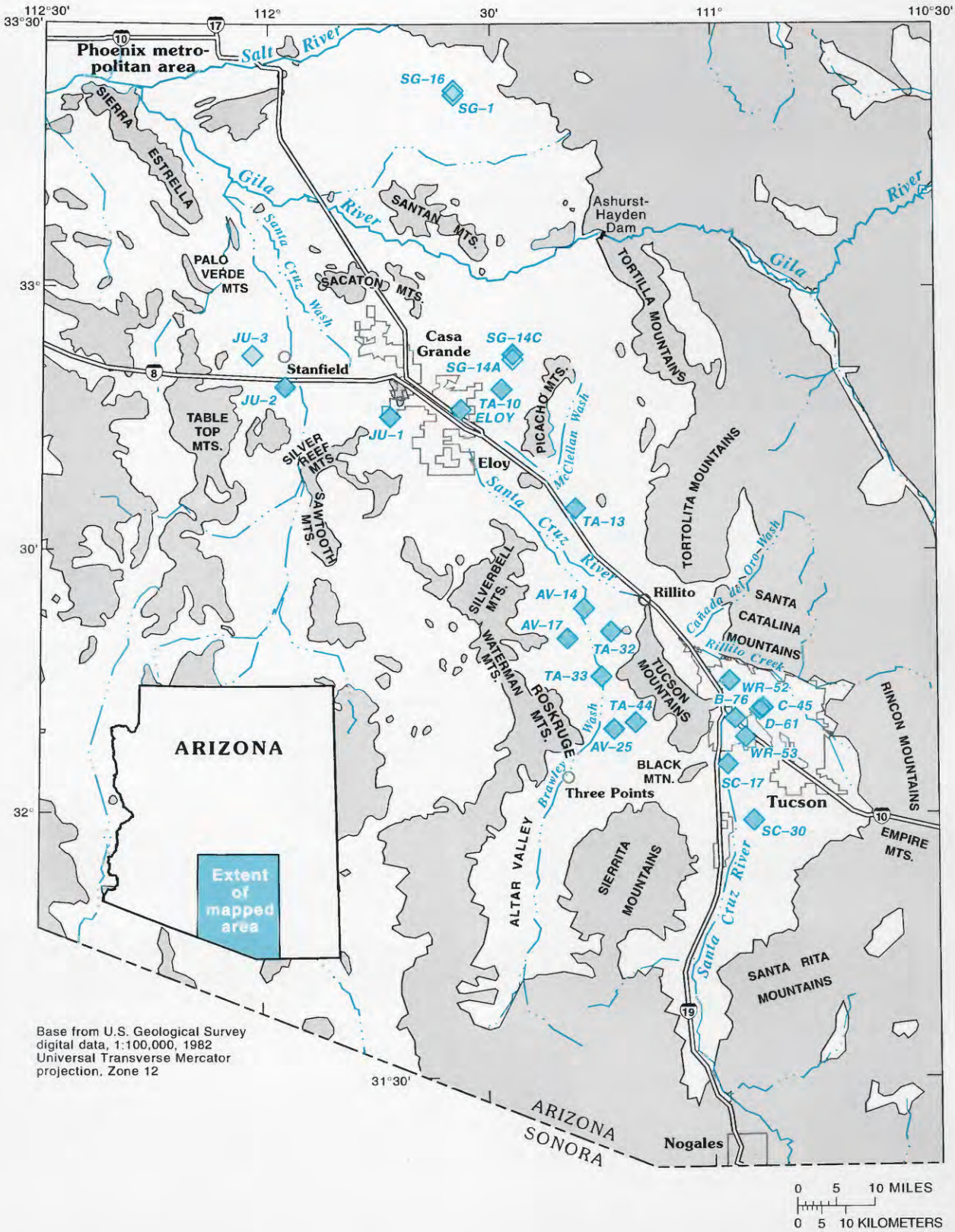

Figure 1. Study area and location of borehole extensometers, south-central Arizona.

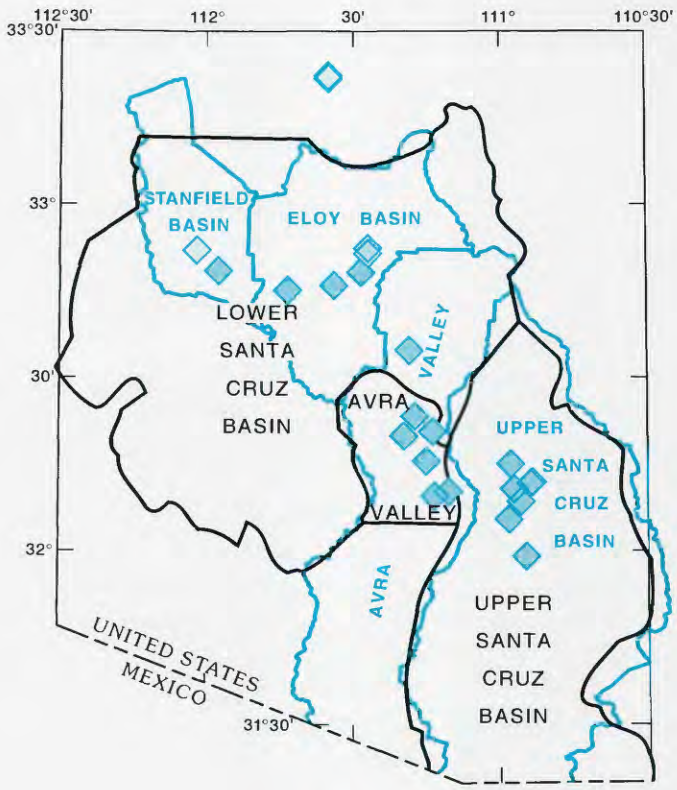

EXPLANATION

- BASIN SEDIMENTS AND SURFICIAL ALLUVIAL DEPOSITS
- BEDROCK
- BOUNDARY OF GROUND-WATER BASIN USED FOR DETERMINATION OF GROUND-WATER WITHDRAWALS
- BOUNDARY OF GROUND-WATER BASIN USED FOR GEOHYDROLOGIC CHARACTERIZATION
- SC-30 — EXTENSOMETER SITE CURRENTLY MONITORED BY U.S. GEOLOGICAL SURVEY—Number is site identifier
- JU-3 — EXTENSOMETER SITE NOT CURRENTLY MONITORED BY U.S. GEOLOGICAL SURVEY—Number is site identifier

Figure 1. Continued.

in the Upper Santa Cruz Basin, 1984 to 1996 for wells in Avra Valley, and 1989 to 1996 for wells in the Eloy and Stanfield Basins. This report provides water-level and compaction data for 19 borehole extensometers in south-central Arizona, stratigraphic information, and interpretation of aquifer-storage properties by calculations of elastic and inelastic storage.

Previous Investigations

Federal, State, county, municipal, and university studies have focused on various aspects of the geohydrological framework of the Eloy Basin, Stanfield Basin, Avra Valley, and the Upper Santa Cruz Basin. Geohydrology and water resources were studied by Davidson (1973), Pool (1984), and Schmidt (1985), and stratigraphy was studied by Allen (1981) and Anderson (1987a). Models of ground-water flow were detailed by Anderson (1972), Moosburner (1972), Clifton (1981), Travers and Mock (1984), Mock and others (1985) and Rampe (1985). The potential for aquifer compaction, land subsidence, and earth fissures was evaluated by Platt (1963), Caito and Sogge (1982), Anderson (1987a, 1989), Carpenter (1988, 1993), Leake and Prudic (1991), Hanson (1989), Hanson and others (1990), and Hanson and Benedict (1994). General ground-water conditions were defined by White and others (1966), Reeter and Cady (1982), Whallon (1983), and Cuff and Anderson (1987). Hydrologic and geologic terms used in this report are summarized by Poland and others (1972), and Laney and Davidson (1986). Hydrologic and geologic factors of land subsidence at the Eloy well were studied by Epstein (1987). Earth fissures in southern Arizona were studied by Carpenter (1988, 1993). Hanson (1989) gives a brief description of physical setting, hydrogeology, and components of aquifer-system compaction in the Tucson Basin and Avra Valley. Holzer and others (1979) and Jachens and Holzer (1979) describe fissuring and subsidence related to ground-water withdrawals in the Eloy Basin. For the purposes of this report, the hydrogeology of the Stanfield Basin is considered to be similar to that of the Eloy Basin. Several studies listed in this section refer to the Tucson Basin, which is a 1,000-square-mile area in the north-central part of the Upper Santa Cruz Basin.

Acknowledgments

Stan Leake, USGS, Tucson, Arizona, provided technical advice. Andrew Hesse, USGS, Tucson, Arizona, digitized data, checked calculations, and provided assistance in correcting data.

Physical Setting

The Eloy Basin, Stanfield Basin, Avra Valley, and Upper Santa Cruz Basin are in the Basin and Range lowlands physiographic province of Arizona. The Eloy Basin is an area of about 900 mi^2 midway between Phoenix and Tucson (fig. 1). Mountains partly surround the basin and include ranges that are less than 5,000 ft above sea level. The basin is bounded on the south and southwest by the Silverbell and Sawtooth Mountains. The west edge of the basin is formed by the Silver Reef and Sacaton Mountains. The Santan Mountains and the Gila River form the north boundary of the basin. The Tortilla Mountains form the northeastern boundary of the basin, and the Picacho Mountains and Picacho Peak form the east boundary. The Stanfield Basin lies adjacent to the Eloy Basin to the west and is bounded on the northwest and southwest by the Palo Verde and Vekol Mountains, respectively. Annual precipitation in the Eloy and Stanfield Basins averages 10.5 in. at Casa Grande and is slightly greater in the mountains (D.R. Pool, hydrologist, USGS, written commun., 1995). The valley floor, which includes about 615 mi^2, ranges in altitude from about 1,900 ft between Picacho Peak and the Silverbell Mountains to about 1,000 ft at Casa Grande and along the Gila River in the northeast part of the Stanfield Basin.

The Gila River is the major surface-water drainage in the area. Before development of surface-water supplies, the Gila River was an intermittent stream that flowed for long periods of the year and probably was perennial throughout the reach within the study area. At present, the flow in the river is controlled partly by upstream reservoir releases and diversions at Ashurst-Hayden Dam.

Other streams flow only in response to local precipitation and include the Santa Cruz Wash and McClellan Wash, which have poorly defined distributary channels in the western part of the basin. Intense rainfall along the Santa Cruz River drainage occasionally produces large flows in the study area.

The Upper Santa Cruz Basin and Avra Valley lie to the southeast of the Eloy Basin. The Upper Santa Cruz Basin encompasses about 2,870 mi^2 in northern Sonora, Mexico, and in Pima, Pinal, and Santa Cruz Counties, Arizona. The Upper Santa Cruz Basin is bounded on the west by the Tucson and Sierrita Mountains and Black Mountain; on the north by the Tortolita and Santa Catalina Mountains; and on the east by the Rincon and Empire Mountains. The southern boundary is south of the study area in Mexico. These mountains range in altitude from about 3,000 ft to about 9,500 ft above sea level. Within the basin, the valley floor ranges in altitude from 2,000 ft above sea level near Rillito and the northwest edge of the basin to 3,500 ft near the international boundary with Mexico. Annual precipitation ranges from 11 in. on the valley floor to about 30 in. in the surrounding mountains.

Avra Valley encompasses about 520 mi^2 and is bounded on the south by the Sierrita Mountains and Altar Valley; on the west by Silverbell, Waterman, and Roskruge Mountains; on the northwest by Picacho Peak; and on the northeast by the Tortolita Mountains. These mountains range in altitude from about 4,500 ft to 6,000 ft above sea level. The valley floor ranges from 1,800 ft above sea level near Picacho Peak to 2,600 ft near Three Points. Annual precipitation in Avra Valley ranges from less than 10 in. on the valley floor to about 12 in. in the mountains.

The Santa Cruz River is the major surface-water drainage in the Upper Santa Cruz Basin and Avra Valley. Before large-scale ground-water pumping began in the basin, the Santa Cruz River was perennial in most of the study area. As of 1998, the base flow in the river is effluent and is controlled by three water-treatment plants. Natural flow is strictly runoff from storms. Other streams generally flow only in response to local precipitation and include the Rillito River and the Cañada del Oro Wash in Tucson and Brawley Wash in Avra Valley.

Hydrogeology

Basins in the study area were formed as a result of crustal extension during the Cenozoic Basin and Range orogeny. The Basin and Range orogeny was accompanied by block faulting, the formation of a horst-and-graben terrain, and the accumulation of sedimentary basin fill. The disturbance, which overlaid earlier formed structural features, transformed the landscape of the Eloy Basin, Stanfield Basin, Avra Valley, and the Upper Santa Cruz Basin from an area of generally moderate relief into one of high relief characterized by deep structural basins bounded by high mountain ranges (Anderson, 1987a).

In this report, some published reports from studies of the Picacho structural basin were used as references for describing hydrogeologic conditions within the Eloy Basin because the two basins are essentially equivalent. Published reports from studies of the Tucson Basin were used as references for describing the hydrogeologic conditions within the Upper Santa Cruz Basin because Tucson Basin was the preferred nomenclature for the north-central part of the Upper Santa Cruz Basin where the extensometers in this study are located. Additionally, hydrogeologic conditions in the Stanfield Basin are considered to be similar to those documented for the Eloy Basin of which more detailed studies have been done.

Alluvial deposits that accumulated in the basins can be grouped into three stratigraphic units of basin fill on the basis of structural relations. The oldest unit was deposited before and during the early phases of extensional tectonism associated with low-angle faulting and includes the Pantano Formation in the Upper Santa Cruz Basin and Avra Valley and the lower hydrostratigraphic unit in the Eloy and Stanfield Basins. The middle unit was deposited during the transition from low- to high-angle faulting and includes the lower Tinaja beds in the Upper Santa Cruz Basin and Avra Valley, and the middle hydrostratigraphic unit in the Eloy Basin. The upper unit is relatively undisturbed by faulting in comparison to the older units and includes the upper Tinaja beds and Fort Lowell Formation in the Upper Santa Cruz Basin and Avra Valley and the upper hydrostratigraphic unit in the Eloy and Stanfield Basins. A thin layer of alluvium was deposited along major drainage

channels subsequent to the accumulation of basin fill.

The Eloy and Stanfield Basins are two of several basins in central Arizona that are known collectively as the Gila Low (Peirce, 1974). The Gila Low, which is a region of closed drainage formed during the early stages of the Basin and Range structural disturbance, contains more than 10,000 ft of basin sediments and evaporites within three major basins (Oppenheimer and Sumner, 1981). The sediments of the Eloy and Stanfield Basins consist primarily of continental basin sediments that accumulated during the Cenozoic Era under restricted or closed drainage. Fine sand, silt, clay, and evaporites were deposited in playas or ephemeral lakes in topographic low regions. Areas around the topographic lows were dominated by alluvial deposition of interbedded sand, gravel, silt, and clay.

The sediments of the Eloy Basin are divided into lower, middle, and upper stratigraphic units. The units are divided on the basis of apparent water-bearing characteristics inferred from subsurface lithologic and physical-property information; therefore, these units are referred to as hydrostratigraphic units (D.R. Pool, hydrologist, USGS, written commun., 1995). The lower unit consists of an alluvial facies that is primarily conglomerate and a playa facies that includes mudstone and evaporites. Much of the lower unit is disturbed by normal faults, and the degree of deformation increases with depth. The unit overlies bedrock throughout the basin and is as much as several thousand feet thick. The middle unit is composed largely of playa deposits, may be structurally deformed near the major normal faults in the basin, and is as much as 1,500 ft thick. The upper unit generally is flat lying but may be deformed near the major graben-bounding faults. The upper unit is primarily alluvial deposits of interbedded sand, gravel, silt, and clay that generally range in thickness from 500 to 1,500 ft. In general, the basin sediments become increasingly fine grained with depth in the basin center and increasingly coarse grained with depth on the basin margin (D.R. Pool, hydrologist, USGS, written commun., 1995).

The principal aquifers in the Eloy Basin are the conglomerate of the lower unit and the sand and gravel interbeds within the alluvial facies of the middle and upper units. The principal confining units are the crystalline rocks that underlie the basin sediments; the playa facies of the lower unit, middle, and upper units; and silt and clay interbeds within the alluvial facies of the middle and upper units. Most ground-water flow occurs in aquifers of the middle and upper units, which are more permeable than the deeper aquifers (D.R. Pool, hydrologist, USGS, written commun., 1995).

The major sources of recharge in the Eloy Basin are streamflow infiltration, mountain-front recharge, and underflow from the south. The Gila River is the largest river in the basin; McClellan Wash and the Santa Cruz River also provide recharge. The main underflow to the area occurs between Picacho Peak and the Silverbell Mountains from areas south of the Eloy Basin.

The Upper Santa Cruz Basin and Avra Valley are north- to northwest-trending alluvial basins bounded by block-faulted mountains that consist of igneous, metamorphic, and sedimentary rocks of Precambrian to Tertiary age (Wilson and others, 1969). Three sedimentary units of Cenozoic age—the Pantano Formation of Oligocene age, the Tinaja beds of Miocene to Pliocene age, and the Fort Lowell Formation of Pleistocene age—compose the alluvial aquifer system (Davidson, 1973; Allen, 1981; Anderson, 1987a, 1987b, 1989; and Hanson 1989). The three sedimentary units of the Upper Santa Cruz Basin and Avra Valley are correlative with the lower, middle, and upper hydrostratigraphic units of the Eloy Basin (fig. 2).

The Pantano Formation consists of conglomerate, sandstone, mudstone, and gypsiferous mudstone as well as megabreccia, tuff beds, and interbedded volcanic flows (Anderson, 1987a). The Pantano Formation was deposited before and during the early stages of extensional tectonism associated with low-angle faulting. The lower Tinaja beds were deposited during the transition from low to high-angle faulting, consist of gravel and conglomerate to clayey silt and mudstone, and are hundreds of feet thick. The middle Tinaja beds consist of gravel conglomerate to gypsiferous and anhydritic clayey silt and mudstone and are hundreds to thousands of feet thick. The upper units generally are undisturbed by faulting in comparison to the older units and include the upper Tinaja beds and the Fort Lowell Formation. The upper Tinaja beds are gravel to clayey silt and are

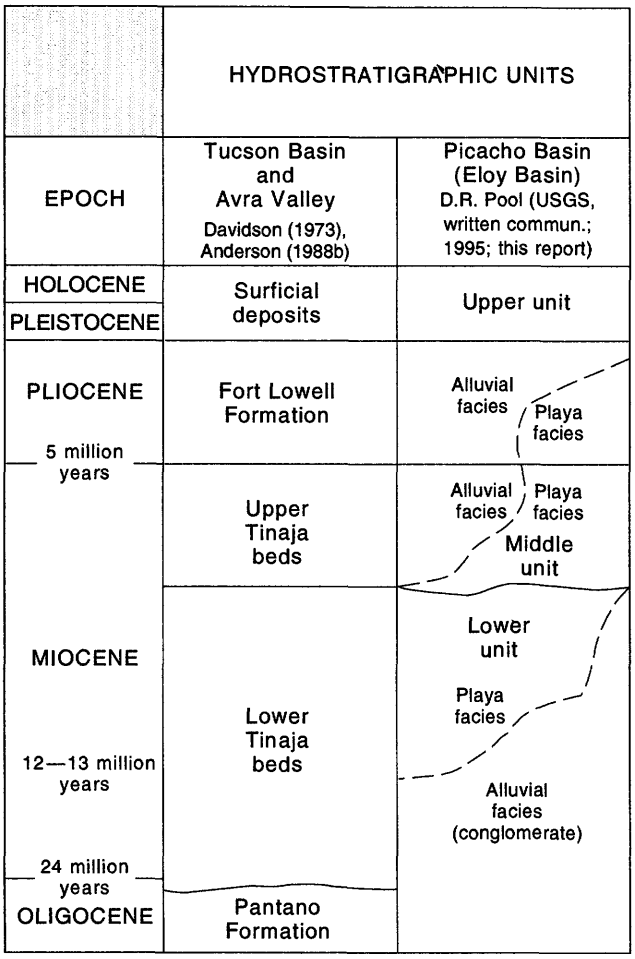

Figure 2. Correlation of local and regional-basin sedimentary units.

hundreds to thousands of feet thick. The Fort Lowell Formation consists of gravel to clayey silt and also includes thin surficial alluvial deposits of late Pleistocene and Holocene age. The Fort Lowell Formation ranges in thickness from several feet to several hundreds of feet (Anderson, 1987a).

The aquifers in the Upper Santa Cruz Basin and Avra Valley consist of the Pantano Formation, the Tinaja beds, and the Fort Lowell Formation (Davidson, 1973). The Pantano Formation and Tinaja beds yield small to moderate amounts of water to wells. The Fort Lowell Formation is the most permeable unit of the aquifer and yields moderate to large amounts of water to wells (Davidson, 1973).

Ground water is replenished by mountain-front recharge in the Upper Santa Cruz Basin and by underflow in Avra Valley (Hanson, 1989). Additional streamflow infiltration from effluent and floods contributes to recharge along the Santa Cruz River and its tributaries in the Upper Santa Cruz Basin. The Santa Cruz River and ground-water outflow from the Upper Santa Cruz Basin enter Avra Valley northwest of Rillito. Additional underflow enters Avra Valley from Altar Valley to the south. Ground-water outflow from Avra Valley occurs between the Silverbell Mountains and Picacho Peak and enters the Eloy Basin in the southern part of the Lower Santa Cruz River Basin. Natural ground-water flow paths and head distributions have been altered by ground-water withdrawals (Hanson, 1989).

Continued withdrawal of ground water has developed perched-aquifer zones as a result of hydraulic disconnection and irrigation return flow in some places; however, in other places, vertical hydraulic gradients are maintained between aquifers across confined and semiconfined beds (Leake and Hanson, 1986; and Cuff and Anderson, 1988). Cuff and Anderson (1987) outlined an area of perched ground water in the north-central part of Avra Valley that is similar to an area in west-central Tucson. Perched aquifers, which are caused by irrigation return flow or artificial recharge, can increase geostatic stress, and transient vertical gradients can result in seepage stresses. Both conditions can increase the change in effective stress on aquitards (Hanson, 1989).

Potential for Aquifer Compaction

The much lower values of density and the larger porosity in the fine-grained sediments of the middle and upper units in the Eloy Basin in relation to those of the lower unit indicate that the middle and upper units contain more void space available for compression and are more compressible than the lower unit (D.R. Pool, hydrologist, USGS, written commun., 1995). The lower unit generally is incompressible in relation to the upper and middle units. Additional qualitative information on compressibility is available from drillers' logs, lithologic logs, and drill cuttings. The amount of dense fine-grained sediments generally increases with depth in the middle unit (D.R. Pool, hydrologist, USGS, written commun., 1995). For the most part, areas with greater rates of inelastic compaction are those in the saturated

zones of the middle and upper units that have a larger silt-clay content and are associated with ground-water withdrawals.

The sediments in the Eloy and Stanfield Basins generally contain more fine-grained material than sediments in the Upper Santa Cruz Basin and, therefore, are more likely to compact inelastically in response to pumping. Four of the five highest rates of compaction per unit of monitored thickness in the network are in the Eloy and Stanfield Basins. When compared to the Fort Lowell Formation and the upper Tinaja beds in the Upper Santa Cruz Basin and Avra Valley areas, the upper hydrostratigraphic unit in the Eloy Basin has been pumped more extensively and has responded with higher rates of compaction as well as with greater amounts of total subsidence.

Potential for aquifer compaction in the Upper Santa Cruz Basin and Avra Valley was explored by Anderson (1987a) and Hanson (1989). The Pantano Formation, lower Tinaja beds, and middle Tinaja beds consist largely of moderately indurated to indurated deposits that generally may be resistant to deformation related to ground-water withdrawal (Anderson, 1987a). The potential for aquifer compaction and its effects in the basin may depend more on the character of the upper units of the Tinaja beds and the Fort Lowell Formation than on the character of the lower units in the basin. The thickness and clay content of the upper units and the relation between the upper units and bedrock has more effect on the potential for aquifer compaction than for the attributes of the lower units in the basin. The thickness of the Fort Lowell Formation and the upper Tinaja beds varies throughout the basin as a result of structural deformation of the underlying rock. Generally, areas of greater rates of inelastic compaction are those areas that contain a larger silt-clay percentage in the saturated zones of the Fort Lowell Formation and upper Tinaja beds and are associated with ground-water withdrawals.

Land subsidence and aquifer compaction in the Upper Santa Cruz Basin and Avra Valley has not been as great as that in the Eloy and Stanfield Basins because these areas have not been pumped as extensively as the Eloy and Stanfield Basins (Anning and Duet, 1994). The Fort Lowell Formation and the upper Tinaja beds do not contain the high percentage of easily compressible clay layers that the upper hydrostratigraphic unit of the Eloy Basin does and, therefore, would not compact as much under similar ground-water withdrawal conditions. The Fort Lowell Formation and the upper Tinaja beds do, however, contain compressible clay layers that have shown high rates of inelastic compaction in response to ground-water withdrawals.

Methods of Data Collection

All monitoring sites are equipped with borehole extensometers that measure compaction between the land surface and the depth at which the bottom of the extensometer is anchored. The extensometer is anchored in bedrock or is grouted into a stationary platform in a less compressible layer of a sedimentary unit (fig. 3). Most of the extensometers in this study were completed to depths between 800 and 1,400 ft and were anchored in the less compressible layers of the middle and lower Tinaja beds or equivalent units. Each site is equipped with a Stevens Type-F recorder to continuously record compaction.

Manual-compaction measurements are made with a steel tape affixed at one end to a table and to the extensometer pipe at the other end and can be made by reading a dial gage that is anchored to a table and pushes against a plate attached to the extensometer pipe (fig. 3). As the land surface moves down relative to the pipe, the recording instrument measures compaction, and as the land surface moves up relative to the pipe, the recording instrument measures expansion. Compaction is measured to the nearest 0.0001 ft and recorded to the nearest 0.001 ft.

The record of compaction data may be affected by downhole frictional forces, temperature changes, and buoyancy of the extensometer pipe. Temperature changes inside the well from barometric effects and the resulting shrinking and swelling of the pipe are evident in some of the data as noise. Water-temperature variations from contributing layers of different depths in the borehole also can have an effect on the pipe. Downhole friction typically is the limiting factor in determining extensometer accuracy (Riley, 1984). Buoyant forces were minimized by using an

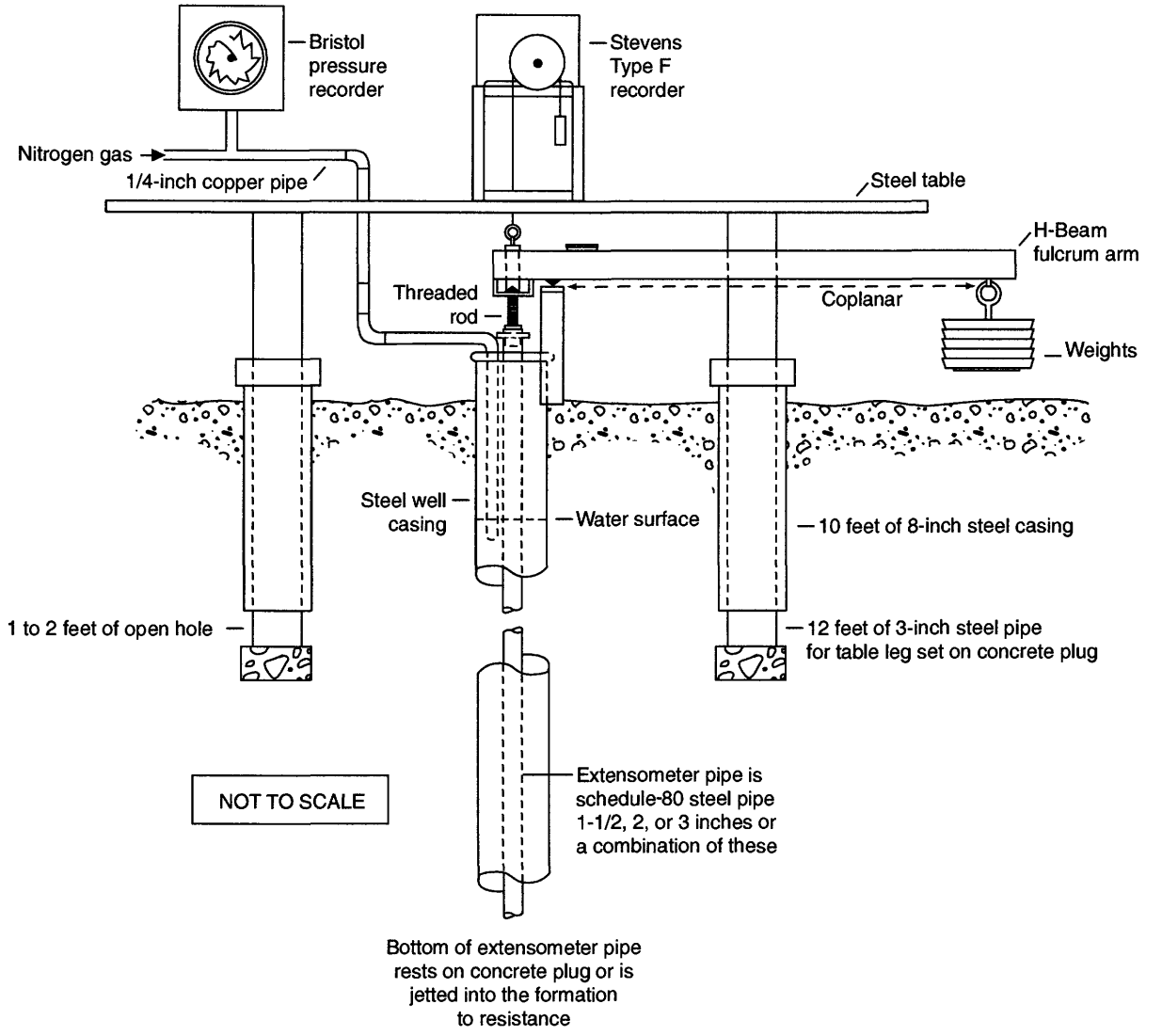

Figure 3. Typical borehole-extensometer installation.

open-ended extensometer pipe so that water levels are equal inside and outside the pipe.

Water levels are recorded with a Bristol pressure recorder. Instantaneous measurements are made with an electric sounder or a steel tape. Water levels are measured and recorded to the nearest 0.1 ft. After collection, the field data are digitized, checked, and stored in the data base. Discrepancies between the instantaneous measurements and the continuous data are adjusted to agree with the instantaneous readings

Land subsidence is not measured as a part of this monitoring study; however, amounts of subsidence through the mid-1980's are provided as supplemental information. Total land subsidence caused by aquifer compaction may not be recorded by an extensometer unless the installation fully penetrates the aquifer.

RELATION BETWEEN WATER-LEVEL CHANGE AND AQUIFER COMPACTION

In addition to measuring aquifer-system compaction, a major purpose of borehole extensometers is to establish relations between water-level change and compaction. Knowledge of

these relations is critical in the prediction of possible future subsidence. The method of analysis of extensometer data for determination of aquifer mechanical properties was presented by Riley (1969). Riley (1969) applied basic principles from the Terzaghi theory of soil mechanics to derive aquifer-system storage properties in terms commonly used by hydrogeologists.

Relations between water-level change and compaction use the principle that effective stress at any point in an aquifer system is the difference between the geostatic load and the pore pressure. Lowering the ground-water head by pumping lowers the pore pressure and thus increases the effective stress on the aquifer system. When effective stress is less than the previous maximum effective stress on the sediments, compaction and expansion is elastic; however, when effective stress exceeds the past maximum value, some fine-grained sediments compact inelastically. This inelastic or nonrecoverable component of compaction is responsible for most of the observed land subsidence in areas of major ground-water withdrawals.

Basic relations between water-level change and compaction are summarized by Leake and Prudic (1991). For a more detailed discussion of these relations, refer to Jorgenson (1980) and Leake (1991). This discussion assumes that compaction is proportional to change in effective stress and that geostatic load is constant. Under these conditions, elastic compaction, Δb_e, can be related directly to water-level or head change, Δh, as

$$\Delta b_e = -\Delta h S_{ske} b_0, \qquad (1)$$

where S_{ske} is the skeletal component of elastic specific storage, and b_0 is the thickness of compressible sediments. The sign convention used here is that a positive compaction, Δb_e, refers to a decrease in thickness of sediments and a positive head change, Δh, refers to an increase in head or water level. The skeletal component of elastic specific storage, S_{ske}, has units of length^{-1}, and thickness of sediments, b_0, has units of length. The product of these quantities is the dimensionless elastic skeletal storage coefficient, denoted as S_{ke}. Note that S_{ke} is the coefficient of proportionality between compaction and head change in equation 1. If compaction in the elastic range and head change are known, then S_{ke} can be computed as

$$S_{ke} = -\Delta b_e / \Delta h. \qquad (2)$$

Similarly, compaction in the inelastic range, Δb_i, can be related to water-level or head change as

$$\Delta b_i = -\Delta h S_{skv} b_0, \qquad (3)$$

where S_{skv} is the skeletal component of inelastic or virgin specific storage. If compaction and head change in the inelastic ranges are known, then inelastic skeletal storage coefficient, S_{kv}, can be computed as

$$S_{kv} = -\Delta b_i / \Delta h. \qquad (4)$$

Riley's (1969) method of analysis of extensometer data uses relations in equations 2 and 4 to compute storage coefficients S_{ke} and S_{kv}. Application of the method requires a graphical analysis of water-level and compaction records from an extensometer to determine ratios of responses of Δb_e and Δb_i to head change, Δh. Data are plotted on an arithmetic scale with compaction on the abscissa and applied stress on the ordinate axis (fig. 4).

With a constant geostatic load, a unit change in water level or head results in a unit change in applied stress. The ordinate axis usually is labeled as "depth to water" with values of depth to water increasing away from the origin. The hypothetical response curve shown in figure 4 is similar to relations analyzed by Riley (1969). For his method, parts of the curves representing elastic and inelastic responses are identified. When water levels recover, sediments expand instead of compact. The inverse slope of this part of the curve is taken to be the elastic skeletal storage coefficient, S_{ke}, as

indicated by equation 2. When water levels begin to recover, the lower limbs of the curve sometimes form hysteresis loops. Riley (1969) attributes these loops to hydrodynamic lag in release of water from fine-grained beds and states that approximately zero excess pore pressure occurs at the point at which the recompression part of the curve crosses the previous expansion part of the curve. The slope of the line fit to pass through or near these points for several cycles will reflect the inelastic storage properties as indicated in equation 4.

Extensometer records from central and southern Arizona seldom are similar to those presented by Riley (1969). Problems encountered in this study include lack of cyclical water-level drawdown and recovery periods, insufficient water-level change to force significant compaction, an insufficient knowledge of the water levels at different depths, delayed effects from previous water-level fluctuations on aquitards, and factors affecting the way instruments record compaction. Only the depth penetrated by the extensometer pipe is monitored by the compaction recorder. Compaction beneath the pipe is not recorded or compared to water-level fluctuations. The depth to water, as recorded by the water-level recorder, is a composite of the total area penetrated by the screened intervals of the casing, and individual layers are not monitored. Because many of the extensometer sites are former water-supply wells or test holes with large contributing aquifers, head changes represent a combination of water-table and confined aquifer conditions.

An inverse correlation between water-level fluctuation and compaction is evident in many of the sites described in this report. Delayed responses to stresses created from previous water-level declines are to be expected from aquitards. The hydraulic conductivity of a deposit controls the rate of compaction. An increase in hydraulic conductivity increases the compaction rate. Specific storage affects the ultimate amount of compaction that can occur. An increase in specific storage will increase the total compaction that will ultimately occur in response to an increased stress (Epstein, 1987). A clay lens with a low hydraulic conductivity will compact over a longer time period than a coarse-grained sediment and will have a greater amount of compaction. As a result,

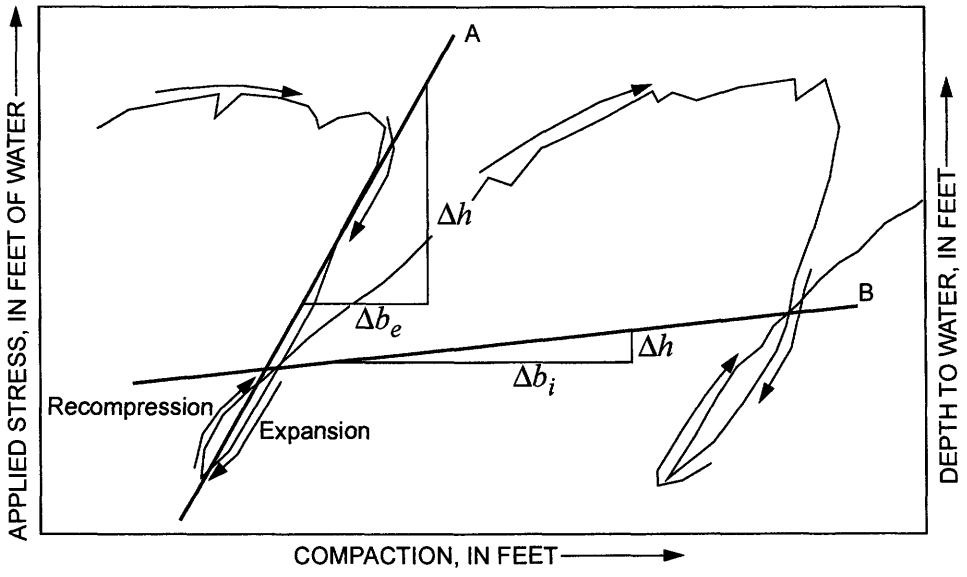

Figure 4. Relation between water-level change and compaction for a hypothetical extensometer. Response shown is typical for extensometers in agricultural areas with annual cycles of drawdown from ground-water pumping followed by a period of recovery. Line A represents elastic recovery, and line B represents long-term inelastic compaction.

water levels may recover; however, compaction will continue.

Often in the calculations of specific storage, there are apparent changes in elastic and inelastic trends. These changes may not be entirely a result of change in material properties. These apparent changes may be partly or entirely due to other factors such as change in pore pressures in an interval not monitored by a piezometer that is used in generating a stress-strain diagram and equipment changes that may introduce a more sensitive compaction or water-level record.

Regardless of these factors, parts of extensometer records representing elastic and inelastic responses can be identified and analyzed as was done by Hanson (1989). Continued data collection into periods with greater water-level and compaction responses will improve the usefulness of these records in establishing relations between water-level change and compaction.

AQUIFER COMPACTION AND WATER LEVELS IN THE ELOY AND STANFIELD BASINS

In the lower Santa Cruz Basin, which encompasses the Eloy and Stanfield Basins (fig. 1), ground-water withdrawals have decreased from 1,400,000 acre-ft in 1953, to 890,000 acre-ft in 1970, and further to 417,000 acre-ft in 1990 (Anning and Duet, 1994). Overall, from 1990 to 1996, ground-water withdrawals have remained fairly constant or have slightly increased (Arizona Department of Water Resources, unpublished data, 1990–95). By 1977, about 655 mi^2 of land area had subsided around Eloy, and the maximum subsidence was 12.5 ft. About 425 mi^2 had subsided around Stanfield, and the maximum subsidence was 11.8 ft (Laney and others, 1978). In addition, areas of significant subsidence corresponded with areas of significant water-level decline (Schumann and Poland, 1970).

In the early 1980's, the water level at the Eloy well (D-07-09)31bba began to recover. From 1980 to 1994, decreased pumping caused by less irrigation and greater use of surface water to supplement ground water, resulted in as much as 150 ft of recovery at the Eloy well. From January 1994 to January 1997, the water level at the Eloy well declined 10 ft. From 1987 through 1996, 0.085 ft of compaction was recorded at the Eloy well (table 1). Data for wells in the Eloy and Stanfield Basins are shown in figures 5–14 in Section A of the section entitled "Basic Data" at the back of this report.

Wells TA-10 and SG-14c are about 4.6 mi apart; however, compaction rates at the two wells are not the same. Compaction at well TA-10 was 0.22 ft, and the compaction rate per foot of monitored thickness was more than five times that of well SG-14c. Water levels recovered 16 ft at well TA-10 and 19 ft at well SG-14c during the period of record. Both wells fully penetrate the upper hydrostratigraphic unit. Sediments at well TA-10 may be more compressible than those of SG-14c, although measurement error may occur at well SG-14c because of friction between the pipe and the well casing. Data at well TA-10 show a compaction rate of 0.053 ft/yr from the beginning of record until mid-1992 when the rate decreased to 0.023 ft/yr. This decrease probably is a result of sediments reacting to recovering water levels in the area.

Three sites in the Eloy and Stanfield Basins show an inverse relation between compaction of sediments and water-level fluctuations (table 2). Wells JU-1, JU-2, and TA-10 had recovering water levels and increasing compaction that probably was due to continued dewatering of aquitards caused by delayed responses to stresses from previously lower ground-water levels in the area. The data for JU-1, JU-2, and TA-10, however, were inconclusive for calculating elastic storage coefficients.

The finer-grained sediments of the Eloy and Stanfield Basins are more compressible than those of the Upper Santa Cruz Basin and more likely to compact in response to pumping. Four of the five highest rates of compaction per foot of monitored thickness are in the Eloy and Stanfield Basins.

AQUIFER COMPACTION AND WATER LEVELS IN AVRA VALLEY

In 1935, ground-water withdrawals in Avra Valley were 1,000 acre-ft; in 1960, 140,000 acre-ft; and in 1970, 157,000 acre-ft. Withdrawals declined to 83,000 acre-ft in 1980 and 38,000 acre-ft in

Table 1. Summary of data from borehole extensometers, south-central Arizona, 1980–96

Well name	Years of record	Date of record	Depth of extensometer, in feet	Depth to water, in feet				Saturated thickness, in feet[1]	Compaction of aquifer, in feet
				Starting	Ending	Maximum	Minimum		
Eloy and Stanfield Basins									
Eloy[2]	8	1989–96	828	312	261	408	245	516	0.085
JU-1	8	1989–96	684	199	182	199	181	485	.094
JU-2	7.5	1989–96	996	671	653	671	648	325	.179
TA-10	7.5	1989–96	1,630	305	288	306	285	1,325	.220
SG-14C	7	1990–96	1,150	267	248	289	235	873	.032
Avra Valley									
AF-14[3]	12.5	1984–96	1,009	286	268	301	266	723	.027
AF-17	11.5	1985–96	1,002	350	338	350	337	652	.120
AV-25[3]	12.5	1984–96	790	338	373	373	335	452	.082
TA-13	7.5	1989–96	1,400	244	246	246	240	1,156	.001
TA-32	8	1989–96	990	352	347	354	347	638	.045
TA-33	8	1989–96	790	358	360	361	358	432	.009
TA-44	8	1989–96	1,400	400	413	413	400	1,000	.012
Upper Santa Cruz Basin									
B-76[3]	16.5	1980–96	871	197	210	211	192	674	.168
C-45	17	1980–96	475	253	300	301	253	222	.197
D-61	17	1980–96	1,025	270	308	308	270	755	.140
SC-17[3]	17	1980–96	805	118	116	121	106	687	.148
SC-30[3]	16.5	1980–96	960	200	211	225	180	760	.160
WR-52[3]	14	1982–96	808	177	230	230	175	631	.080
WR-53	13	1983–96	1,030	144	148	148	143	886	.025

[1]Saturated thickness was calculated by subtracting the water level at the beginning of record from the depth of the extensometer.

[2]For previously estimated aquifer-system properties, see Epstein (1987).

[3]For previously estimated aquifer-system properties, see Hanson (1989).

1990 (Anning and Duet, 1994). From 1940 through 1984, ground-water pumping resulted in widespread water-level declines that ranged from 50 to 150 ft (Cuff and Anderson, 1987). Declines were accompanied by localized compaction of the aquifer, subsidence of the land surface, and formation of earth fissures (Anderson, 1987b). Between 1950 and 1985, land subsidence ranged from 0 to 1 ft (Anning and Duet, 1994).

Most of the extensometers continued to record compaction through 1996. From 1989 through 1996, the greatest amount of compaction (0.12 ft) and a water-level recovery (about 12 ft) occurred at well AF-17 (table 1; figs. 15–33 in Section B of the section entitled "Basic Data" at the back of the report).

Data from wells AF-17 and TA-32 showed an inverse stress-strain relation (table 2). Although water levels have recovered at both sites, subsidence has continued. Instruments at wells AF-14 and AF-17, which are 4.6 mi apart, recorded different compaction rates. Both wells are drilled to the same depth and water-level recoveries were similar at the two wells. Data from well AF-17 shows five times the compaction rate per unit of monitored thickness than that of well AF-14. At well AF-17, the inelastic aquifer storage coefficient changed (fig. 18). From 1985 to late 1992, the elastic aquifer-storage coefficient was determined to be 2.6×10^{-3} from the slope of line AB (fig. 18). After 1992, a coefficient of 1.7×10^{-3} was found from the slope of line A'B'. In early 1994, water levels at well AV-25 began to drop rapidly even

Table 2. Compaction rate and elastic- and inelastic-storage coefficients at borehole extensometers in selected wells, south-central Arizona

[Dashes indicate no change]

Well name	Compaction rate, in feet x 10^{-3} per year	Compaction per unit of monitored thickness of aquifer system, in feet per year per foot x 10^{-6}			Elastic-storage coefficient			Elastic specific-storage coefficient x 10^{-6}	Inelastic-storage coefficient			Inelastic specific-storage coefficient x 10^{-6}
		Rate	Early[1]	Late[1]	x 10^{-3}	x 10^{-3} Early[1]	x 10^{-3} Late[1]		x 10^{-3}	x 10^{-3} Early[1]	x 10^{-3} Late[1]	
Eloy and Stanfield Basins												
Eloy	10.6	21	---	---	1.1	---	---	2.1	(2)	---	---	(2)
JU-1	11.8	24	---	---	(2)	---	---	(2)	[3]-1	---	---	[3]-1
JU-2[1]	23.9	74	---	---	(2)	---	---	(2)	[3]-1	[3]-1	(2)	[3]-1
TA-10[1]	29.3	22	40	17	(2)	---	---	(2)	[3]-1	---	---	[3]-1
SG-14C	4.6	5	---	---	1.1	---	---	1.3	(2)	---	---	(2)
Avra Valley												
AF-14	2.2	3	---	---	1.8	---	---	2.5	(2)	---	---	0
AF-17[1]	10.4	16	---	---	2.2	2.6	1.7	3.3	[3]-1	---	---	[3]-1
AV-25[1]	6.6	15	---	---	0	---	---	(2)	2.7	4.3	1.1	6.1
TA-13	.1	0	---	---	5.0	---	---	4.3	(2)	---	---	(2)
TA-32	5.6	9	---	---	(2)	---	---	(2)	[3]-1	---	---	[3]-1
TA-33	1.1	3	---	---	(2)	---	---	(2)	1.7	---	---	3.9
TA-44	1.5	2	0	[4]3	(2)	---	---	(2)	1.5	---	---	---
Upper Santa Cruz Basin												
B-76	10.2	15	---	---	1.4	---	---	2.1	12.0	---	---	17.8
C-45	11.6	52	---	---	(2)	---	---	(2)	4.2	---	---	19.8
D-61[1]	8.2	11	---	---	(2)	---	---	(2)	4.4	2.7	6.1	5.9
SC-17[1]	8.7	13	2.6	10	4.1	---	---	6.0	[3]-1	---	---	[3]-1
SC-30	9.7	13	---	---	1.6	---	---	2.1	14.0	---	---	18.2
WR-52	5.7	9	---	---	(2)	---	---	(2)	1.6	---	---	2.6
WR-53	1.9	2	---	---	(2)	---	---	(2)	6.7	(2)	---	7.6

[1]Early and late values were calculated for stress-strain relations that indicated two distinctly different trends with time. Specific periods are shown on the stress-strain graphs.

[2]Insufficient data.

[3]Negative value indicates an inverse stress-strain relation.

[4]Change is due to equipment sensitivity.

though the compaction rate generally remained constant. More data are needed to accurately calculate a change in elastic storage properties at well AV-25. Data from well TA-44 showed a change in compaction rate from 0 ft/yr to 0.003 ft/yr in late 1992. This change in rate of compaction probably is a result of a change in instrumentation to a more sensitive recorder that was installed in 1992. Elastic-storage coefficients and specific-storage coefficients for wells TA-32, TA-33, and TA-44 could not be calculated because of poorly defined elastic responses.

Retirement of farmlands and the inception of the Central Arizona Project resulted in decreased pumping and, in some instances, water-level recoveries. From 1990 to 1996, withdrawals slightly increased because of increased municipal consumption and slight increases in irrigation (Arizona Department of Water Resources, unpublished data, 1990–95). Regionally, water levels are constant in Avra Valley. From 1984 to 1996, three stations recorded recoveries, and three stations recorded declines. Large changes in water levels did not occur except at well AV-25. Since 1984, the water level at well AV-25 has declined 35 ft; about 25 ft of decline occurred from 1994 through 1996.

AQUIFER COMPACTION AND WATER LEVELS IN THE UPPER SANTA CRUZ BASIN

Between 1940 and 1985, water levels declined from 100 to more than 150 ft throughout most of north-central metropolitan Tucson and along the Santa Cruz River northeast of Black Mountain (Babcock and others, 1986). Other effects of pumping include a shift of natural ground-water flow paths toward pumping centers, increased vertical hydraulic gradients, development of perched ground water above the regional aquifer in areas underlain by shallow fine-grained beds, decreased transmissivity resulting from dewatering of permeable sediments of Quaternary age, and increased vertical effective stress resulting in compaction of the aquifer system (Hanson and Benedict, 1994). Ground-water withdrawals were 35,000 acre-ft in 1920, to 62,000 acre-ft in 1940, and 240,000 acre-ft in 1970.

From 1970 to 1996, ground-water withdrawals fluctuated slightly (Anning and Duet, 1994; Arizona Department of Water Resources, unpublished data, 1990–95). Unlike extensometer sites in the Eloy and Stanfield Basins and Avra Valley, the sites in the Upper Santa Cruz Basin are continuing to record water-level declines. From 1980 through 1996, declines ranged from near 0 at well SC-17 to nearly 50 ft at wells C-45, SC-30, and WR-52 (figs. 32–52 in section C of the Basic Data section). The Central Arizona Project has not had a significant influence on ground-water pumping in the Tucson area, which is reflected by the trend in withdrawal rates and the subsequent water-level declines. Between 1950 and 1980, measured subsidence ranged from 0 to 0.5 ft (Anderson, 1989).

In the Upper Santa Cruz Basin, most extensometers continued to record compaction through 1996. The least compaction was recorded at well WR-53 (near 0 ft; table 1), and the most compaction was recorded at well C-45 (about 0.20 ft; table 1). Between 1980 and 1996, most sites recorded about 0.15 ft of compaction.

Data from well SC-17 had an inverse stress/strain relation (table 2). Although water levels have increased slightly, compaction has continued. This relation, as described for many of the sites in the Eloy and Stanfield Basins, may be due to continued dewatering of aquitards from stresses created from previous water-level declines. Compaction at well SC-17 also varied diurnally, which probably was due to temperature effects on the pipe from the blowing and sucking actions of the well. Wells C-45 and D-61, which are about 0.5 mi apart, fully penetrate the Fort Lowell Formation and partially penetrate the upper Tinaja beds. Since 1980, instruments at well C-45 recorded 0.197 ft of compaction, and instruments at well D-61 recorded 0.140 ft of compaction although well D-61 penetrates about twice the depth of well C-45 (table 1). Instruments at well C-45 recorded one of the highest rates of compaction per foot of monitored thickness in the network and almost four times the rate of well D-61 (table 2). On the basis of this data, sediments at well C-45 are three to four times more compressible than those at well D-61. Data from well D-61 show a change in inelastic storage properties to a higher rate of compaction per unit

of monitored thickness. Elastic storage and specific storage were not calculated for wells C-45 (fig. 35), D-61 (fig. 38), WR-52 (fig. 47), and WR-53 (fig. 50) because of poorly defined elastic response.

SUMMARY

Since the 1940's, ground-water declines of several feet per year have resulted in measurable land subsidence from aquifer compaction in the Eloy and Stanfield Basins, Avra Valley, and Upper Santa Cruz Basin. Historic overdrafts in the Eloy area of the Eloy Basin are responsible for continued dewatering of aquifers and subsequent land subsidence even with recent water-level recoveries of more than 100 ft in some areas. Water-level declines in Avra Valley and the Upper Santa Cruz Basin are less than in the Eloy and Stanfield Basins; however, measurable amounts of aquifer compaction have been recorded at most stations.

In 1979, the USGS, in cooperation with the City of Tucson, began to study aquifer compaction in the Upper Santa Cruz Basin. In 1983, the study was expanded to include sites in Avra Valley. In 1989, with the cooperation of the Arizona Department of Water Resources, four extensometers in the Eloy Basin and one site in the Stanfield Basin were added to the network. Data have been collected continuously since the activation of each well. As of 1998, the USGS is monitoring 19 extensometer sites in wells in south-central Arizona. At each site, continuous water levels and compaction data are recorded.

In the Eloy and Stanfield Basins, water-level declines continued at rates of several feet per year from the 1940's until the early 1980's. With the advent of the Central Arizona Project and subsequent decreased pumping, water levels began to recover. Since the early 1980's, recoveries of as much as 100 ft were recorded. The effects of historic pumping on the aquifer are still evident. The higher clay content of the sediments in Eloy and Stanfield Basins and the continued dewatering of these aquitards caused about 15 ft of subsidence from overdrafts and caused four of the five highest rates of compaction in the monitoring network.

In Avra Valley, water levels in well AV-25 declined 30 ft during the period of record, of which 17 ft occurred from 1994 through 1996. Water levels at other sites, such as well AF-17, are recovering. Even with the significant water-level recovery, 0.12 ft of compaction occurred at well AF-17 from 1985 through 1996.

In the Upper Santa Cruz Basin, overdrafts resulted in water-level declines of as much as 50 ft from 1980 through 1996. Data for well C-45, in central Tucson, show a water-level decline of 47 ft and the second highest rate of compaction per foot of monitored thickness in the network since 1980. Steady or increased rates of pumping has resulted in steadily declining water levels and increasing compaction. The rapid population growth of Tucson is increasing demand on the ground-water supply. Although alternative water sources are being studied, overdraft continues. As in the Eloy area, even if alternate sources of water are found, the consequences of overdrafts may be long lasting in spite of water-level recoveries.

SELECTED REFERENCES

Allen, T.J., 1981, The subsurface stratigraphy of the northern Avra Valley, Pima County, Arizona: Akron, Ohio, Kent State University, unpublished master's thesis, 71 p.

Anderson, S.R., 1987a, Cenozoic stratigraphy and geologic history of the Tucson Basin, Pima County, Arizona: U.S. Geological Survey Water-Resources Investigations Report 87–4190, 20 p.

___ 1987b, Potential for aquifer compaction, land subsidence, and earth fissures in Avra Valley, Pima County, Arizona: U.S. Geological Survey Hydrologic Atlas HA–718, 3 sheets.

___ 1989, Potential for aquifer compaction, land subsidence, and earth fissures in the Tucson Basin, Pima County, Arizona: U.S. Geological Survey Hydrologic Investigations Atlas HA–713, 3 sheets.

Anderson, T.W., 1972, Electrical-analog analysis of the hydrologic system, Tucson Basin, southeastern Arizona: U.S. Geological Survey Water-Supply Paper 1939–C, 34 p.

Anning, D.W., and Duet, N.R., 1994, Summary of ground-water conditions in Arizona, 1987–90: U.S. Geological Survey Open-File Report 94–476, 1 sheet.

Babcock, J.A., Cameron, J.A., and Heidenreich, L.K., 1986, Annual static water-level basic data report,

Tucson Basin and Avra Valley, Pima County, Arizona, 1985: City of Tucson, Tucson Water Planning Division report, 57 p.

Caito, T.J., and Sogge, R.L., 1982, Fissuring and subsidence in Avra Valley, Arizona: Tucson, Arizona, Desert Earth Engineering report prepared in cooperation with the City of Tucson and Pima County Department of Transportation, 69 p.

Carpenter, M.C., 1988, Land-surface deformation and water-level fluctuations near the Picacho earth fissure, south-central Arizona, 1980–84: U.S. Geological Survey Open-File Report 88–97, 24 p.

___1993, Earth-fissure movements associated with fluctuations in ground-water levels near the Picacho Mountains, south-central Arizona, 1980–84: U.S. Geological Survey Professional Paper 497–H, 49 p.

Clifton, P.M., 1981, Statistical inverse modeling and geostatistical analysis of the Avra Valley aquifer: Tucson, Arizona, University of Arizona master's thesis, 190 p.

Cuff, M.K., and Anderson, S.R., 1987, Ground-water conditions in Avra Valley, Pima and Pinal Counties, Arizona: U.S. Geological Survey Water-Resources Investigations Report 87–4192, 3 sheets.

Davidson, E.S., 1973, Geohydrology and water resources of the Tucson Basin, Arizona: U.S. Geological Survey Water-Supply Paper 1939–E, 81 p.

Epstein, V.J., 1987, Hydrologic and geologic factors affecting land subsidence near Eloy, Arizona: U.S. Geological Survey Water-Resources Investigations Report 87–4143, 28 p.

Hanson, R.T., 1989, Aquifer-system compaction, Tucson Basin and Avra Valley, Arizona: U.S. Geological Survey Water-Resources Investigations Report 88–4172, 69 p.

Hanson, R.T., and Benedict, J.F., 1994, Simulation of ground-water flow and potential land subsidence, Upper Santa Cruz Basin, Arizona: U.S. Geological Survey Water-Resources Investigations Report 93–4196, 47 p.

Hanson, R.T., Anderson, S.R., and Pool, D.R., 1990, Simulation of ground-water flow and potential land subsidence, Avra Valley, Arizona: U.S. Geological Survey Water-Resources Investigations Report 90–4178, 41 p.

Hardt, W. F., and Cattany, R.E., 1965, Description and analysis of the geohydrologic system in western Pinal County, Arizona: U.S. Geological Survey open-file report, unnumbered, 92 p.

Helm, D.C., 1974, Evaluation of stress-dependent aquitard parameters by simulating observed compaction from known stress history: Berkeley, California, University of California doctoral dissertation, 175 p.

___ 1975, One-dimensional simulation of aquifer-system compaction near Pixley, California, 1, Constant parameters: American Geophysical Union, Water Resources Research, v. 11, no. 3, p. 465–478.

Holtzer, T.L., Davis, S.N., and Lofgren, B.E., 1979, Faulting caused by groundwater extraction in south-central Arizona: Journal of Geophysical Research, v. 84, no. B2, p. 603–612.

Jachens, R.C., and Holzer, T.L., 1979, Geophysical investigations of ground failure related to ground-water withdrawal—Picacho Basin, Arizona: Ground Water, v. 17, no. 6, p. 574–585.

Jorgenson, D.G., 1980, Relationships between basic soils-engineering equations and basic ground-water flow equations: U.S. Geological Survey Water-Supply Paper 2064, 40 p.

Laney, R.L., and Davidson, C.B., 1986, Aquifer-nomenclature guidelines: U.S. Geological Survey Open-File Report 86–534, 46 p.

Laney, R.L., and Pankratz, L.W., 1987, Investigations of land subsidence and earth fissures near the Salt-Gila aqueduct, Maricopa and Pinal Counties, Arizona—Altitudes of the tops of the consolidated rocks, surficial geology, and land subsidence in the Florence quadrangle: U.S. Geological Survey Map I–1892–A, 1 sheet.

Laney, R.L., Raymond, R.H., and Winikka, C.C., 1978, Maps showing water-level declines, land subsidence, and earth fissures in south-central Arizona: U.S. Geological Survey Water-Resources Investigations Report 78–83, 2 sheets.

Leake, S.A., 1991, Simulation of vertical compaction in models of regional ground-water flow, *in* Johnson, Ivan, ed., Land Subsidence—Proceedings of the Fourth International Symposium on Land Subsidence, May 1991, Houston, Texas: International Association of Hydrological Sciences Publication No. 200, p. 565–574.

Leake, S.A., and Hanson, R.T., 1987, Distribution and movement of trichloroethylene in ground water in the Tucson area, Arizona: U.S. Geological Survey Water-Resources Investigations Report 86–4313, 40 p.

Leake, S.A., and Prudic, D.E., 1987, New approaches to simulating aquifer-system compaction in models of regional ground-water flow [abs.]: American Geophysical Union Transactions, v. 68, no. 44, p. 1301.

___ 1991, Documentation of a computer program to simulate aquifer-system compaction using the modular finite-difference ground-water flow model: U.S. Geological Survey Techniques of

Water-Resources Investigations, book 6, chap. A2, 68 p. (Supersedes Open-File Report 88–482).

Mock, P.A., Travers, B.C., and Williams, C.K., 1985, Results of the Tucson Airport area remedial investigation—Phase I, Volume 2, Contaminant transport modeling: Phoenix, Arizona Department of Water Resources duplicated report, 106 p.

Moosburner, Otto, 1972, Analysis of the ground-water system by electrical-analog model, Avra Valley, Pima and Pinal Counties, Arizona: U.S. Geological Survey Hydrologic Investigations Atlas HA–215, 2 sheets.

Oppenheimer, J.M., and Sumner, J.S., 1980, Depth-to-bedrock map of southern Arizona: Tucson, University of Arizona, Laboratory of Geophysics, Department of Geosciences, 1 sheet.

Pierce, H.W., 1974, Thick evaporites in the Basin and Range Province, Arizona, *in* Fourth Symposium on Salt: Cleveland, Northern Ohio Geological Society, p. 47–55.

Platt, W.S., 1963, Land-surface subsidence in the Tucson area: Tucson, University of Arizona master's thesis, 38 p.

Poland, J.F., Lofgren, B.E., and Riley, F.S., 1972, Glossary of selected terms useful in studies of the mechanics of aquifer systems and land subsidence due to fluid withdrawal: U.S.Geological Survey Water Supply Paper 2025, 9 p.

Pool, D.R., 1984, Aquifer geology of alluvial basins of Arizona, *in* Replogle, J.A., and Renard, K.G., eds., Water today and tomorrow: American Society of Civil Engineers, Proceedings of the Irrigation and Drainage Specialty Conferences, Flagstaff, Arizona, July 24–26, 1984, p. 683–690.

Rampe, J.J., 1985, Results of the Tucson Airport area remedial investigations, Phase I, Volume 3, An evaluation of the potential sources of groundwater contamination near the Tucson International Airport, Tucson, Arizona: Phoenix, Arizona Department of Health Services duplicated report, 110 p.

Reeter, R.W., and Cady, C.V., 1982, Maps showing ground-water conditions in the Avra-Altar Valley area, Pima and Santa Cruz Counties, Arizona—1981: Phoenix, Arizona Department of Water Map Series Report Number 7, 2 sheets.

Riley, F.S., 1969, Analysis of borehole extensometer data from central California, *in* Tison, L.J., ed., Land Subsidence: International Association of Scientific Hydrology Publication No. 89, v. 2, p. 423–431.

___1984, Developments in borehole extensometry, *in* International Symposium on Land Subsidence, 3d, Venice, Italy, 1984, Proceedings: International Association of Hydrological Sciences Publication 151, p. 169–186.

Schmidt, K.D., 1985, Results of the Tucson Airport area remedial investigations, Phase I, Volume 1, Summary report: Tucson, Arizona Department of Health Services duplicate report, 114 p.

Schumann, H.H., and Genualdi, R.B., 1986, Land subsidence, earth fissures, and water-level change in southern Arizona: Tucson, Arizona Bureau of Geology and Mineral Technology, Geological Survey Branch, Map 23, 1 sheet.

Schumann, H.H., and Poland, J.F., 1970, Land subsidence, earth fissures, and groundwater withdrawal in south-central Arizona, U.S.A., *in* Tison, L.J., ed., Land Subsidence: International Association of Scientific Hydrology Publication 88, v. 1, p. 295–302.

Travers, B.C., and Mock, P.A., 1984, Groundwater modeling study of the upper Santa Cruz Basin and Avra Valley in Pima and Santa Cruz Counties, southeastern Arizona: Phoenix, Arizona Department of Water Resources, Hydrologic Division, 2 volumes, v.p.

Wallace, B.L.,Wrege, B.M., and Schumann, H.H., 1986, Geohydrologic data along the Salt-Gila aqueduct of the Central Arizona Project in Maricopa and Pinal Counties, Arizona: U.S. Geological Survey Open-File Report 86–236, 49 p.

Whallon, A.J., 1983, A geohydrological study of the regional ground-water system in Avra Valley, Pima and Pinal Counties, Arizona: Tucson, Arizona, University of Arizona master's thesis, 68 p.

White, N.D., Matlock, W.G., and Schwalen, H.C., 1966, An appraisal of the ground-water resources of Avra and Altar Valleys, Pima County, Arizona: Phoenix, Arizona State Land Department Water-Resources Report 25, 66 p.

Wilson, E.D., Moore, R.T., and Cooper, J.R., 1969, Geologic map of Arizona: Tucson, Arizona Bureau of Mines map, scale 1:500,000.

BASIC DATA

A. Hydrographs for Selected Well Sites, Eloy and Stanfield Basins

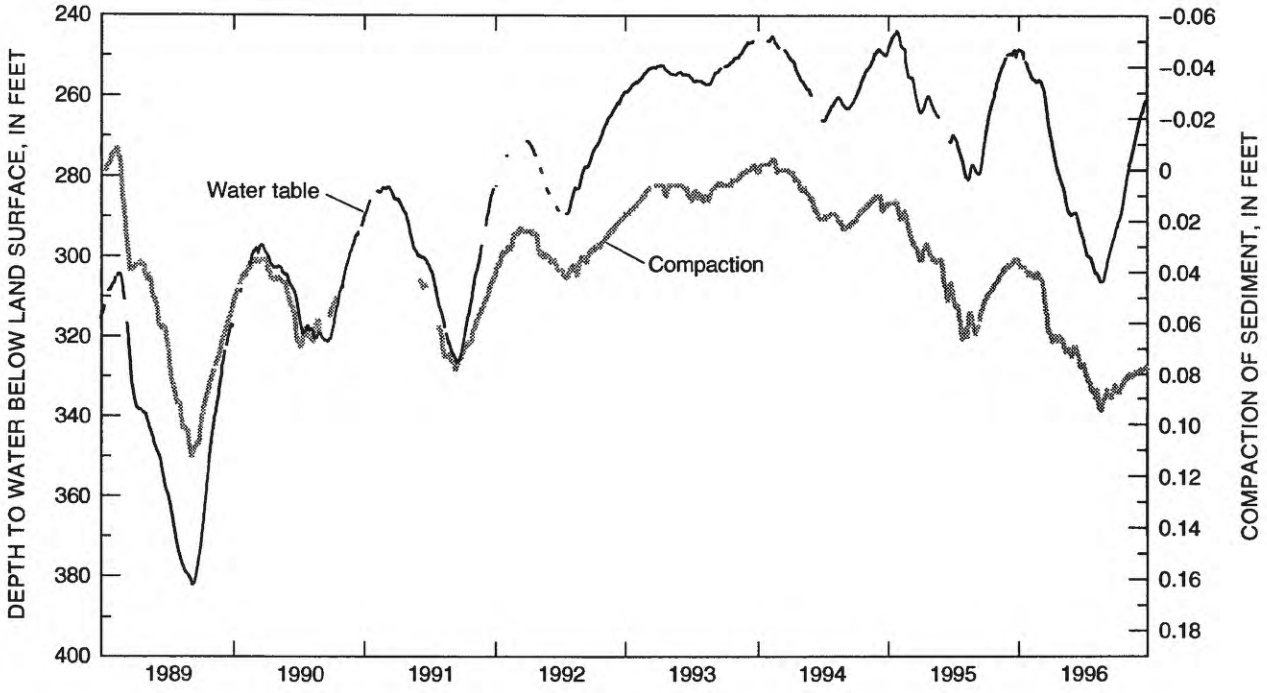

Figure 5. Depth to water and measured compaction in the Eloy well (D-07-08)31bba.

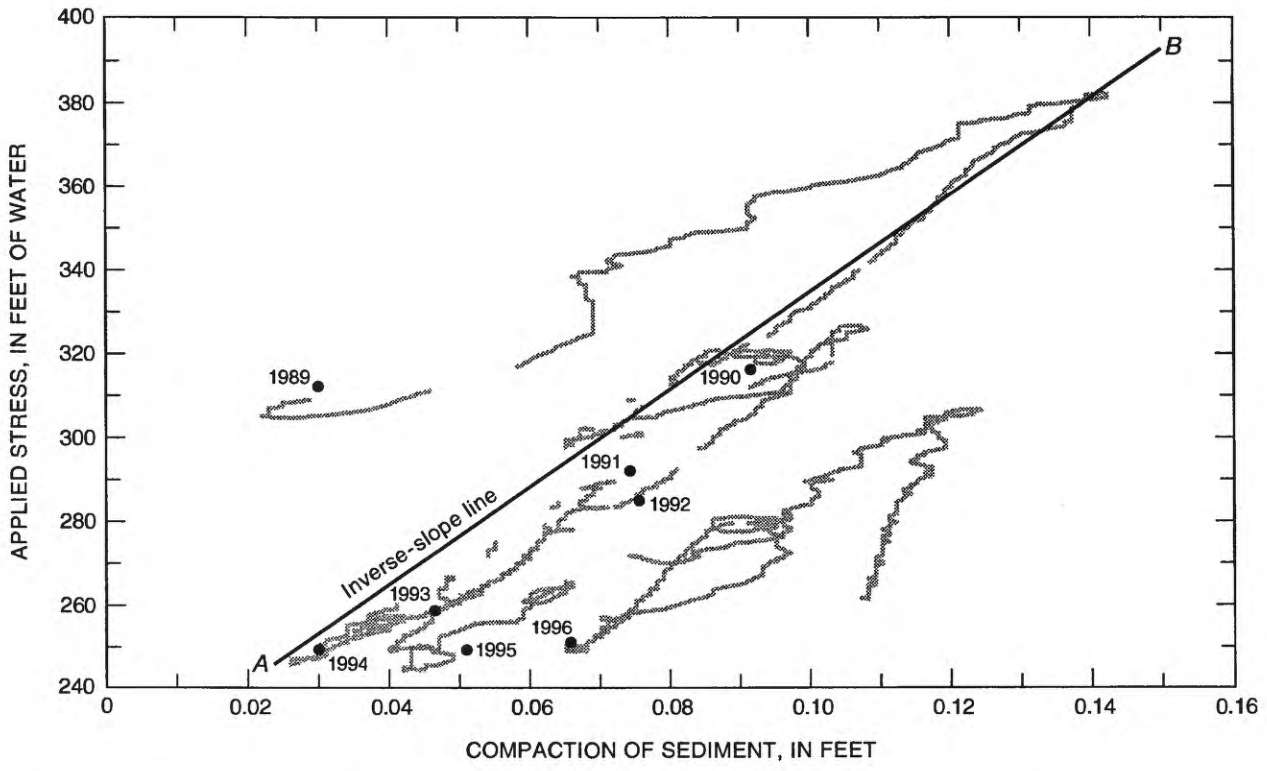

Figure 6. Compaction as a function of measured stress in the Eloy well (D-07-08)31bba.

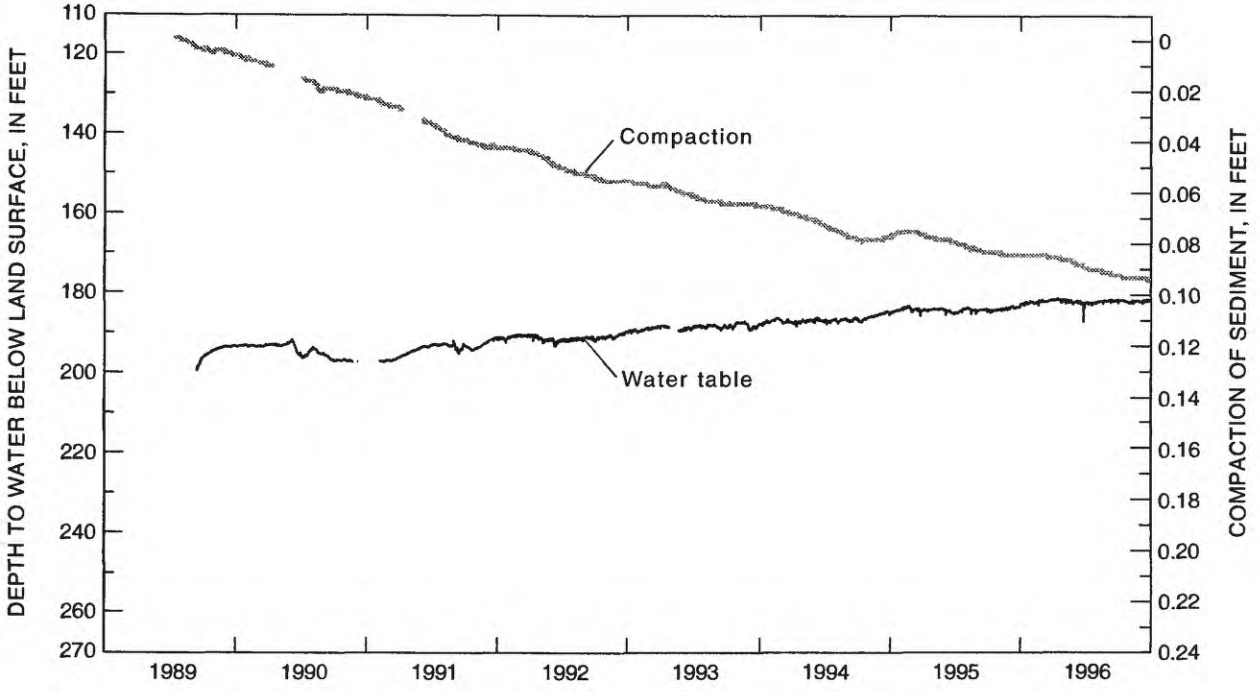

Figure 7. Depth to water and measured compaction in well JU-1 (D-08-06)04aaa.

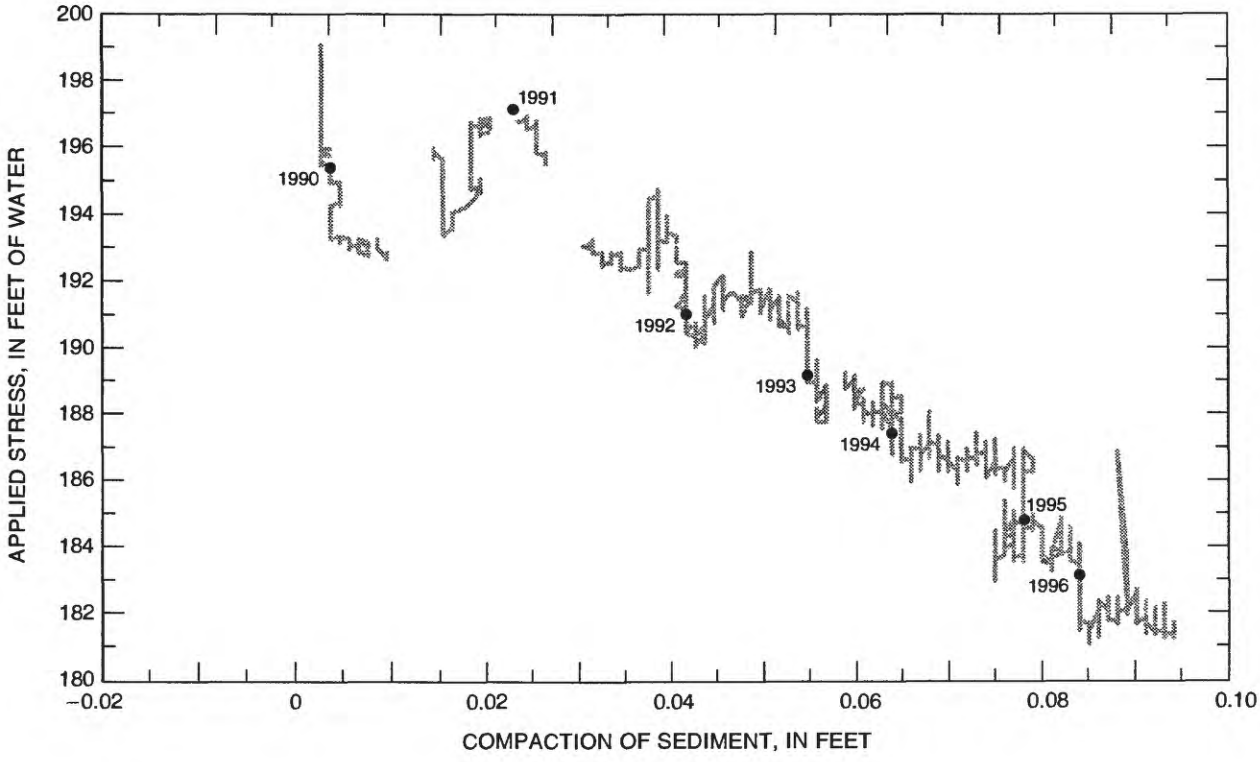

Figure 8. Compaction as a function of measured stress in well JU-1 (D-08-06)04aaa.

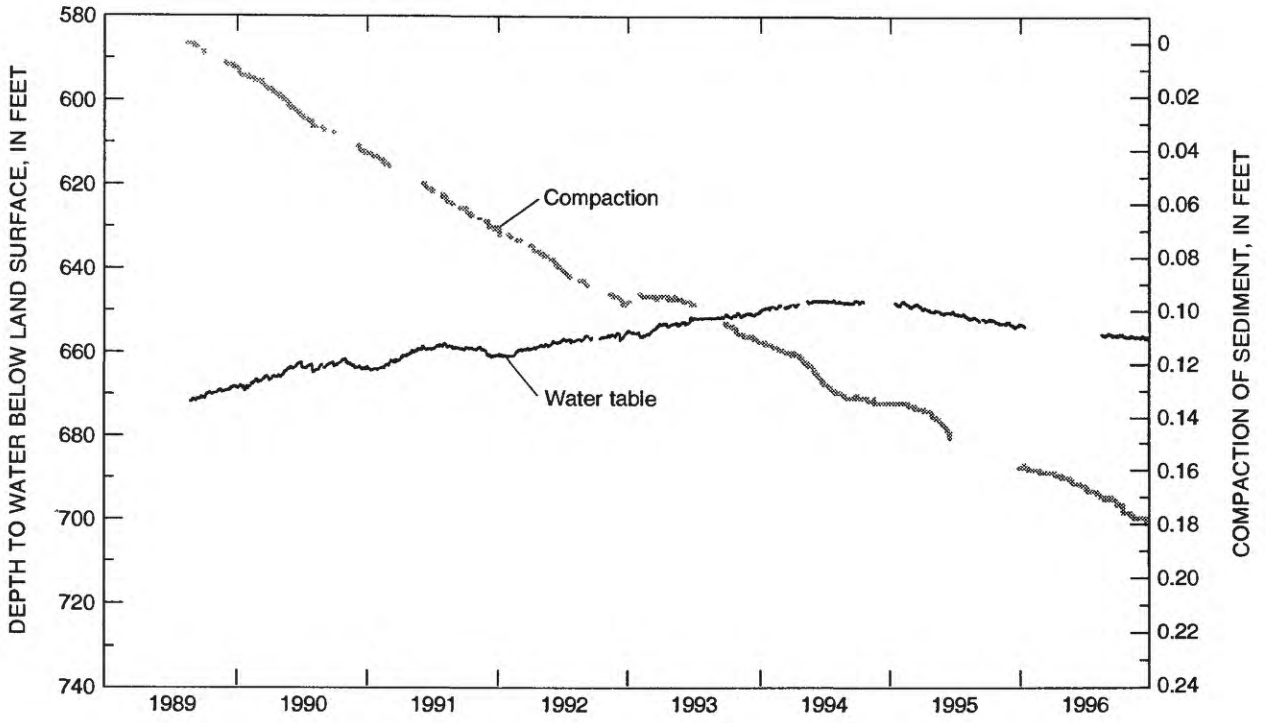

Figure 9. Depth to water and measured compaction in well JU-2 (D-07-04)16bcc.

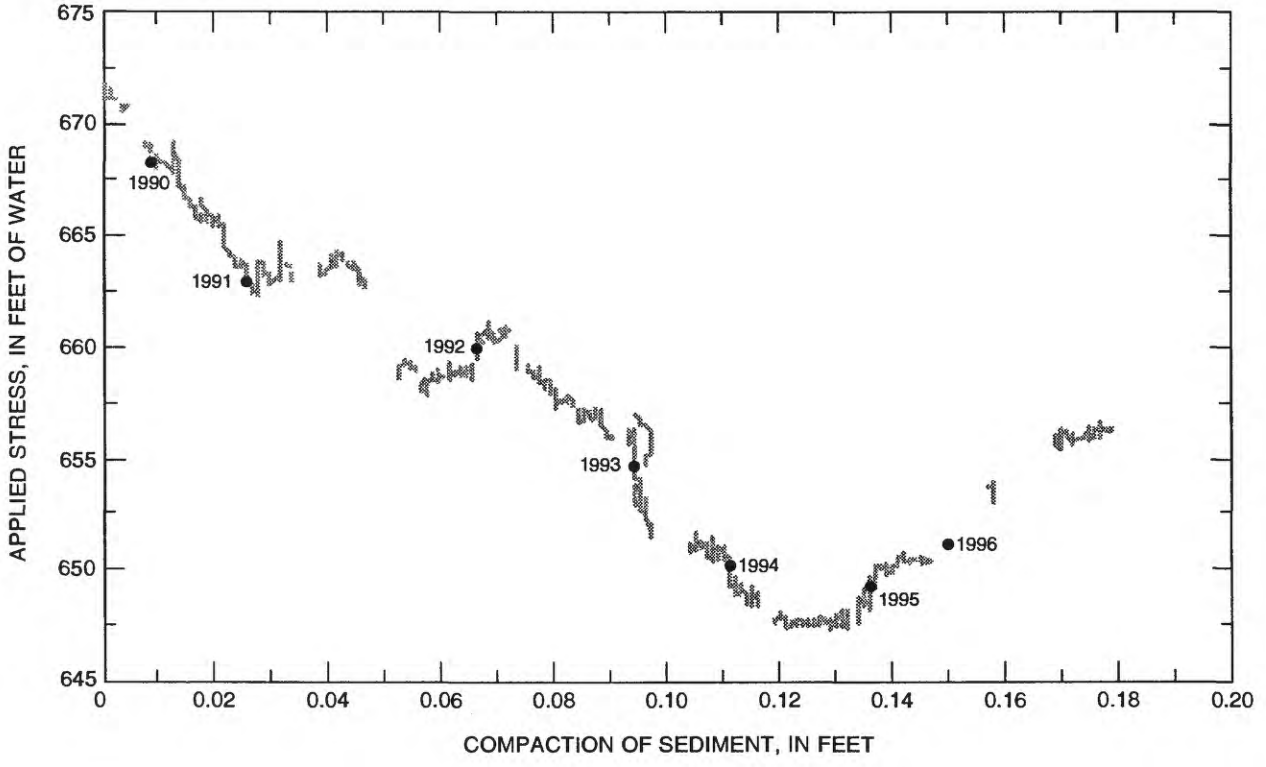

Figure 10. Compaction as a function of measured stress in well JU-2 (D-07-04)16bcc.

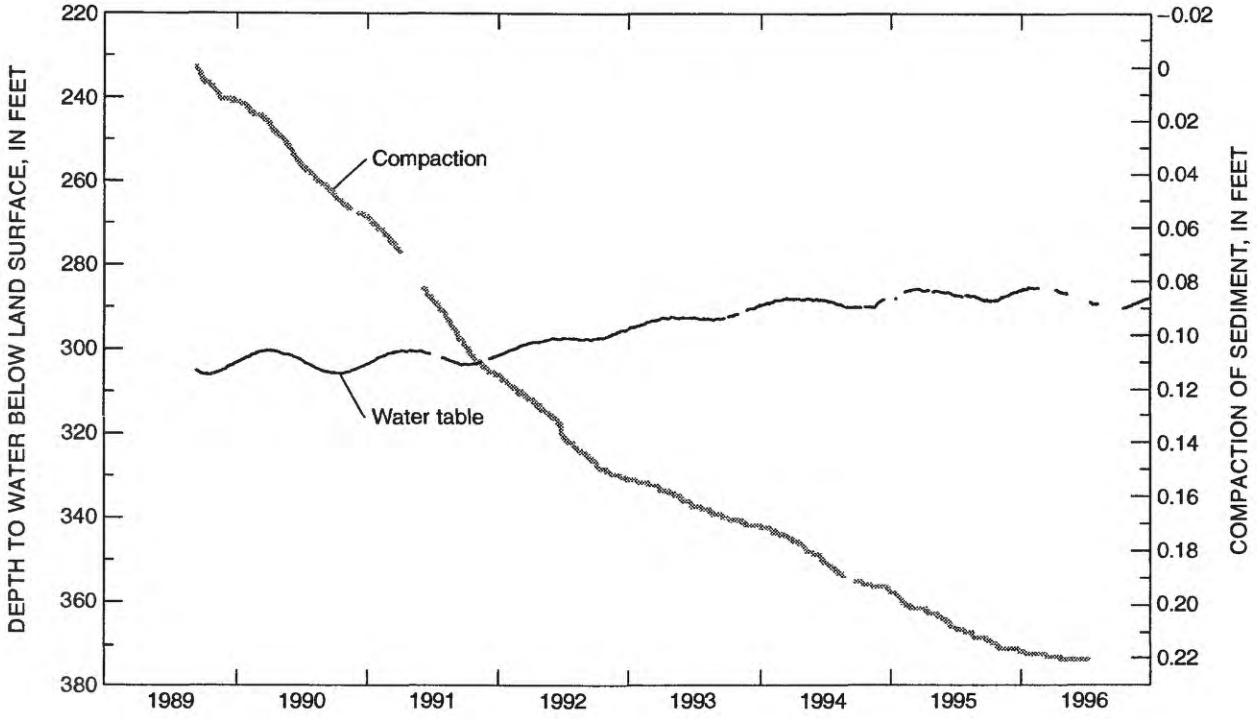

Figure 11. Depth to water and measured compaction in well TA-10 (D-07-09)16aca.

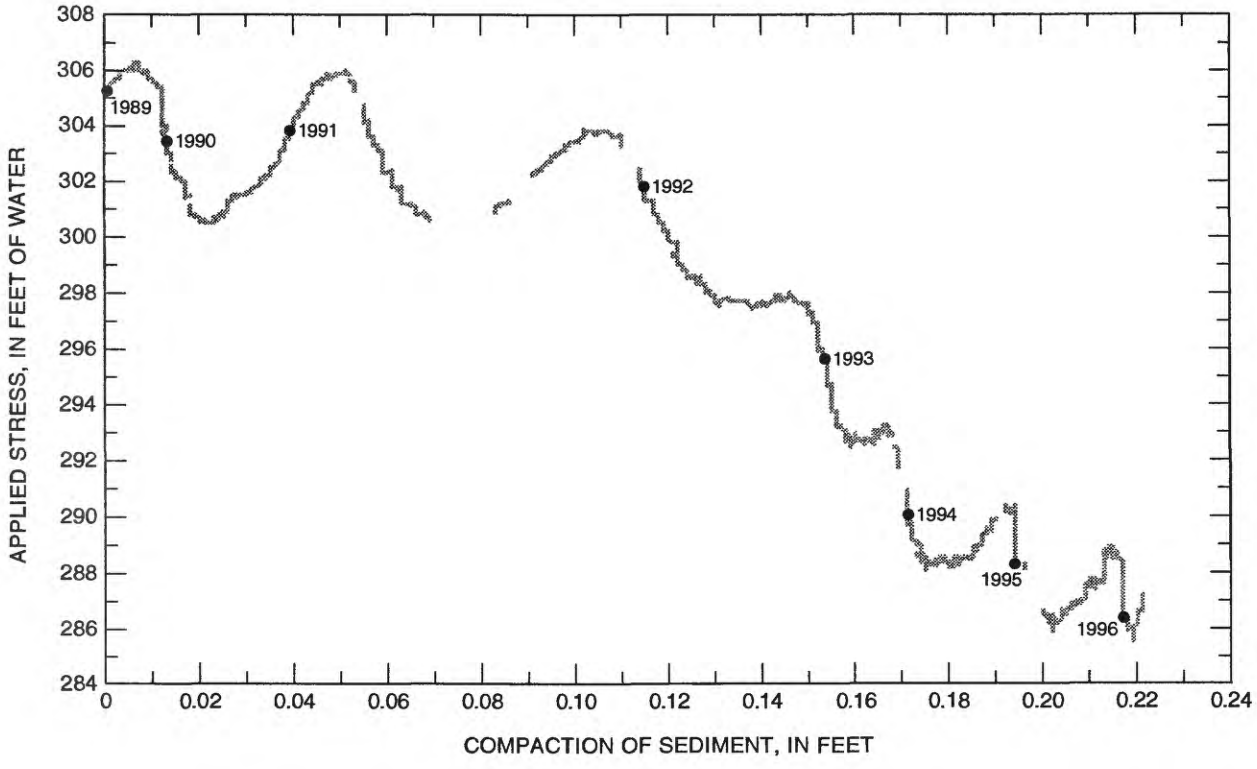

Figure 12. Compaction as a function of measured stress in well TA-10 (D-07-09)16aca.

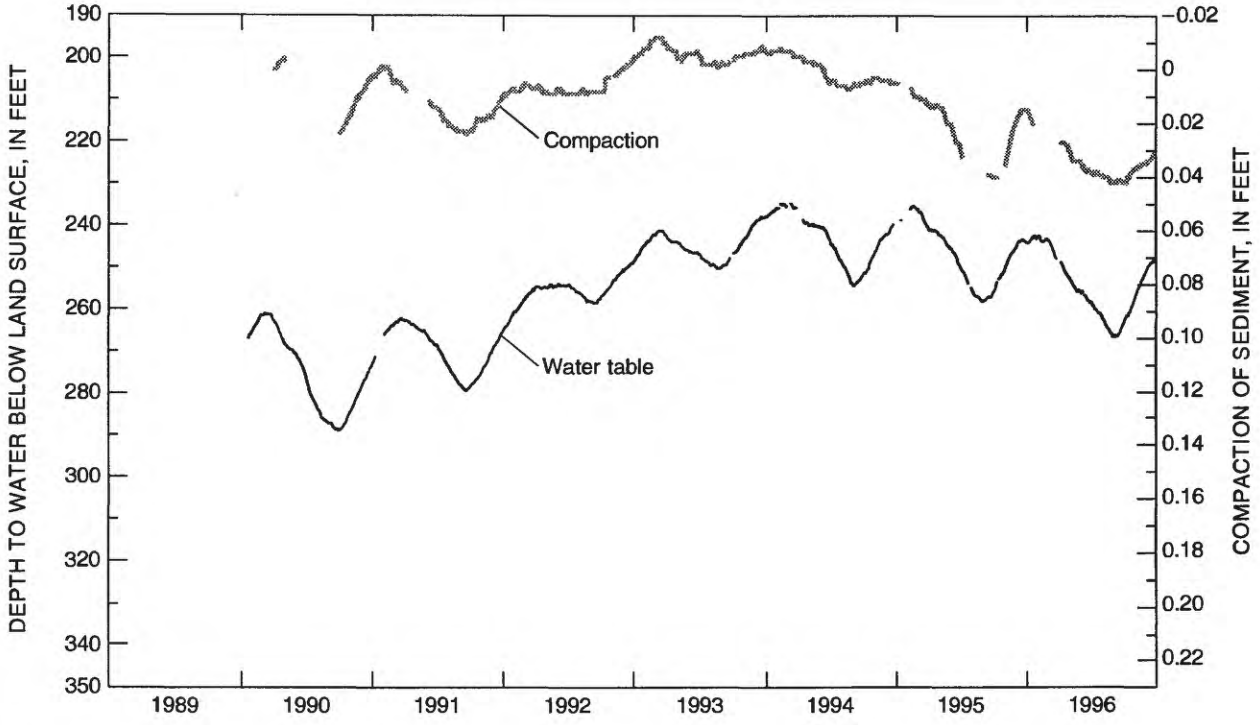

Figure 13. Depth to water and measured compaction in well SG-14C (D-06-09)29bba4.

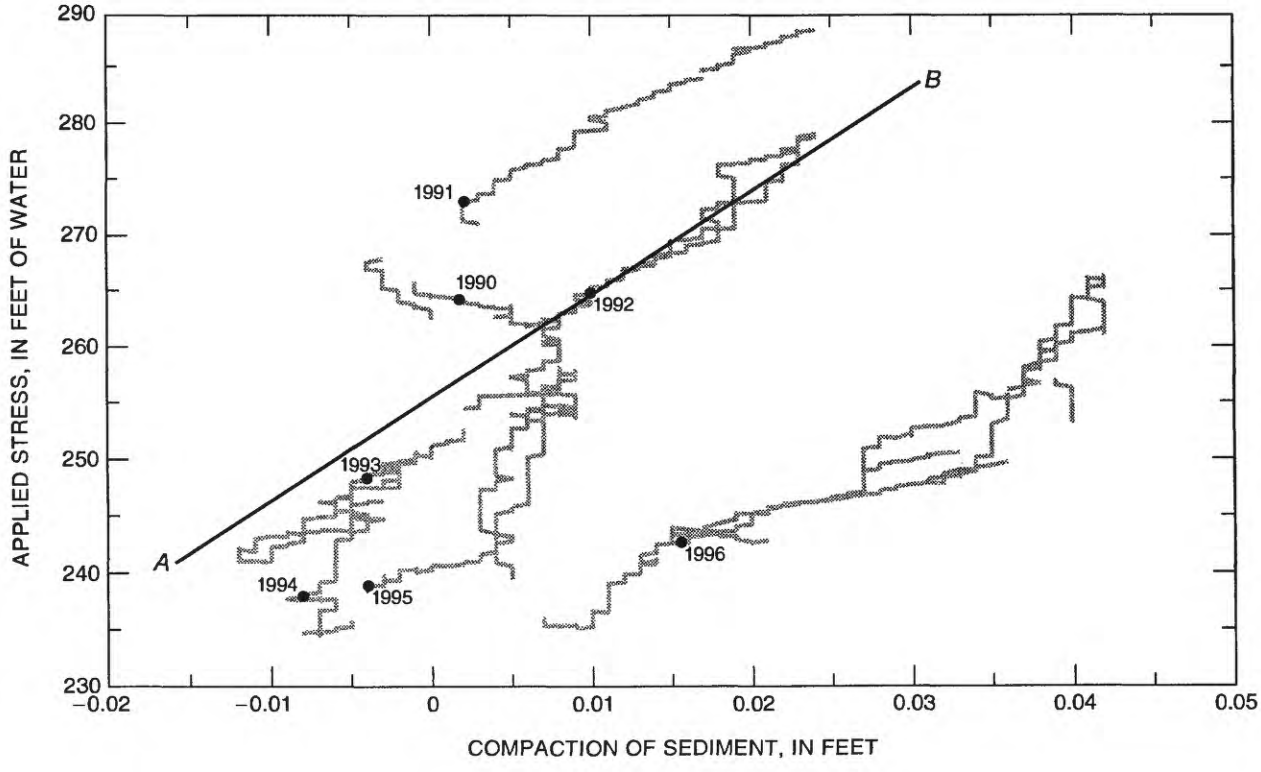

Figure 14. Compaction as a function of measured stress in well SG-14C (D-06-09)29bba4.

BASIC DATA

B. Hydrographs for Selected Well Sites, Avra Valley, Arizona

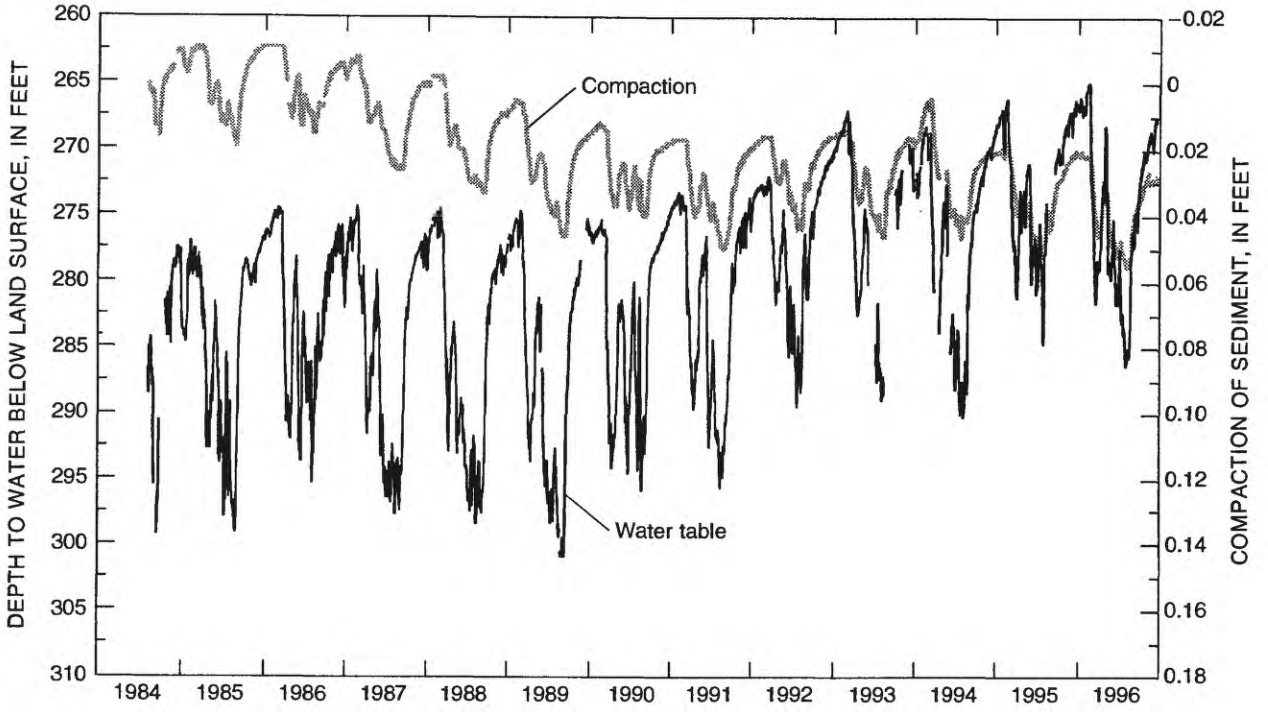

Figure 15. Depth to water and measured compaction in well AF-14 (D-12-10)12ccd1.

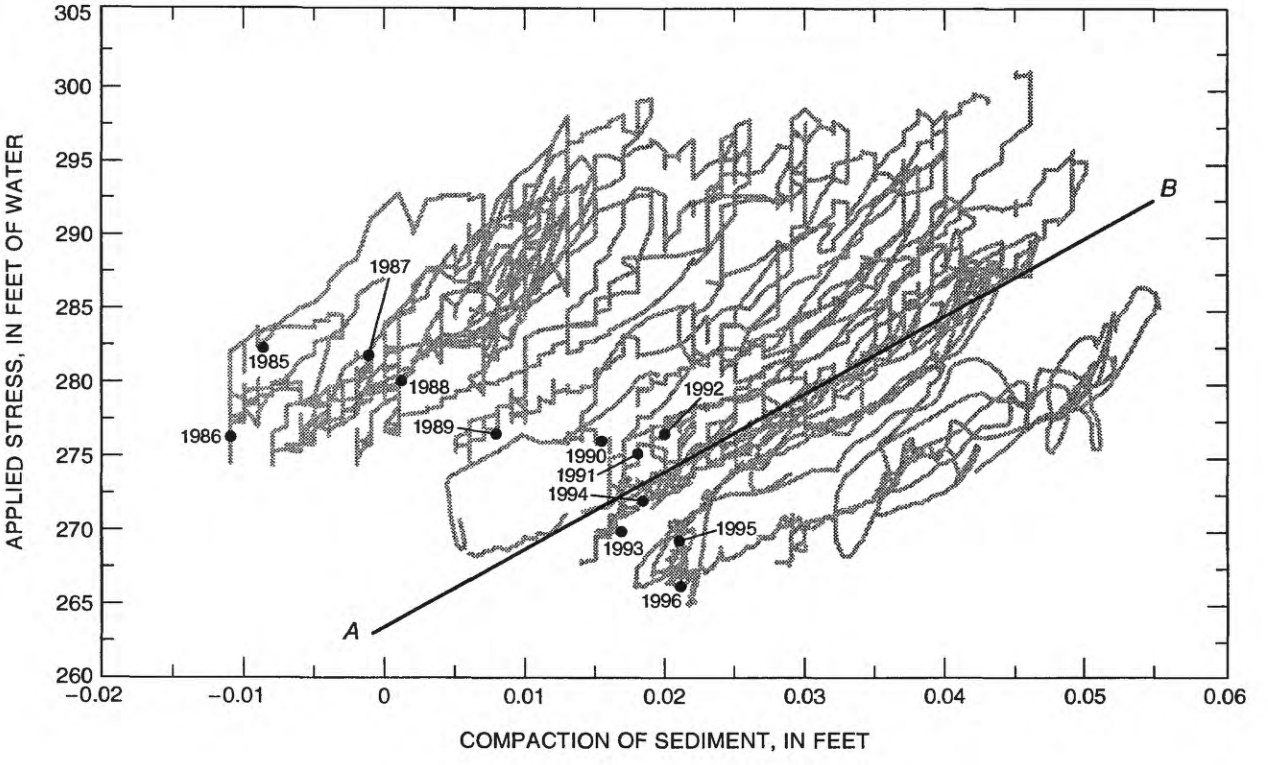

Figure 16. Compaction as a function of measured stress in well AF-14 (D-12-10)12ccd1.

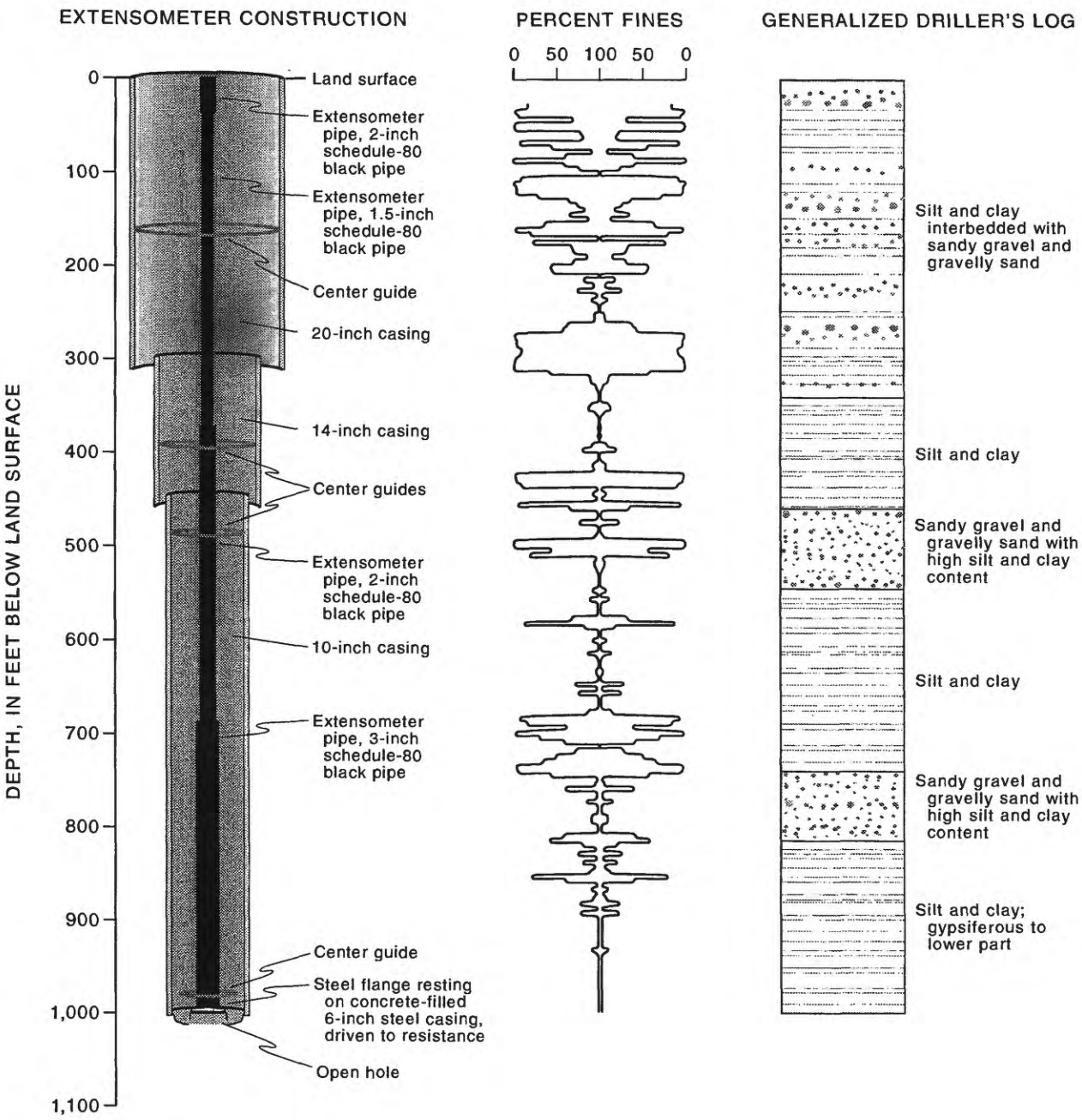

Figure 17. Extensometer construction, percent-fines distribution, and driller's log for well AF-14 (D-12-10)12ccd1.

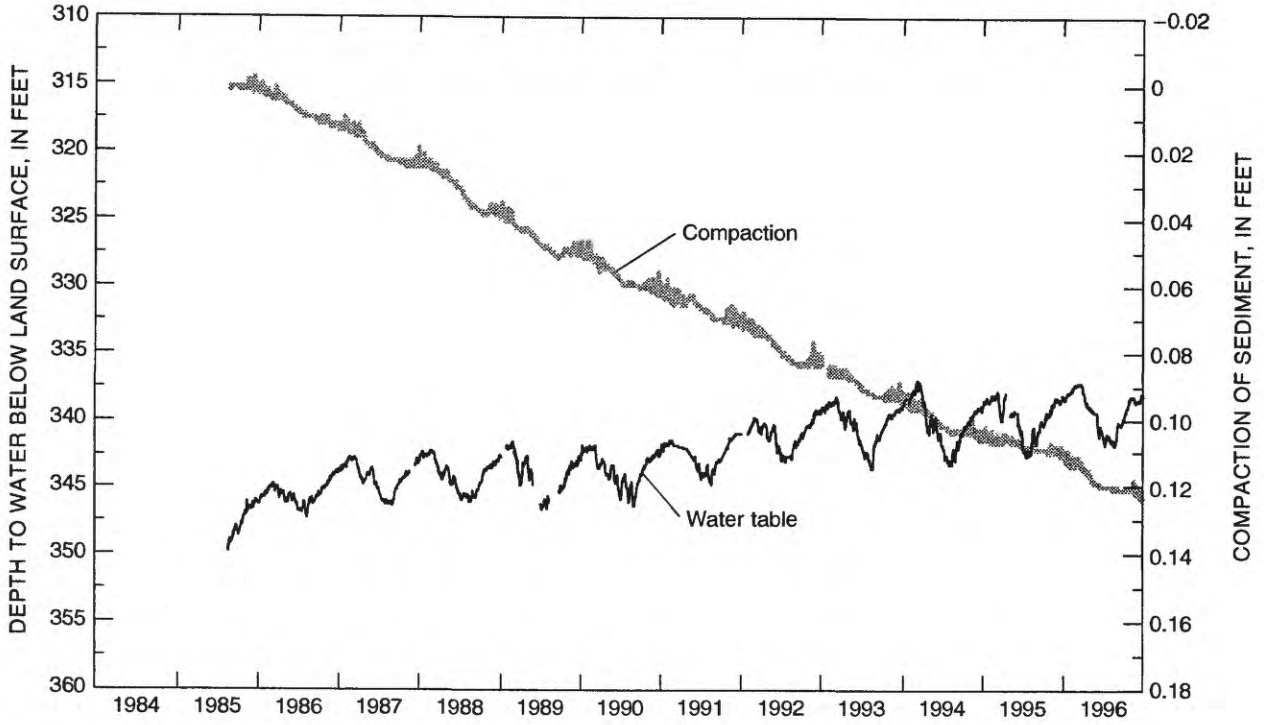

Figure 18. Depth to water and measured compaction in well AF-17 (D-12-10)33ddd.

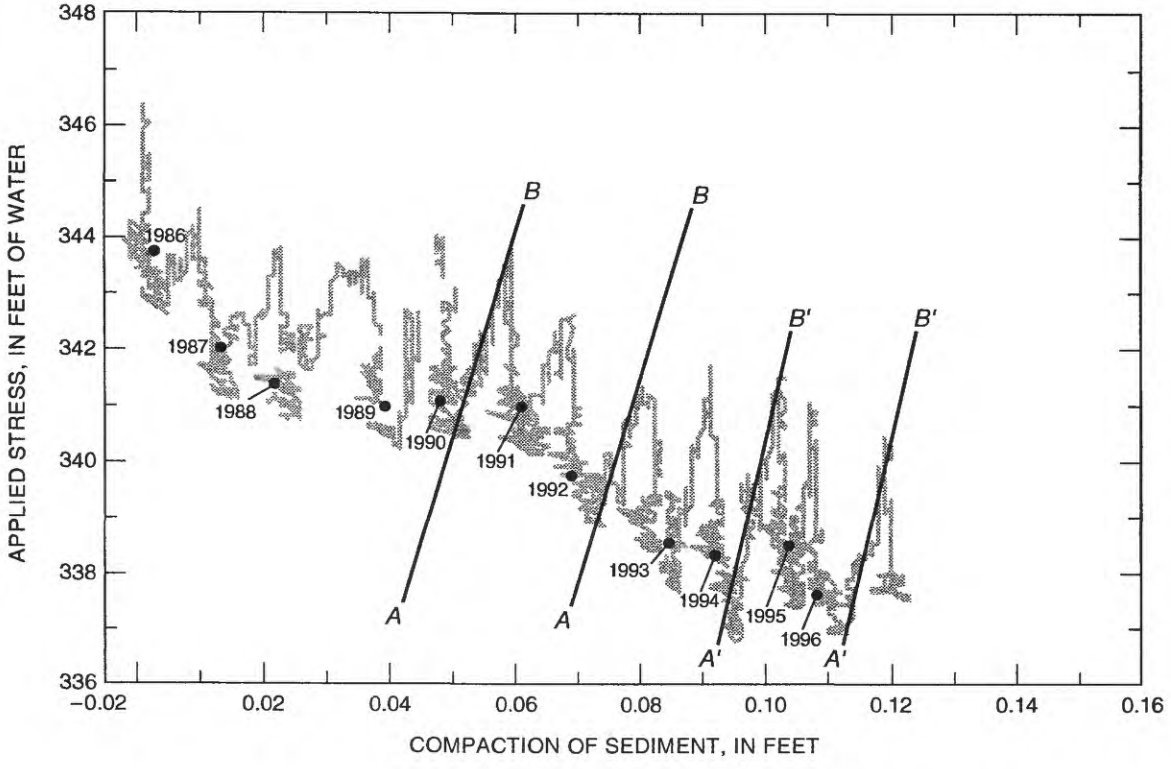

Figure 19. Compaction as a function of measured stress in well AF-17 (D-12-10)33ddd.

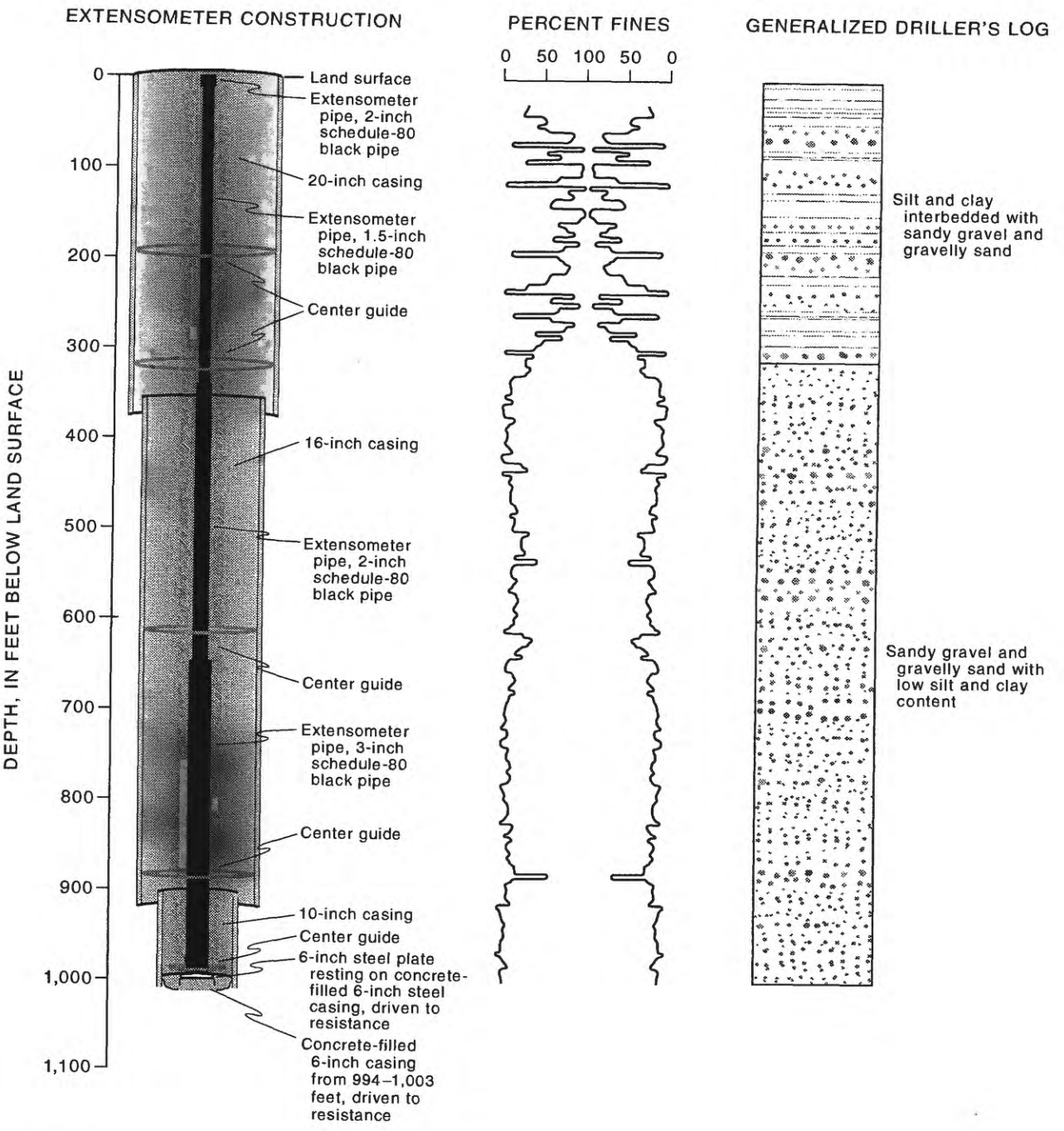

Figure 20. Extensometer construction, percent-fines distribution, and driller's log for well AF-17 (D-12-10)33ddd.

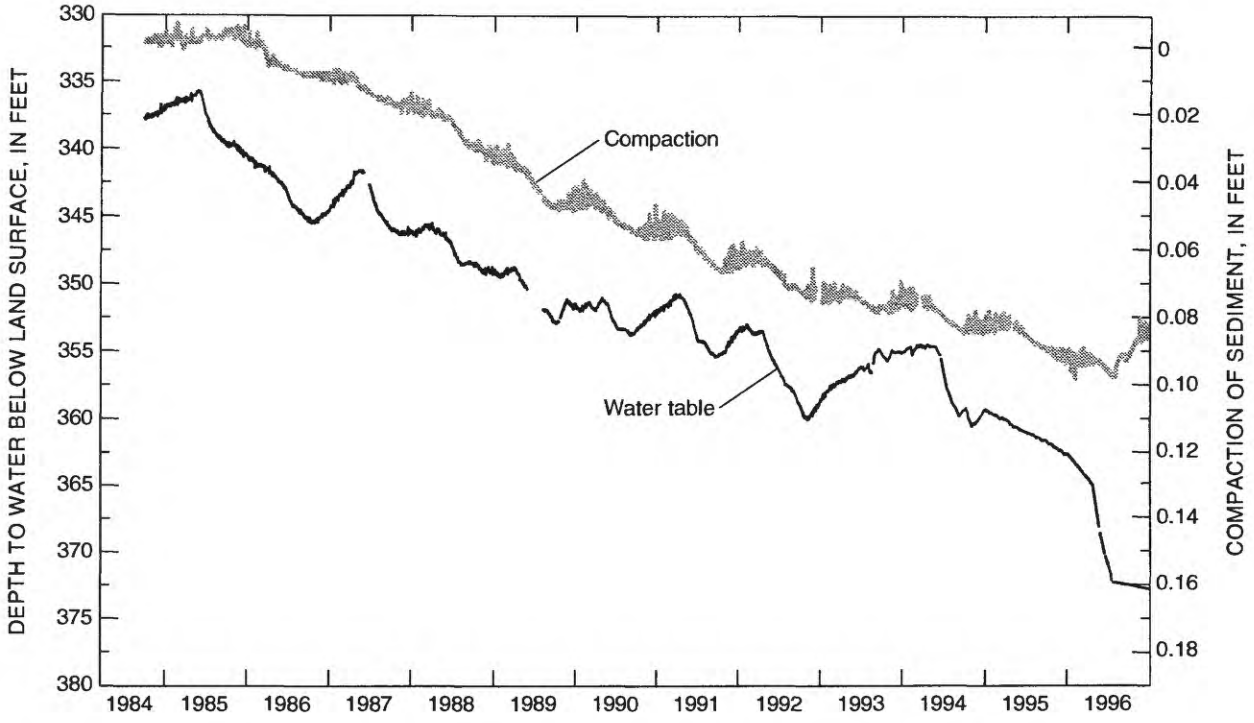

Figure 21. Depth to water and measured compaction in well AV-25 (D-14-11)34ccc.

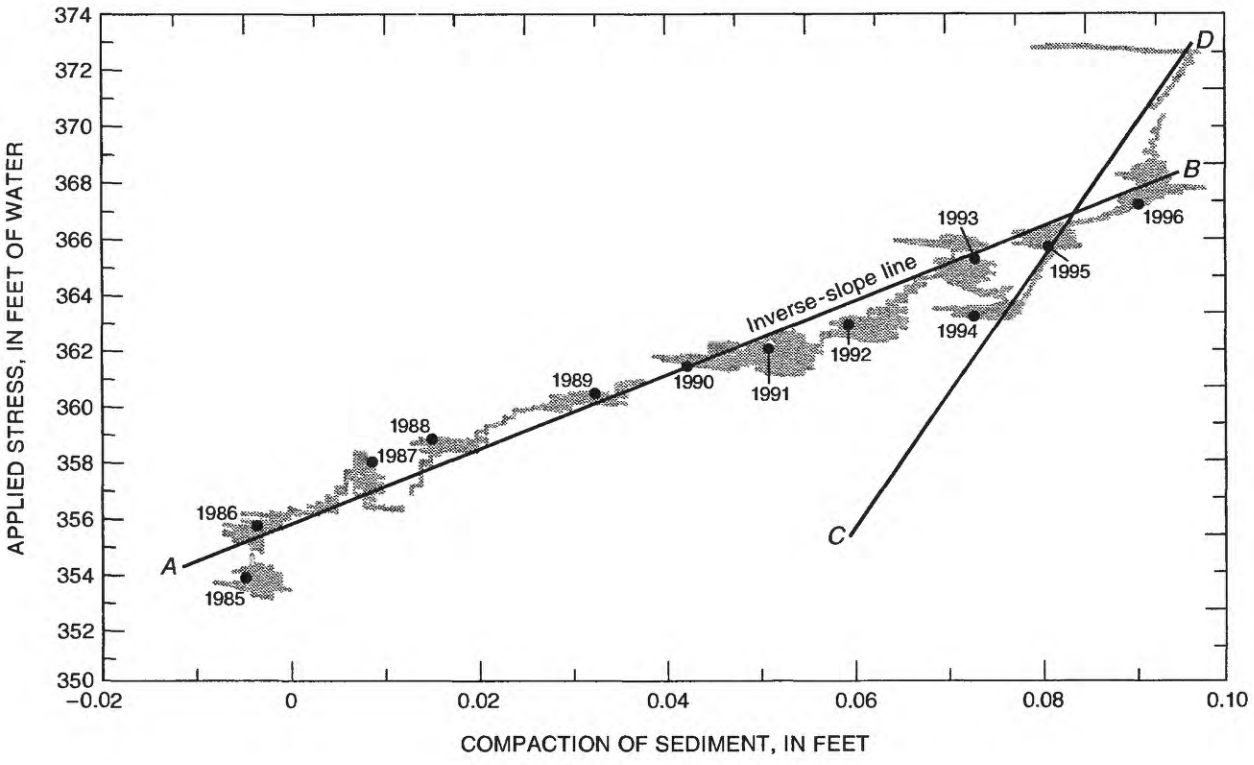

Figure 22. Compaction as a function of measured stress in well AV-25 (D-14-11)34ccc.

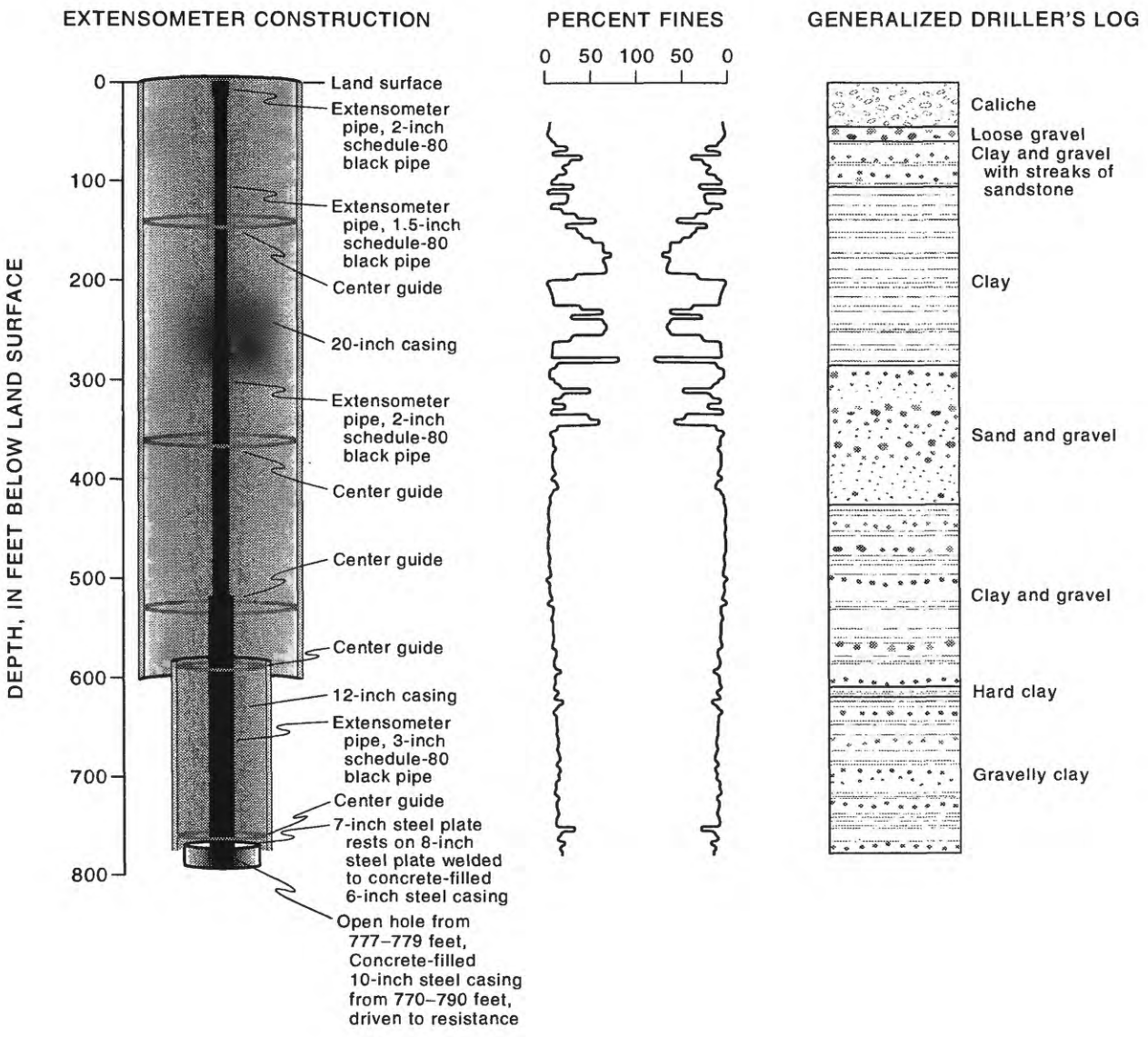

Figure 23. Extensometer construction, percent-fines distribution, and driller's log for well AV-25 (D-14-11)34ccc.

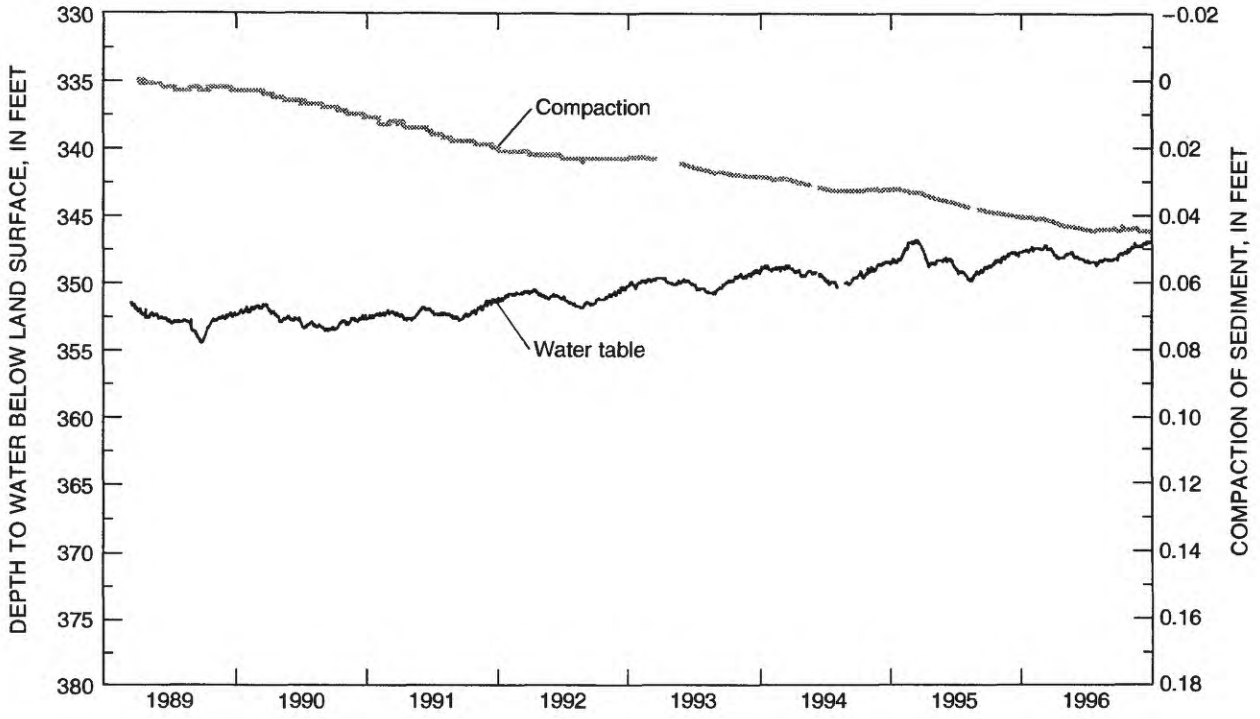

Figure 24. Depth to water and measured compaction in well TA-32 (D-12-11)33bbc.

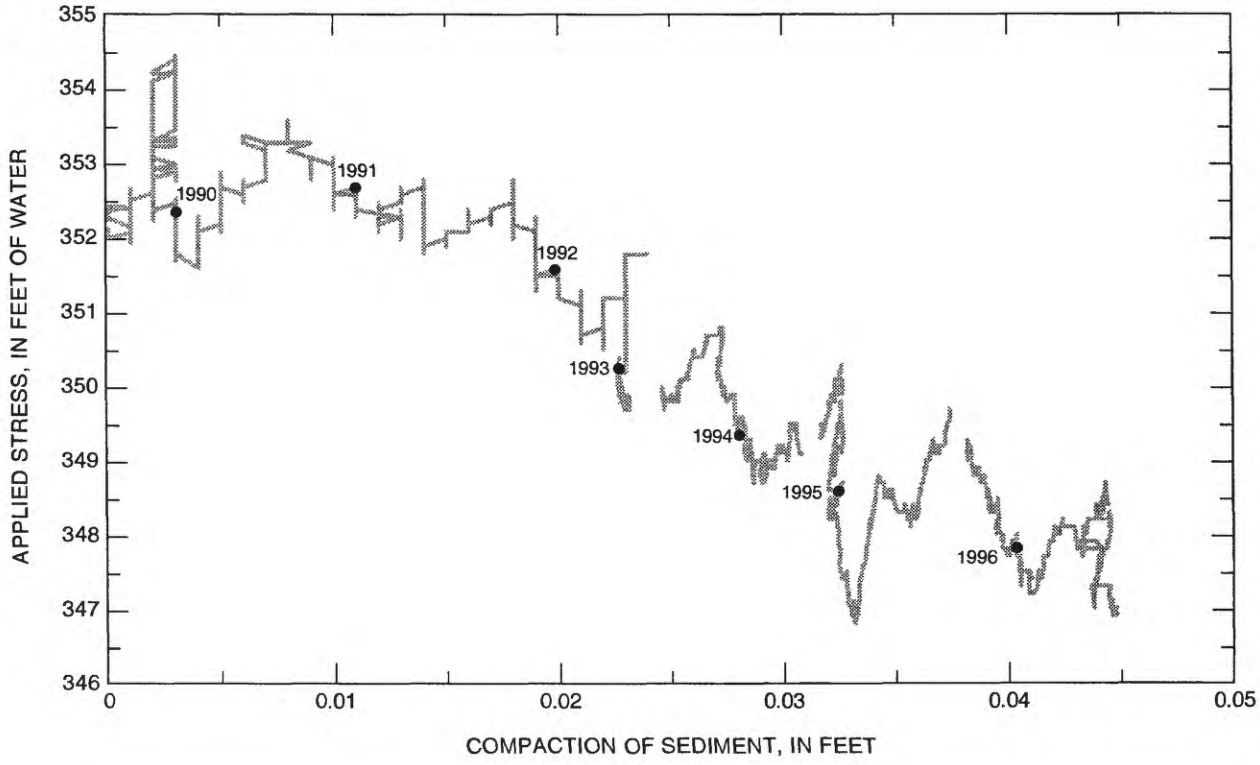

Figure 25. Compaction as a function of measured stress in well TA-32 (D-12-11)33bbc.

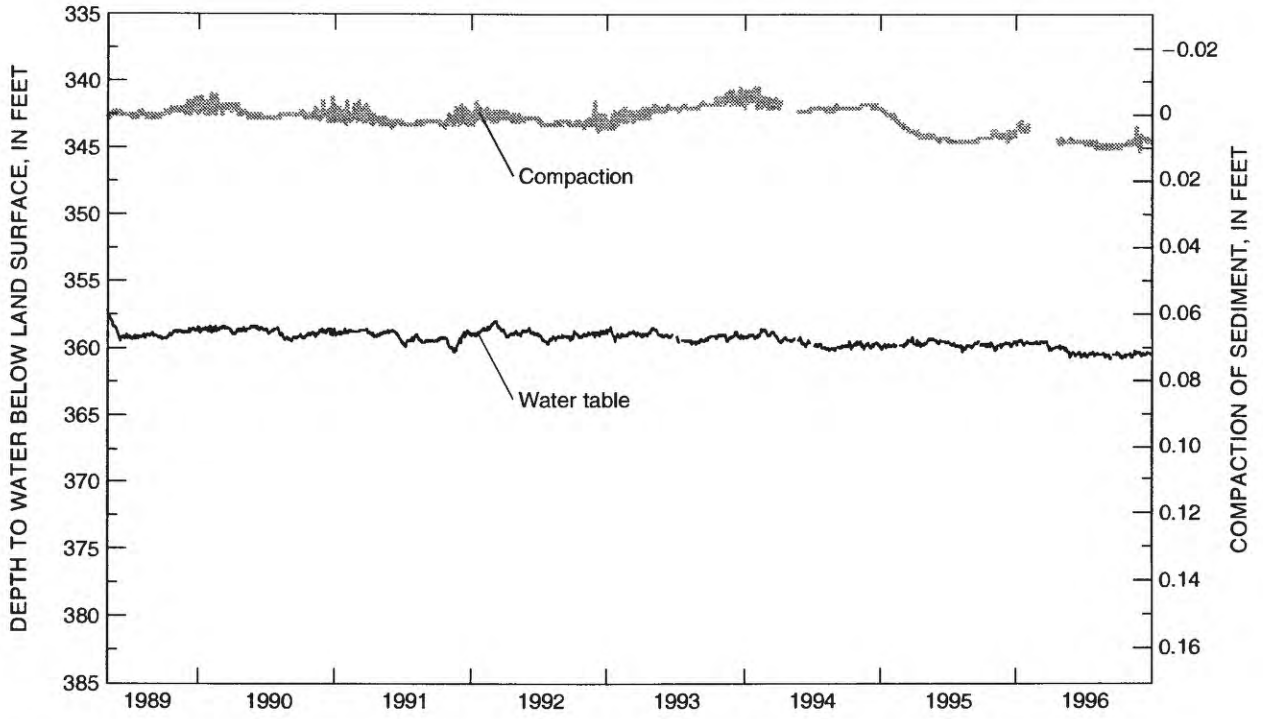

Figure 26. Depth to water and measured compaction in well TA-33 (D-13-11)29cdd.

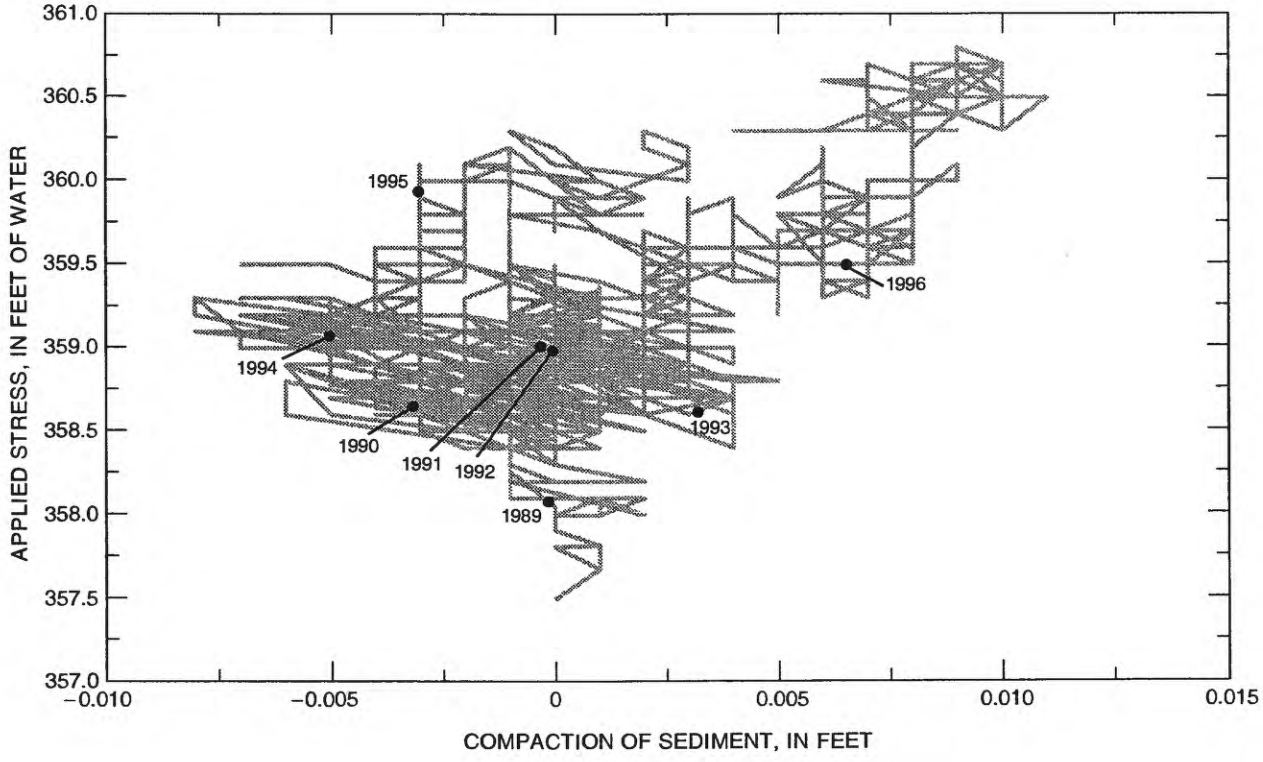

Figure 27. Compaction as a function of measured stress in well TA-33 (D-13-11)29cdd.

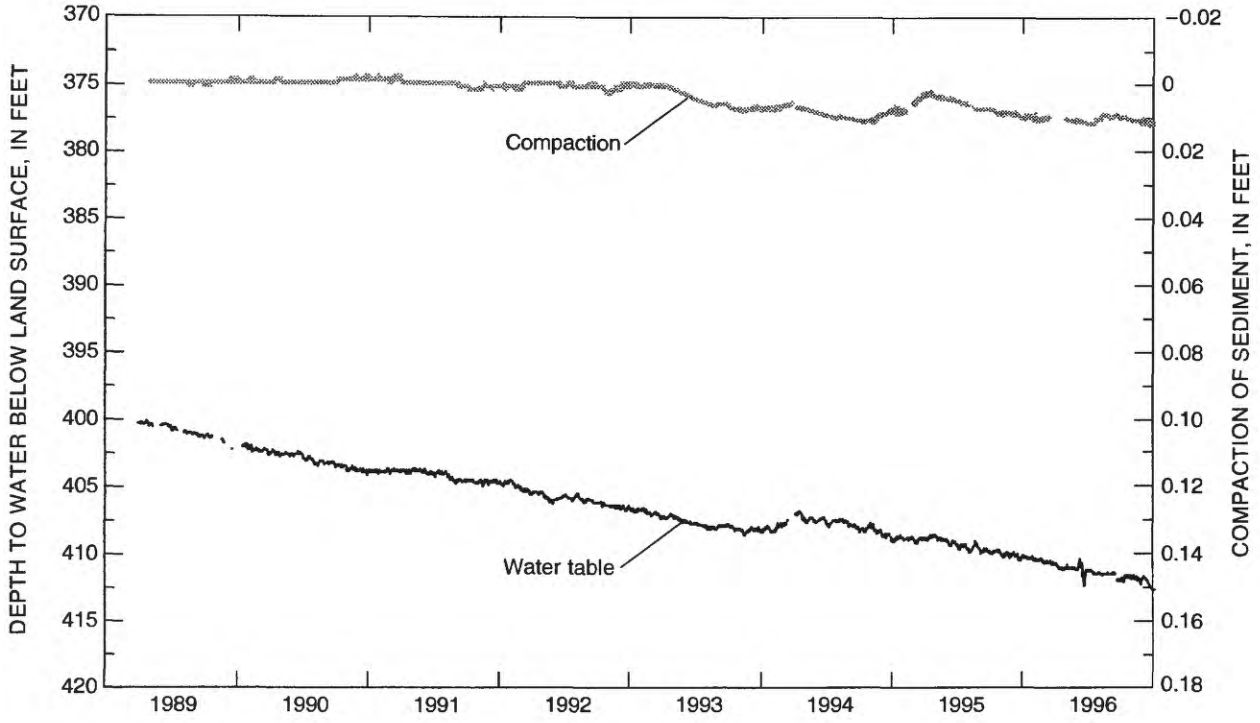

Figure 28. Depth to water and measured compaction in well TA-44 (D-14-11)36aac.

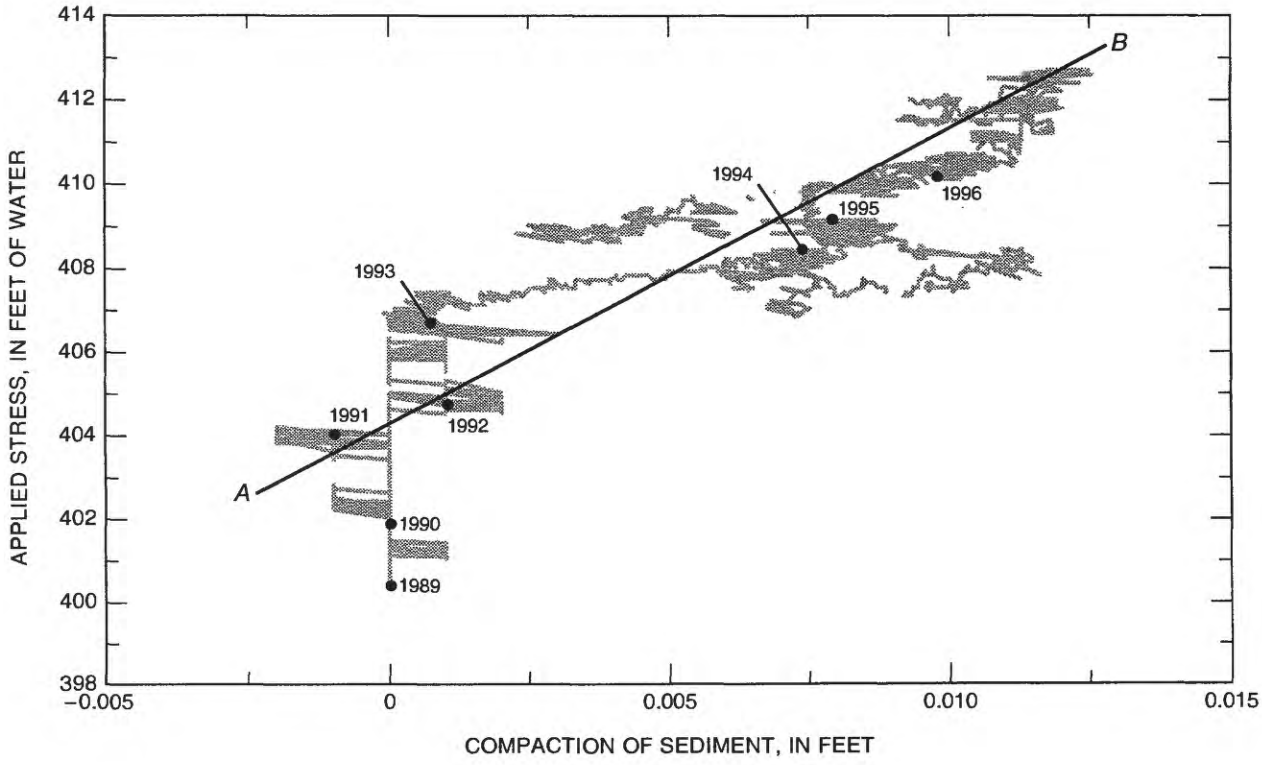

Figure 29. Compaction as a function of measured stress in well TA-44 (D-14-11)36aac.

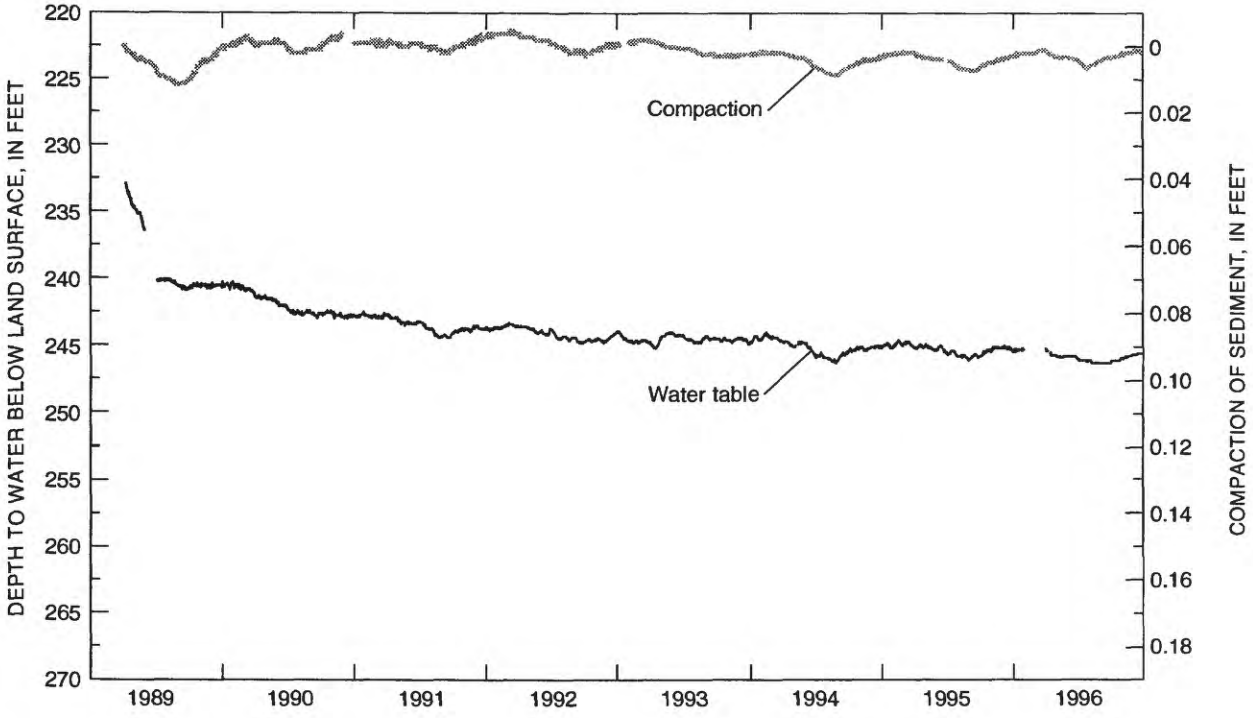

Figure 30. Depth to water and measured compaction in well TA-13 (D-10-10)03abc.

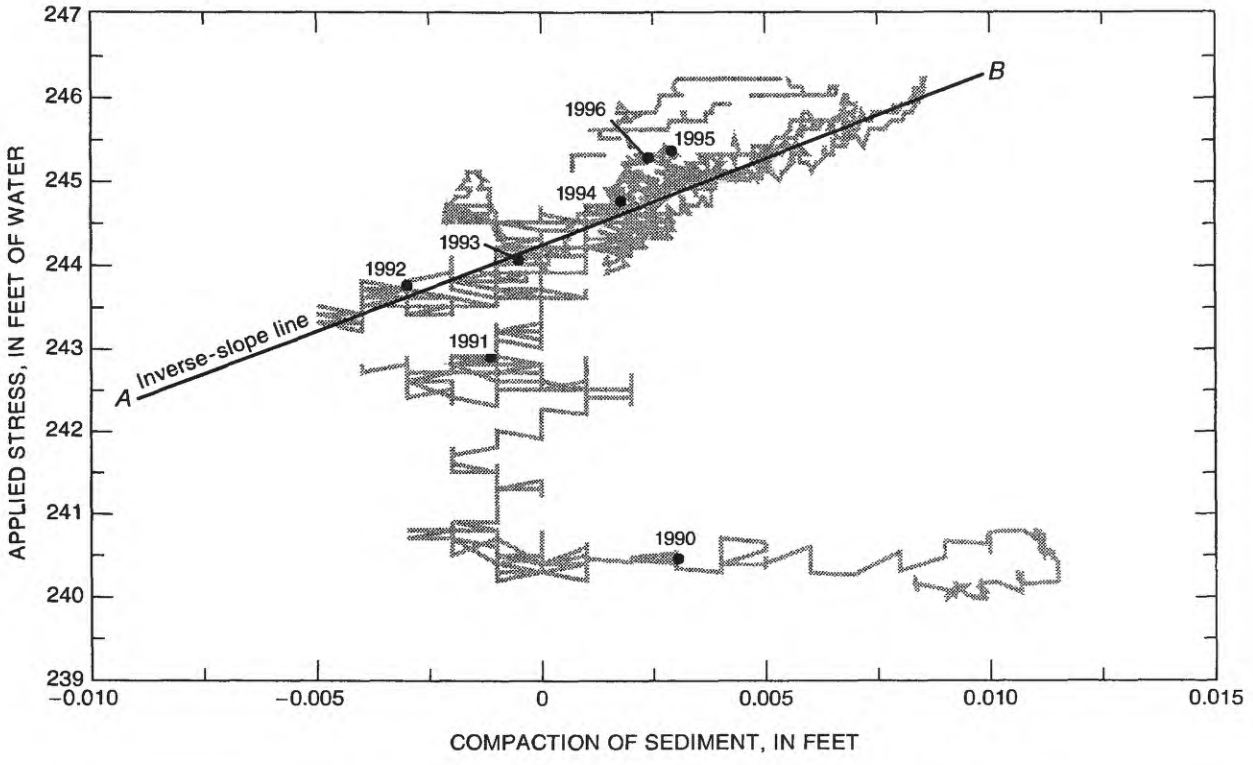

Figure 31. Compaction as a function of measured stress in well TA-13 (D-10-10)03abc.

BASIC DATA

C. Hydrographs for Selected Well Sites, Upper Santa Cruz Basin, Arizona

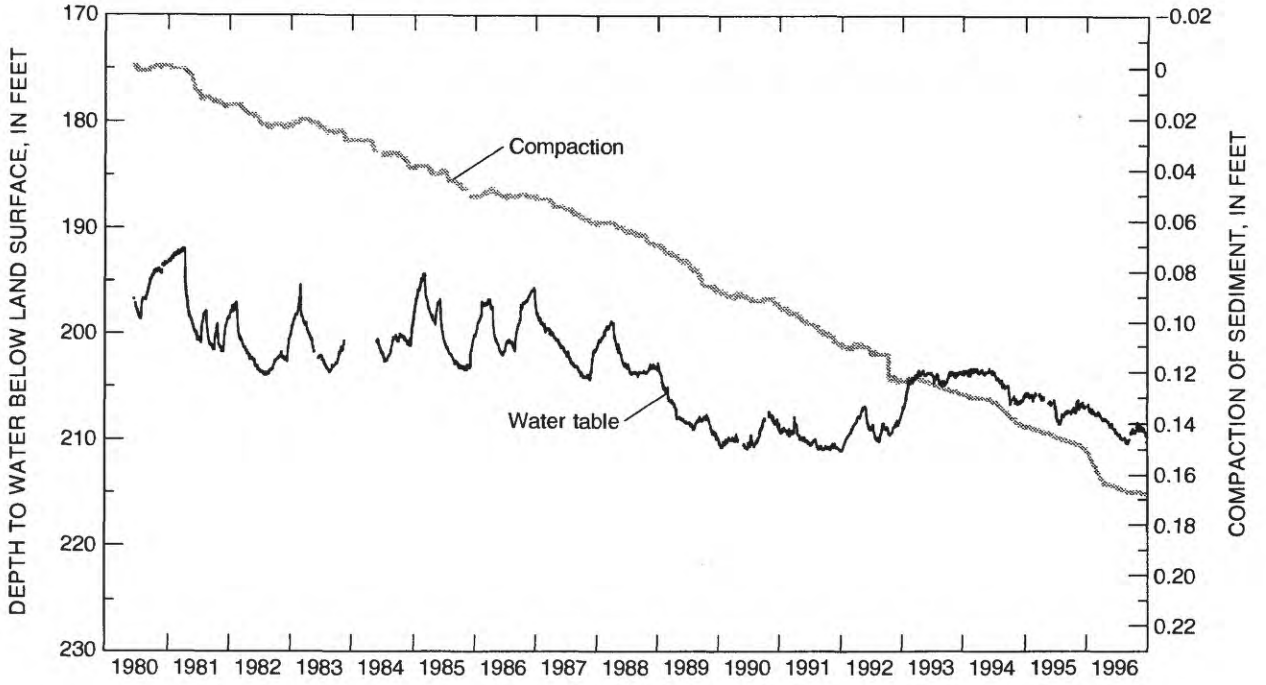

Figure 32. Depth to water and measured compaction in well B-76 (D-14-14)29cbc.

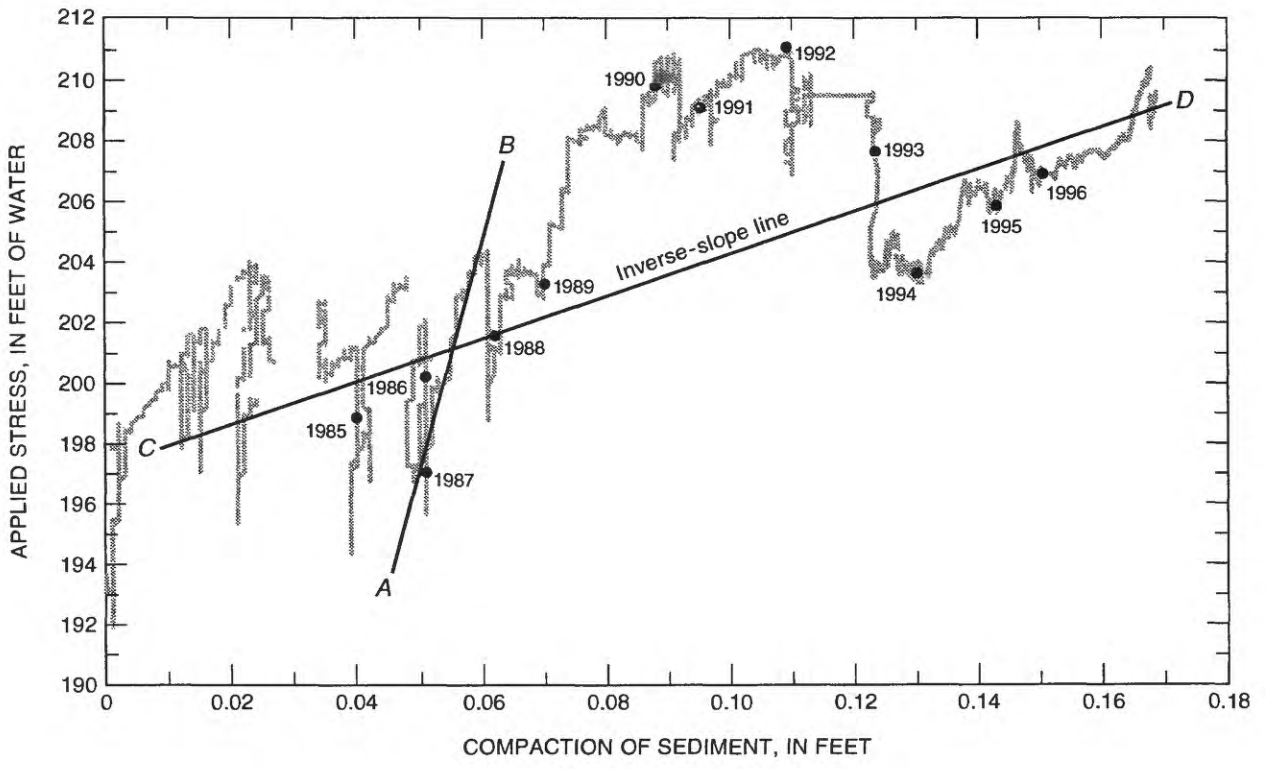

Figure 33. Compaction as a function of measured stress in well B-76 (D-14-14)29cbc.

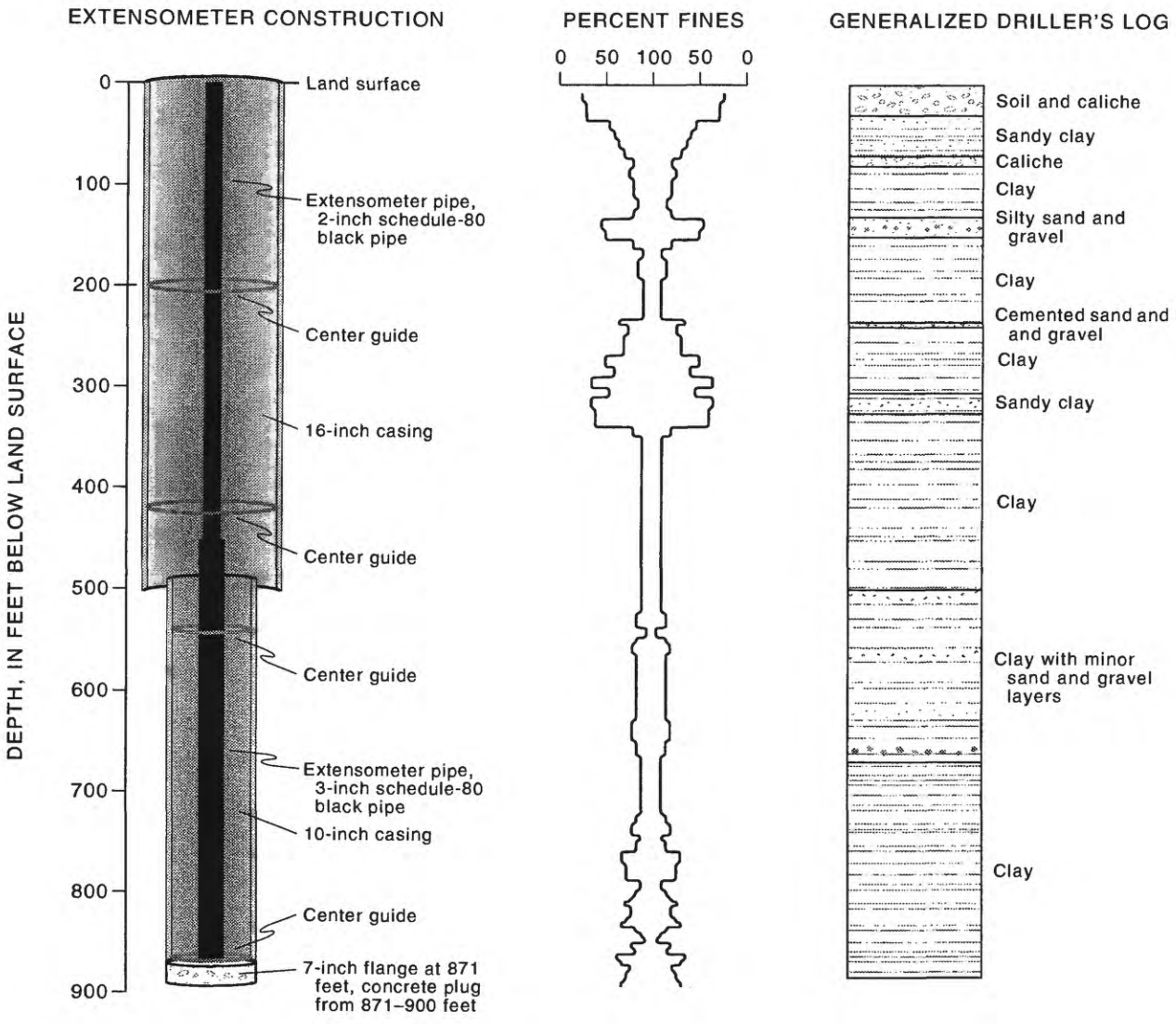

Figure 34. Extensometer construction, percent-fines distribution, and driller's log for well B-76 (D-14-14)29cbc.

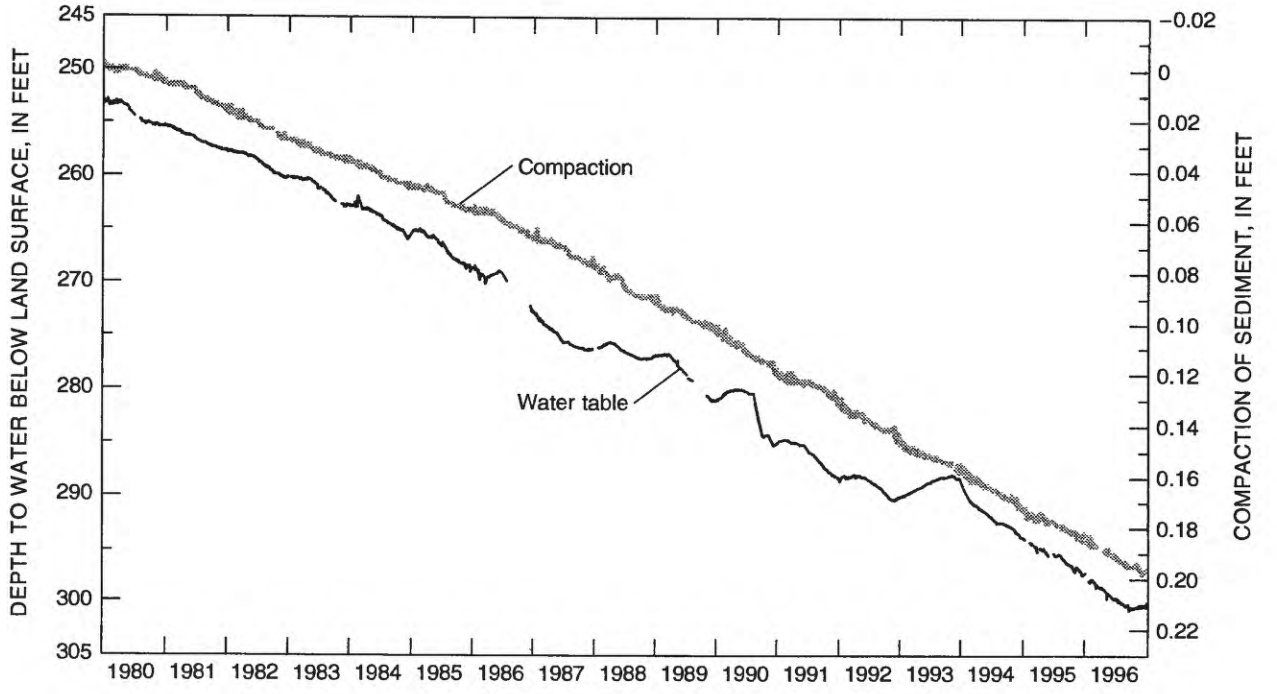

Figure 35. Depth to water and measured compaction in well C-45 (D-14-14)22adb.

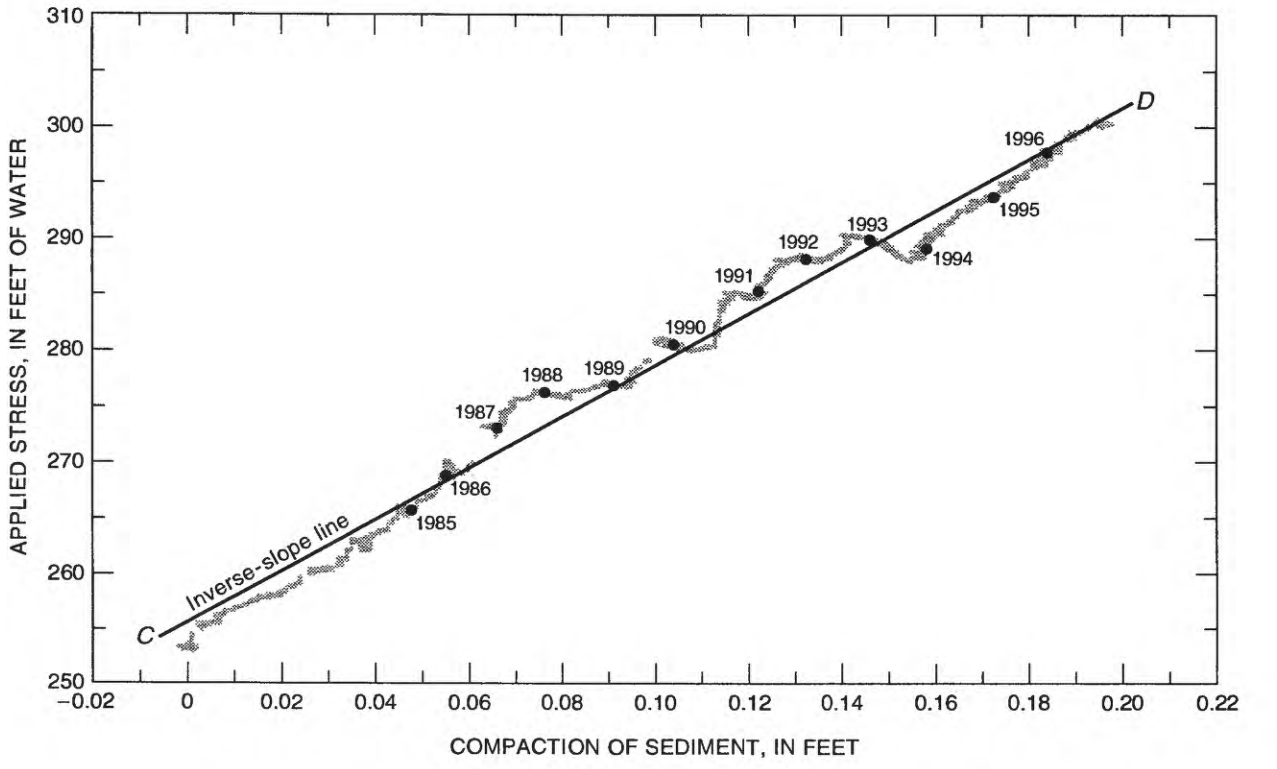

Figure 36. Compaction as a function of measured stress in well C-45 (D-14-14)22adb.

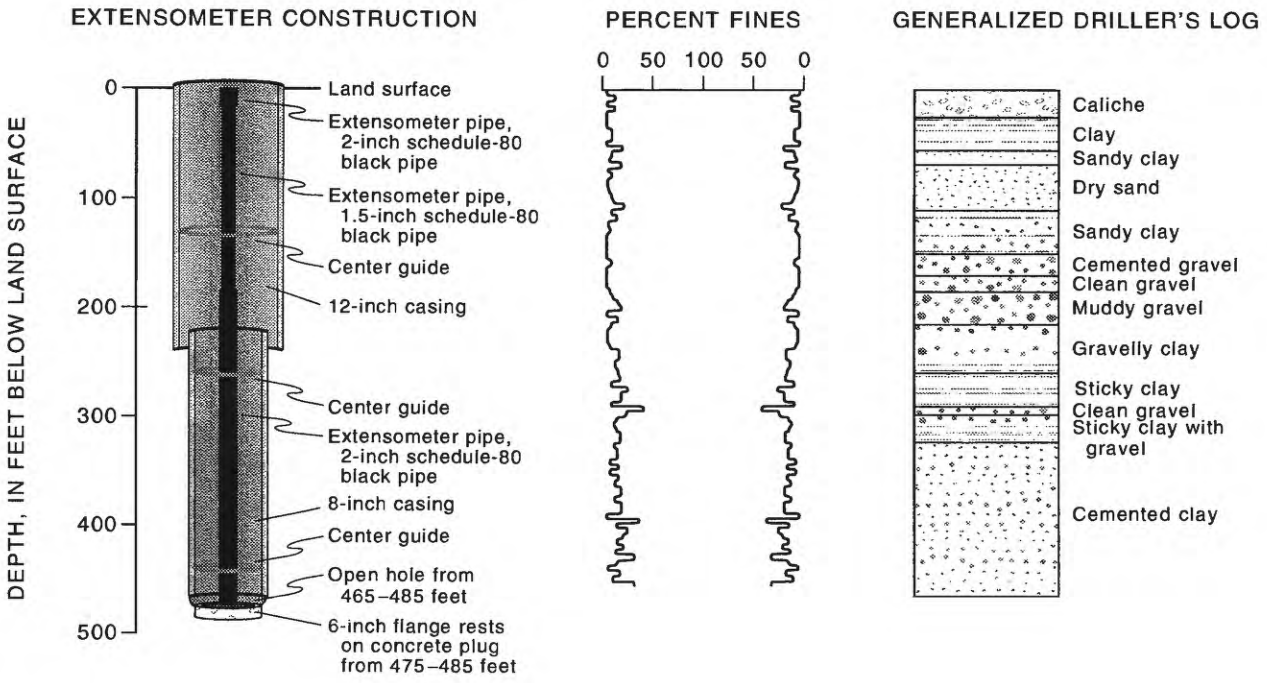

Figure 37. Extensometer construction, percent-fines distribution, and driller's log for well C-45 (D-14-14)22adb.

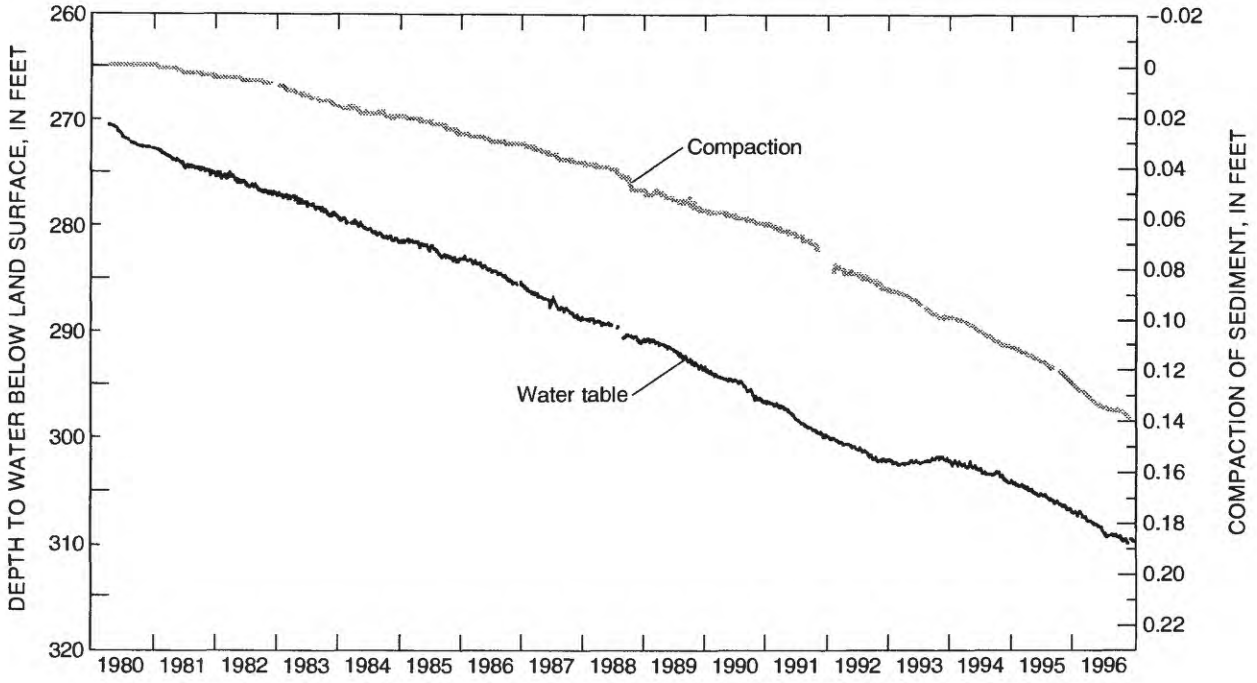

Figure 38. Depth to water and measured compaction in well D-61 (D-14-14)23cab.

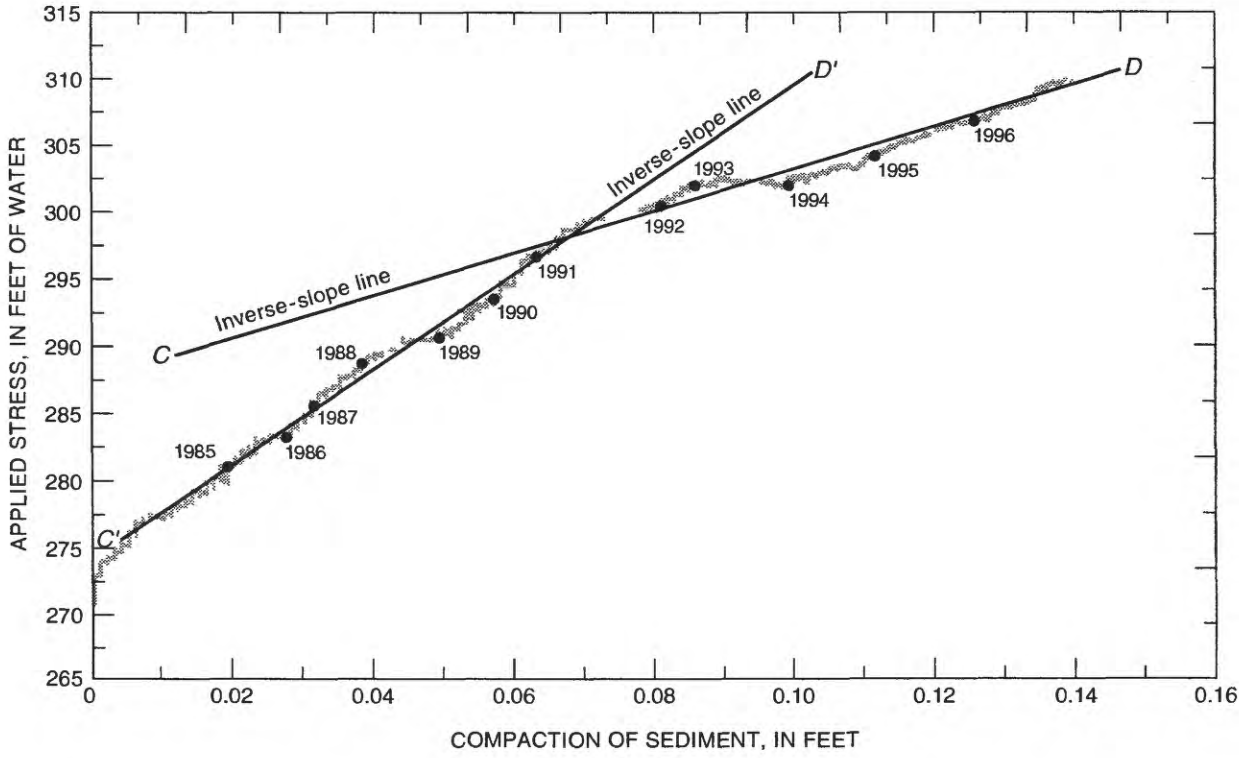

Figure 39. Compaction as a function of measured stress in well D-61 (D-14-14)23cab.

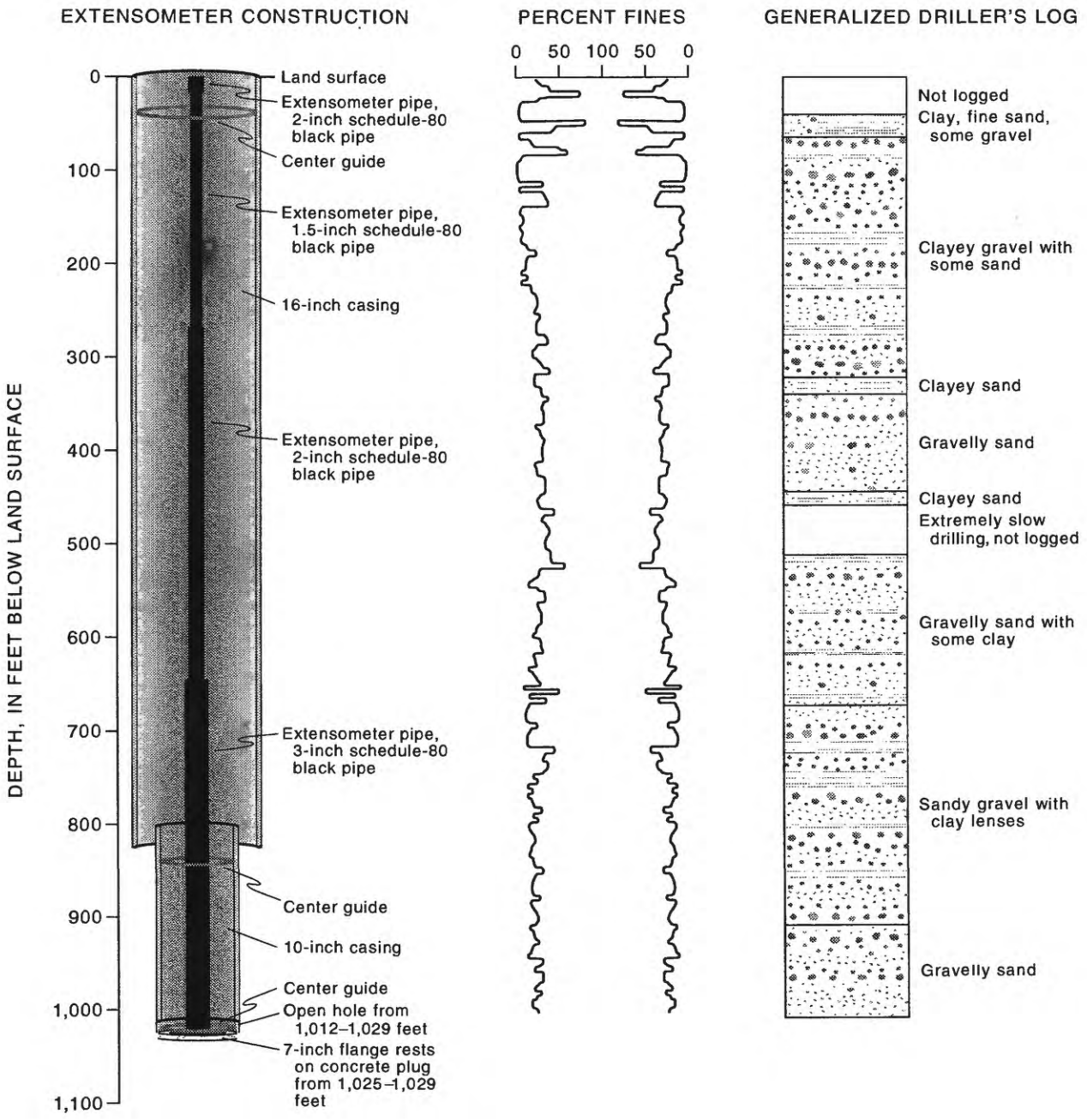

Figure 40. Extensometer construction, percent-fines distribution, and driller's log for well D-61 (D-14-14)23cab.

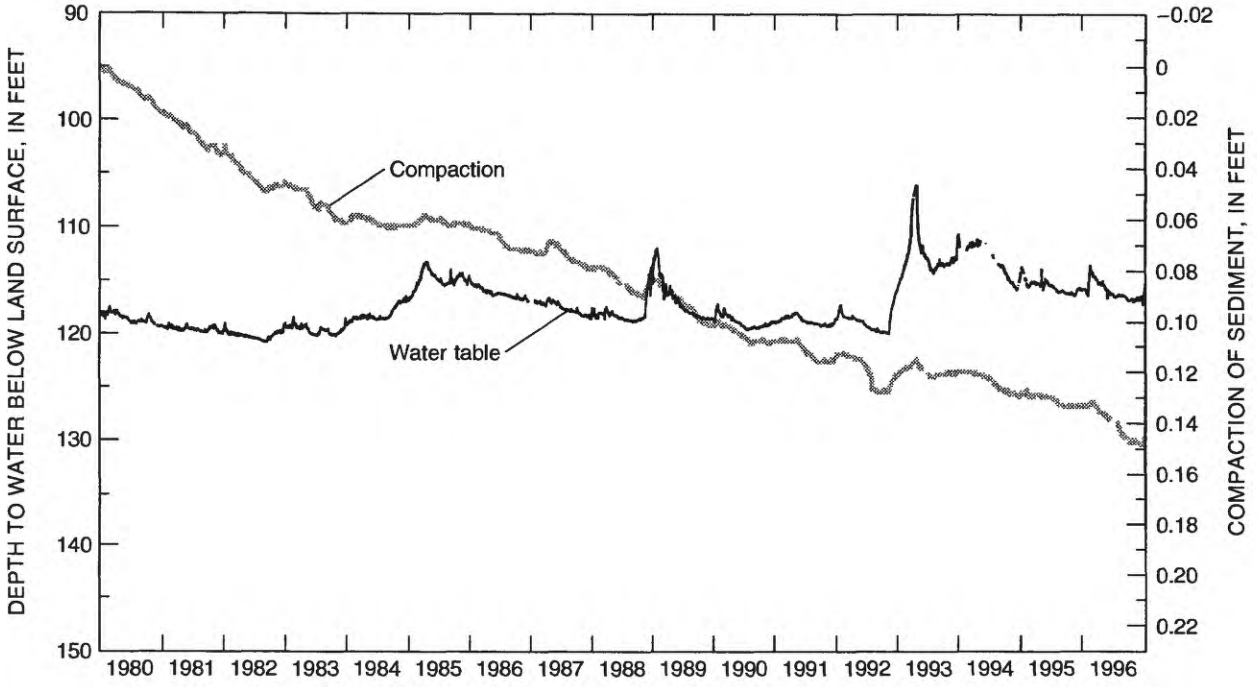

Figure 41. Depth to water and measured compaction in well SC-17 (D-15-14)30cbc.

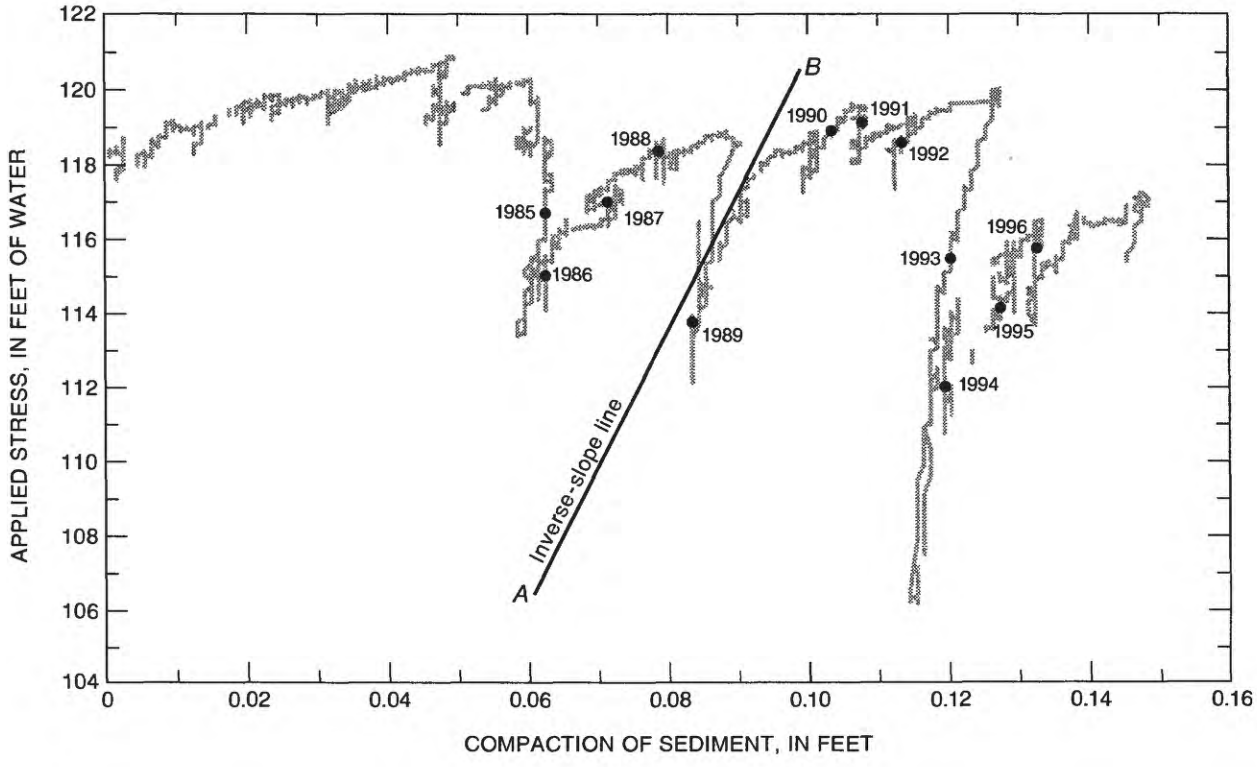

Figure 42. Compaction as a function of measured stress in well SC-17 (D-15-14)30cbc.

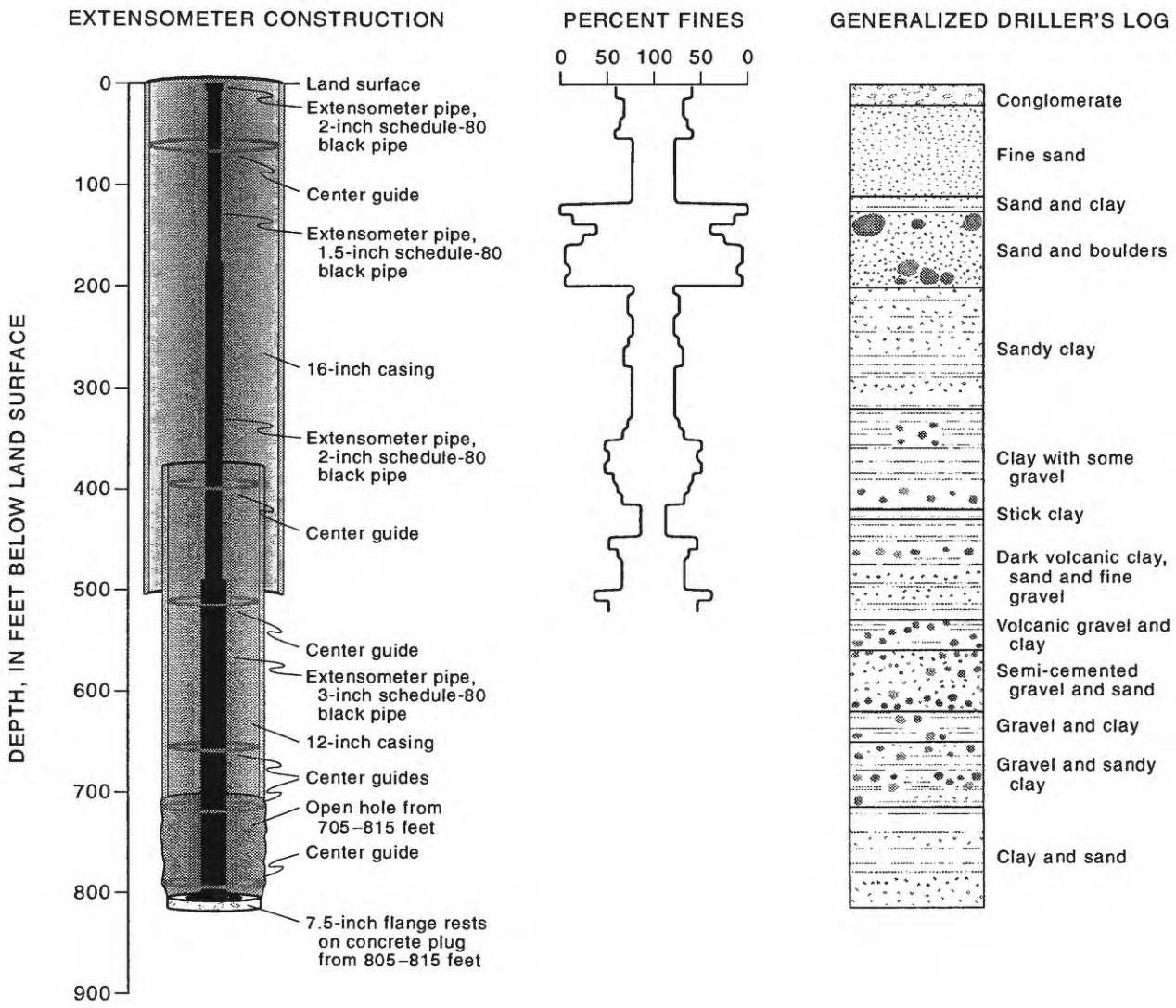

Figure 43. Extensometer construction, percent-fines distribution, and driller's log for well SC-17 (D-15-14)30cbc.

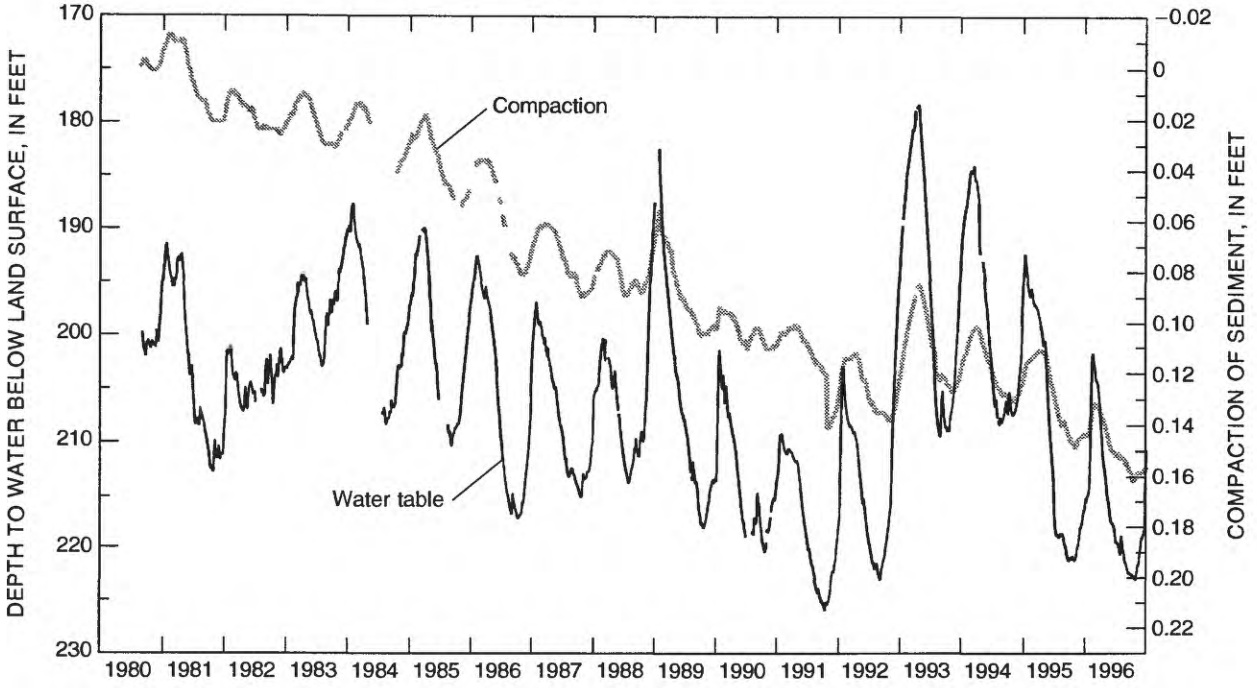

Figure 44. Depth to water and measured compaction in well SC-30 (D-17-14)03baa.

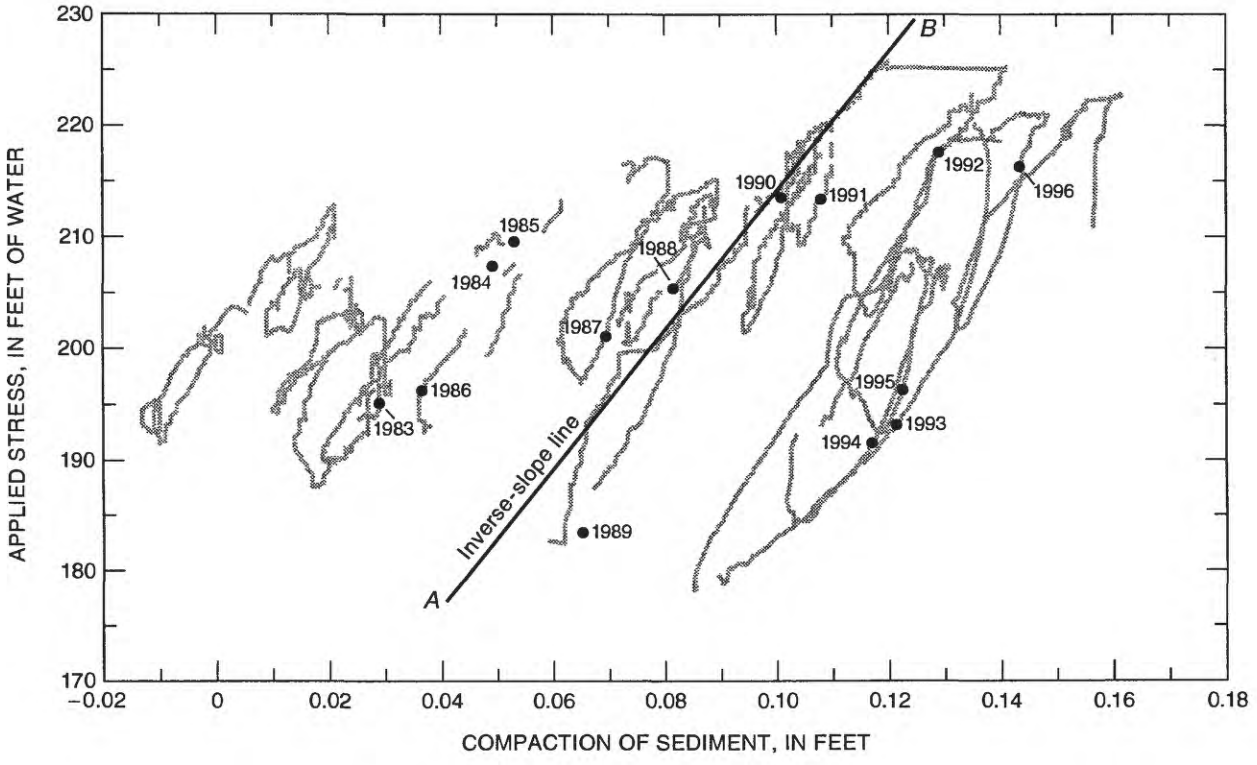

Figure 45. Compaction as a function of measured stress in well SC-30 (D-17-14)03baa.

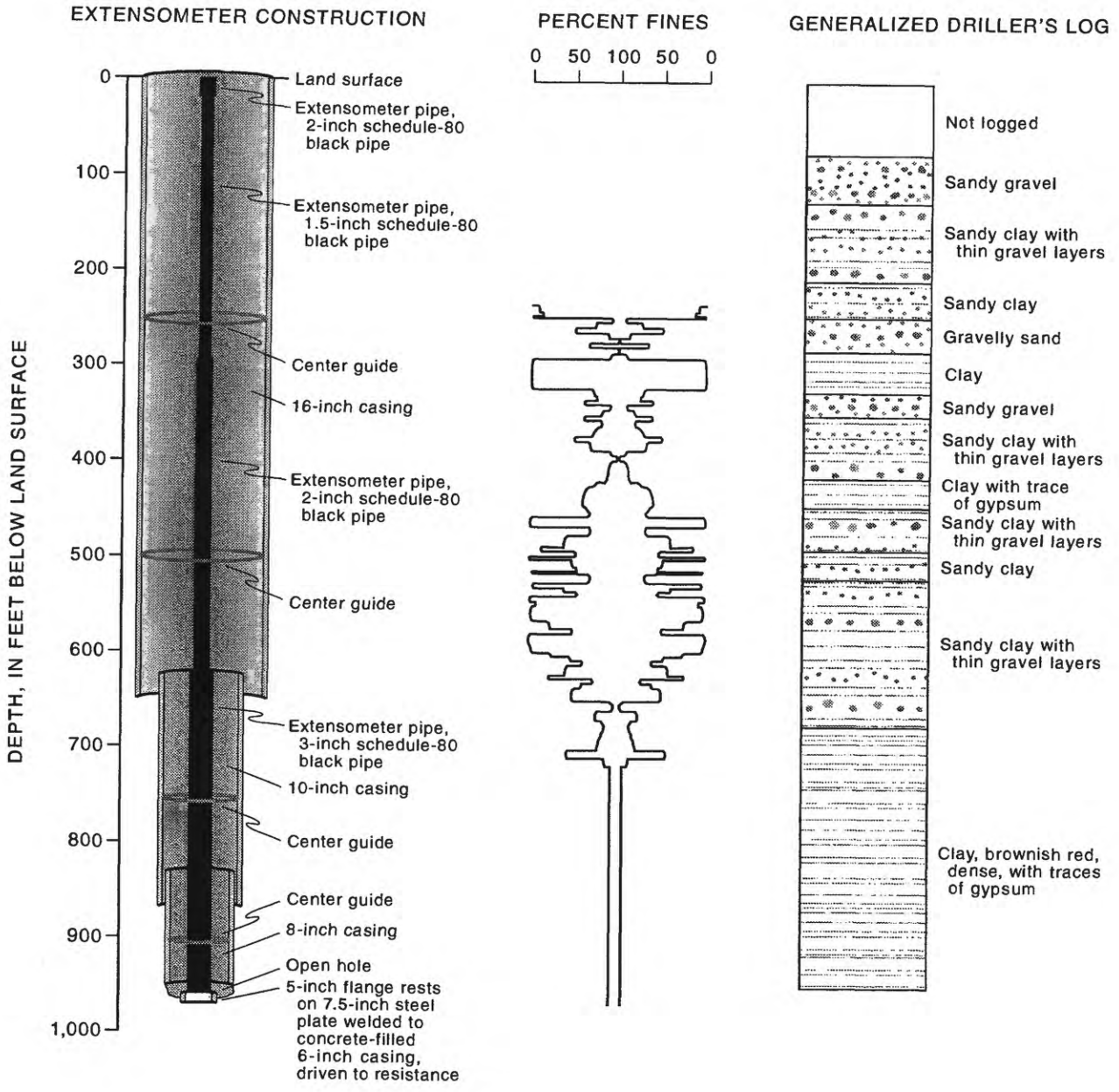

Figure 46. Extensometer construction, percent-fines distribution, and driller's log for well SC-30 (D-17-14)03baa.

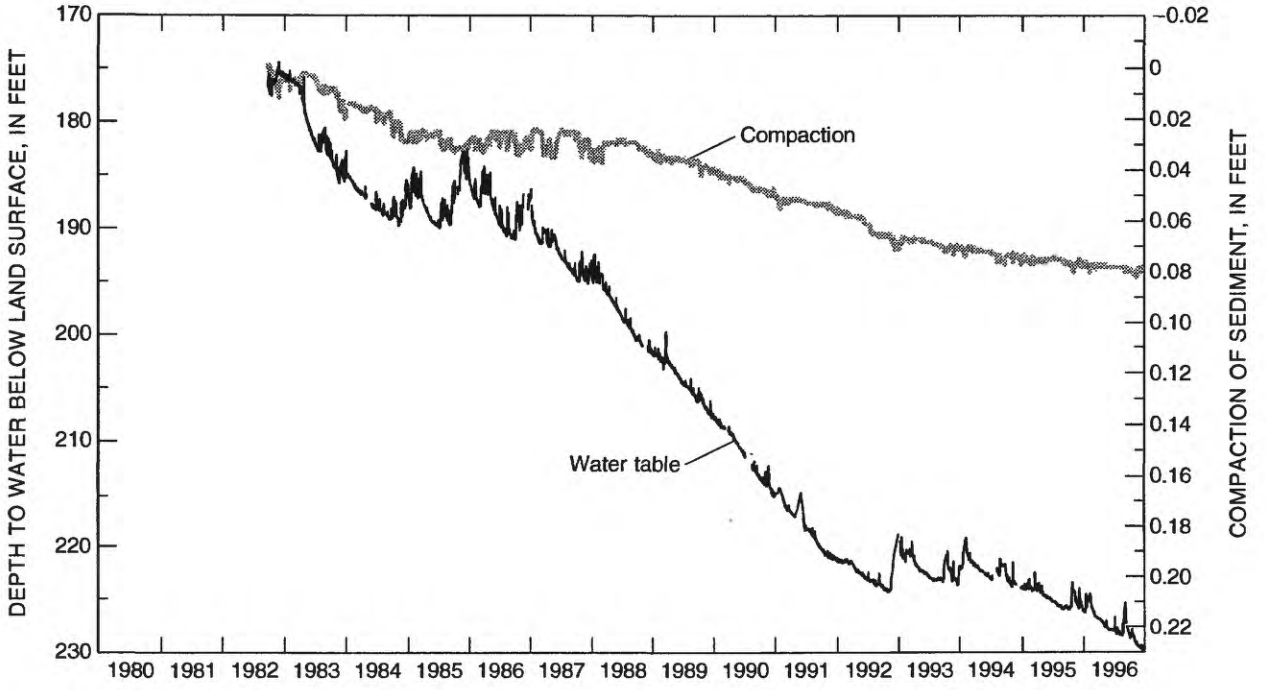

Figure 47. Depth to water and measured compaction in well WR-52 (D-13-14)31cac.

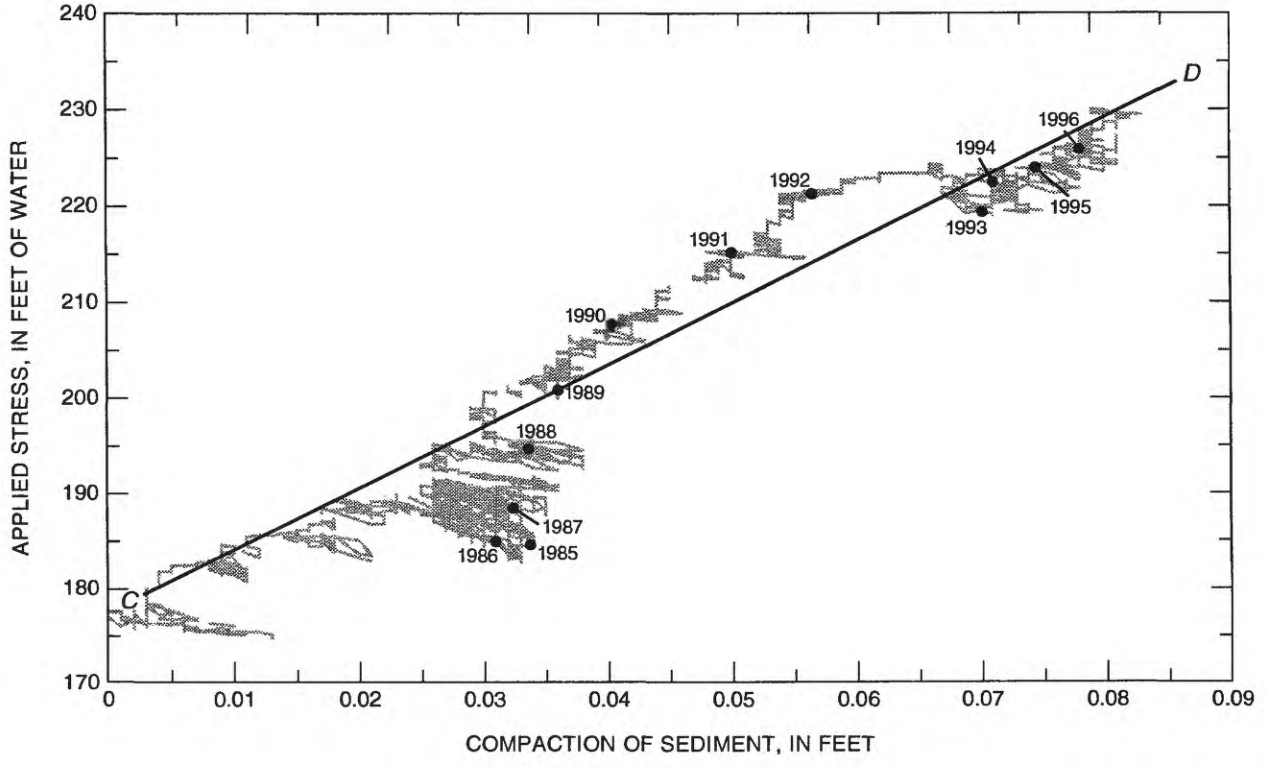

Figure 48. Compaction as a function of measured stress in well WR-52 (D-13-14)31cac.

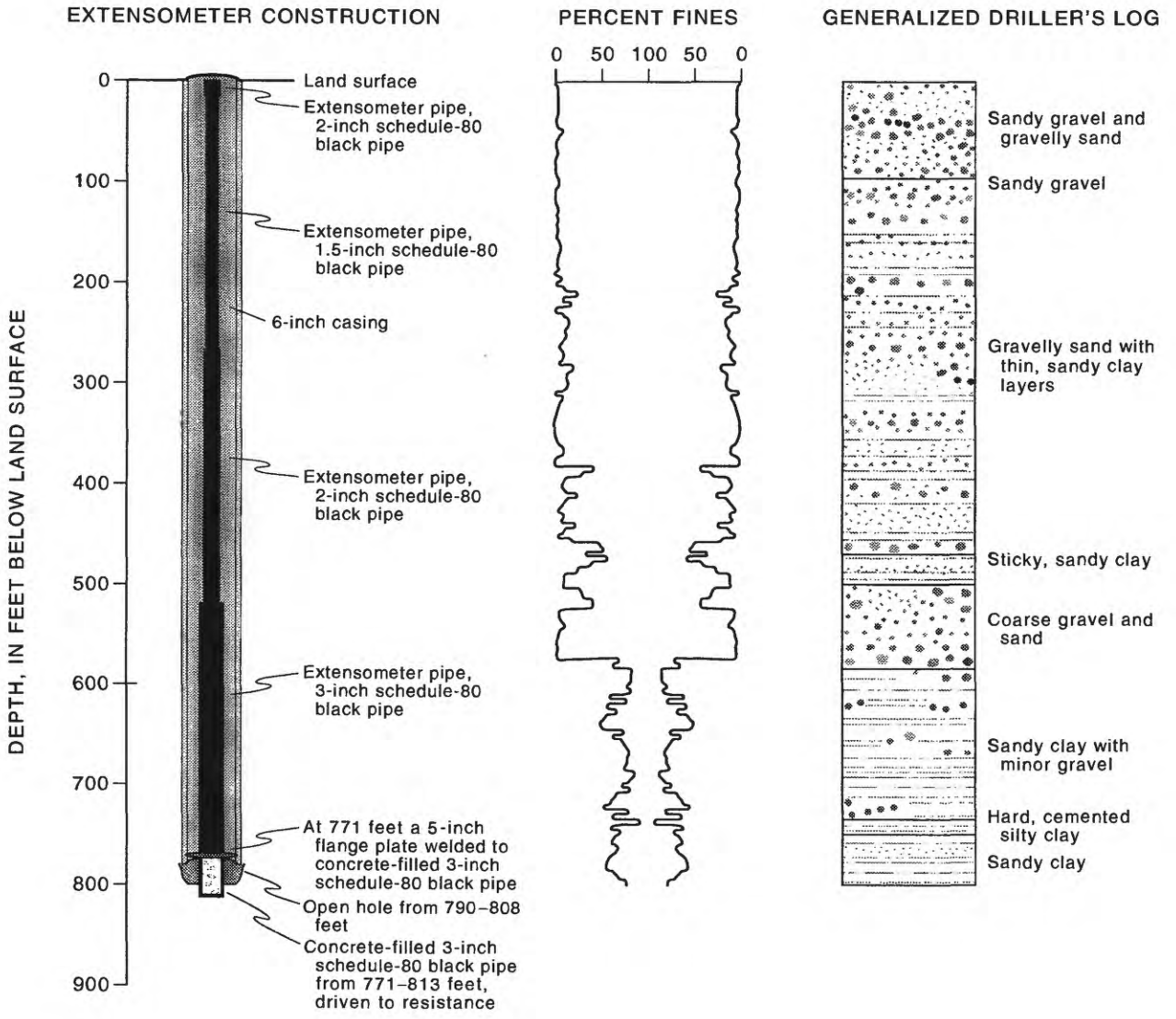

Figure 49. Extensometer construction, percent-fines distribution, and driller's log for well WR-52 (D-13-14)31cac.

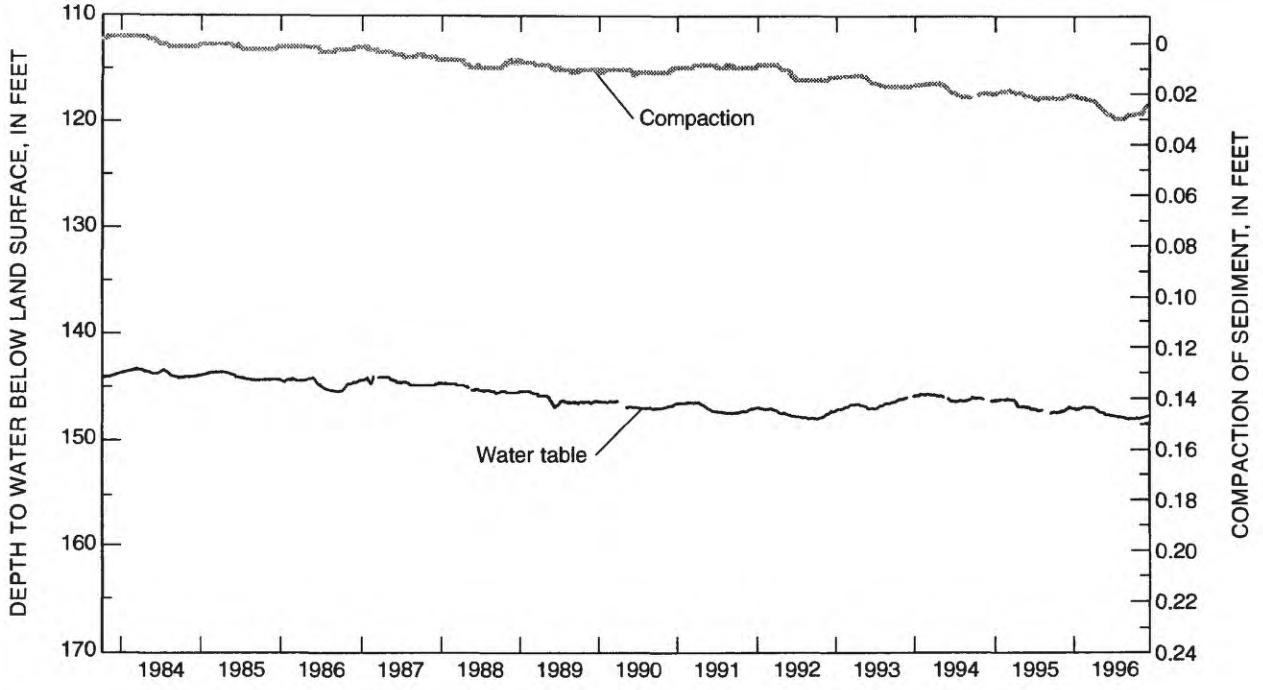

Figure 50. Depth to water and measured compaction in well WR-53 (D-15-14)09bac.

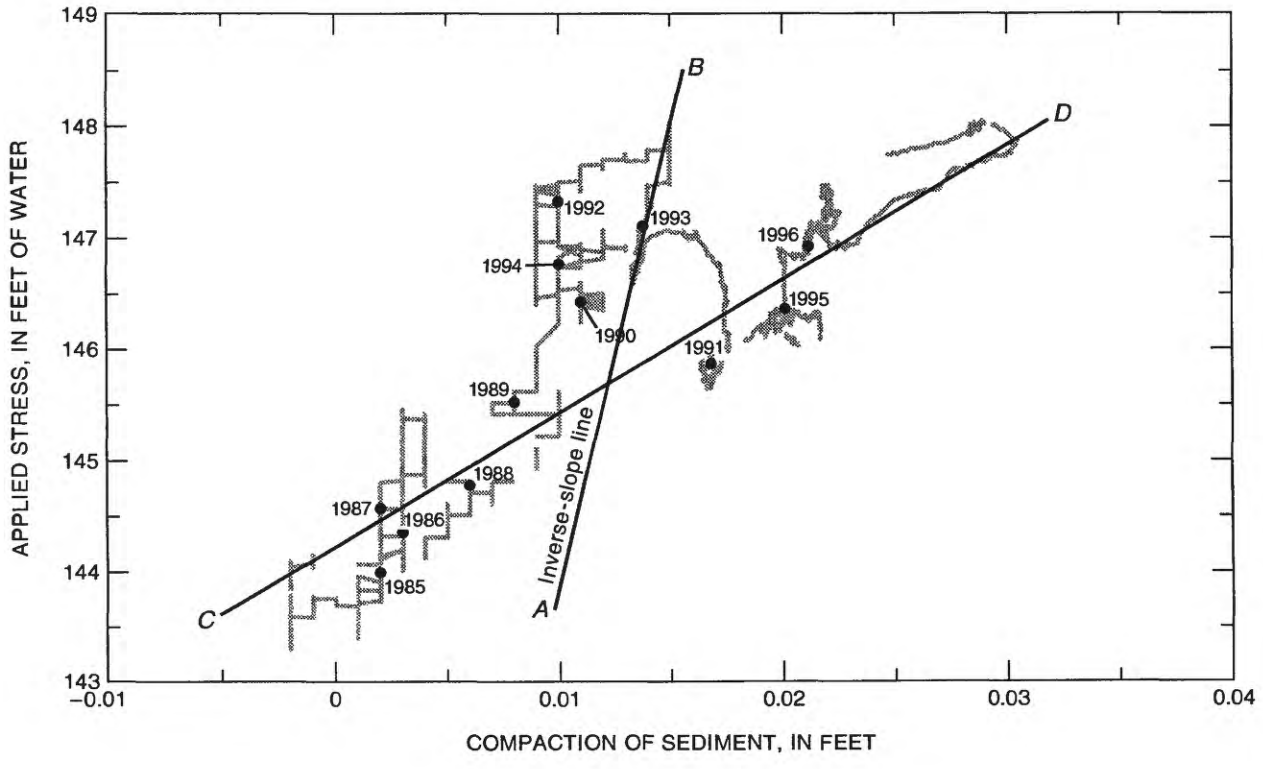

Figure 51. Compaction as a function of measured stress in well WR-53 (D-15-14)09bac.

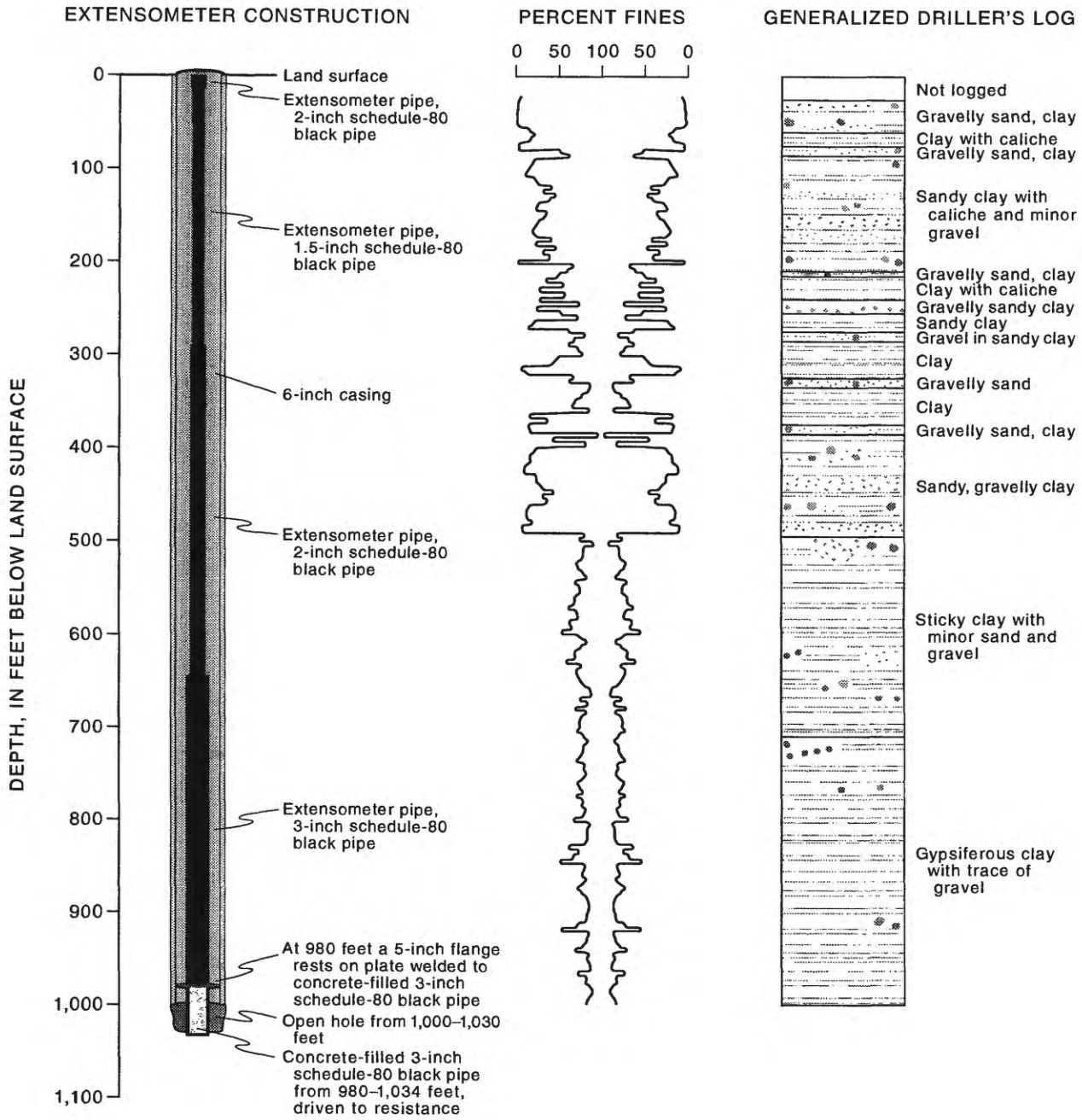

Figure 52. Extensometer construction, percent-fines distribution, and driller's log for well WR-53 (D-15-14)09bac.

*U.S.G.P.O. 1999-0-583-703